Oral Delivery of Neuropeptide(s) to The Brain Utilizing a Ligand Niosomal Delivery System for The Treatment of Neurodegenerative Disorders.

Murad Al Gailani

BPharm

A thesis submitted in partial fulfilment of the requirements for the degree of Doctor of Philosophy (in Pharmacy), The University of Auckland, 2021.

Abstract

Background: Neurological disorders affect hundreds of millions of people worldwide and rapidly rising. One of the biggest hurdles for treating neurological disorders is the limited scope of drugs that can be delivered to the brain via non-invasive routes. Peptide drugs like Glycine-Proline-Glutamate (GPE) and cyclic Glycine Proline (cGP) have been found to be very effective at treating a wide range of neurodegenerative conditions like stroke and Parkinson's Disease (PD). The main issue with these drugs is that they are susceptible to degradation and/or elimination when either orally or parenterally administered to patients. By incorporating these peptide drugs into a formulation, it is possible to both protect and deliver the drugs directly to the brain. Niosomes were chosen as the preferred vesicle of choice as they are biocompatible and able to entrap both hydrophilic and lipophilic drugs. Notably, niosomes are also able to incorporate ligands into its structure to improve both the efficacy of transport and specificity targeting towards the blood-brain-barrier (BBB). Two different ligands were chosen to be incorporated into the formulation to help deliver the drugs to the brain. The two ligands are the non-specific cell-penetrating peptide Poly-L-arginine (PLR) and the monoclonal antibody RI7, which is a non-invasive targeting ligand specific towards the BBB to improve oral drug delivery to the brain. These two ligands can be used to improve the cellular uptake and transport of GPE and cGP to the brain across the BBB.

Aim: The aim of this project is to design an optimised a bi-ligand niosomal delivery system to orally deliver GPE and cGP across the BBB.

Methods: An HPLC method was developed and validated for the determination of both peptide drugs, GPE and cGP. The niosomes were prepared via a thin-film hydration technique and a factorial design was used to efficiently explore and optimise the different formulation parameters. Chemical and physical properties of the niosomes such as particle size, entrapment efficiency, zeta potential and *in vitro* release profiles were characterised. The cytotoxicity of the bi-ligand niosomes and both free drugs were evaluated in both human colorectal adenocarcinoma cells (Caco-2)/HT29-MTX-E12 (E12) and Rat brain microvascular endothelial cell (RBMVEC). Cellular uptake was determined on both Caco-2 and RBMVEC for various niosome formulations and parameters such as time, concentration, temperature, and the use of transport inhibitors. Both a gastrointestinal (Caco-2/E12) and BBB (RBMVEC/Astrocytes) model were used to determine the transport of the free drug and niosomal formulations through Transwell® inserts.

Results and Discussion: The optimum formulation was obtained with the following conditions: 0.5 mg of drug, 1:1 ratio between cholesterol and Span 80 surfactant (total 150 µmol), 5 µmol of dicetyl phosphate, 10 ml hydration volume, and 30 min hydration time. This resulted in entrapment efficiency of 28.3% for GPE niosomes and 68.1% for cGP niosomes. The size of the bi-ligand niosome after sonication did not exceed 300 nm with a PDI of less than 0.2 and zeta potential of more than -50 mV. The small size means that the niosomes are suitable for uptake into the cells and are the overall formulation is stable due to the negative zeta potential causing repulsion between vesicles. The *in vitro* release studies indicated release of drug from the niosome follows an initial burst release of 50% followed by a slow and sustained release of drug over 48 hours. This release profile fits the Korsmeyer-Peppas model and shows that the release of drug from the niosome is via more than 1 phase. The cytotoxicity studies with Caco-2 and RBMVEC is used to determine the dose range to use for subsequent uptake and transport experiments. Uptake results of the niosomal formulation into Caco-2 cells showed that it was time-dependent, concentration-dependent, temperature dependent and the mechanism of uptake is partially via adsorptive-mediated endocytosis pathway. Uptake of the niosomal formulation into RBMVEC showed it was time-dependent, concentration-dependent, temperature dependent and the mechanism of uptake is partially via active transport, adsorptive mediated transport and clathrin mediated transport. Importantly, when free drug uptake is compared to bi-ligand niosome uptake there was 2.5 times more GPE and 3 times more cGP found in the cells when delivered using niosomes. Also, the RI7 ligand only improved uptake into RBMVECs but not Caco-2 cells, whereas the PLR ligand significantly improved uptake into both cell types. Transport experiments utilising a Caco2/E12 gastrointestinal model and RBMVEC/Astrocyte BBB model were carried out, but no detectable amount of drug was found in the basolateral compartment in both models. This suggests that even though uptake of drug into cells was successful, transport of drugs across the cell was not, which could be due the significant degradation of the drug.

Conclusion: This project was meant to develop an optimised novel niosomal delivery system to entrap a wide range of hydrophilic or lipophilic drugs for delivery across the BBB. Successful optimisation, characterisation, and fabrication of the novel bi-ligand niosomes that can entrap both GPE and cGP was achieved. Niosome with both ligands significantly improved GPE or cGP cellular uptake into both Caco-2 and RBMVEC cells, however no detectable amounts of drugs was observed through the cells during transport studies. Further investigation

and correlation with an animal model is required to prove the BBB transport ability of this novel delivery system.

Acknowledgements

First and foremost, I would like to express my sincere gratitude to my supervisor Associate Professor Jingyuan Wen, for her support, advice, and guidance. She was integral in completing my PhD, for her encouragement, patience and enthusiasm is invaluable. There are not enough words about how grateful I am by the opportunities and experiences that were only possible due to her. In my opinion, she goes above and beyond for her students, and I have been given an amazing memory that will never be forgotten. Thank you as well, my co-supervisor Associate Professor Jian Guan as she has given me lots of valuable insight into the brain science and associated areas.

I would also like to acknowledge everyone in A/P Jingyuan Wen's research group like Sanjukta Duarah and Shuo Chen for their great support. Marvin Mengyang Liu and Naibo Yin are of special mentions from the group as they have assisted me with countless tasks, discussions with both intellectual and emotional support. The lab technician Cathy Li have also helped immensely with various orders and equipment and general support.

I am grateful to the University of Auckland and School of Pharmacy as there are countless people who have helped me either by answering a question or just lending an ear. In particular, I would like to thank Associate Professor Suresh Muthukumaraswamy for his help and advice throughout my study. Special thanks to Associate Professor Darren Svirskis, Associate Professor Zimei Wu and Dr. Manisha Sharma have all been great mentors who provided me with lots of encouragement and support.

I would like to specially thank my family and close friends for their support and unconditional love. There are many people who I have likely not specifically gave acknowledgement to, but I still greatly appreciate you and the help you provided me.

Table of contents

List of Abbreviations

AD	Alzheimer's disease
ANOVA	Analysis of variance

ASA	Arylsulfatase A
BBB	Blood Brain Barrier
BCA	Bicinchoninic acid
BP	British Pharmacopeia
Caco-2	Human colorectal adenocarcinoma
CCD	Central composite design
CH	Cholesterol
CNS	Central nervous system
CPP	Cell-penetrating peptides
CV	Coefficient of variation
DCP	Dihexadecyl phosphate
DDS	Drug delivery systems
DLS	Dynamic Light Scattering
DMEM	Dulbecco's Modified Eagle Medium
DMSO	Dimethyl sulfoxide
DNA	Deoxyribonucleic acid
DOE	Design of experiments
DSC	Differential scanning calorimetry
DSPE-PEG	1,2-distearoyl-*sn*-glycero-3-phosphoethanolamine-N-amino(polyethylene glycol)
EDC	N-(3-Dimethlaminopropyl)-N'-ethyl carbodiimide hydrochloride
EDTA	Ethylenediaminetetraacetic acid
EE	Entrapment efficiency
EGF	Epidermal growth factor
E12	HT29-MTX-E12

FBS	Fetal Bovine Serum
FTIR	Fourier transform infrared spectroscopy
GI	Gastrointestinal
GIT	Gastrointestinal tract
GLUT	Glucose transporter
GP	Glycine-proline
GPE	Glycine-proline-glutamate
HB	Heparin binding
HBSS	Hanks balanced salt solution
HPLC	High performance liquid chromatography
IC_{50}	Half-maximal inhibitory concentration
ICH	International Conference on Harmonisation
IGF	Insulin growth factor
LDL	Low-density lipoprotein
LOD	Limit of detection
LOQ	Limit of quantification
LRP	Lipoprotein receptor-related proteins
MA	Monoclonal antibodies
MTT	5-diphenyl tetrazolium bromide
NEAA	Non-Essential Amino Acid Solution
NHS	N-hydroxy succinimide
NP	Nanoparticles
PBS	Phosphate buffered saline
PD	Parkinson’s disease

PDI	Polydispersity index
PLA	Poly-lactic acid
PLGA	Poly(lactic-co-glycolic acid)
PLR	Poly-L-arginine
RBMVEC	Rat brain microvascular endothelial cell
ROS	Reactive oxygen species
RP	Polar-RP C18 Column (250 x 4.6 mm; 4.0 μm particle size)
SATA	Succinimidyl-S-acetylthioacetate
SLN	Solid Lipid Nanoparticles
TAT	Transactivator of transcription
TEER	Transepithelial electrical resistance
TFA	Trifluoroacetic acid
UV	Ultraviolet
VIP	Vasoactive Intestinal Peptide
WHO	World Health Organization

List of Figures

List of Tables

List of Equations

Chapter 1
General Introduction

1.1. Neurodegenerative Diseases

1.1.1. Background

Neurological disorders affect hundreds of millions of people worldwide, with numbers quickly rising. Alzheimer's disease (AD) and Parkinson's disease (PD) are the two most common neurological disorders with huge health burdens on society. Dementia is expected to double every 20 years to an estimated 139 million worldwide in 2050 (1). Treatment options for people living with neurological disorders are limited in scope and application. Majority of these diseases are immedicable with great physical, mental, and social implications to the individual.

Patients with AD develop amyloid plaques and neurofibrillary tangles causing cerebrovascular damage, microglial and astrocyte activation as well as overall neurotoxicity. This results in cognitive decline, chronic neurodegeneration and neuroinflammation. Patients with PD have progressive loss of neuronal cells that produce dopamine in the substantia nigra. Dopamine controls the body's movements, and as a result, patients with PD can develop tremors, have impaired reflexes and experience slower, rigid movements (2,3). The loss of neuronal cells also elicits an immune response from the body, and neuroinflammation is prevalent and problematic. A common result of these neurodegenerative diseases is loss of function due to neuronal cell death. The etiology and pathogenesis of neurodegenerative diseases consist of both genetic and non-genetic components developed through complex mechanisms that are still not yet fully understood. These incurable diseases are exhibited in people through impaired memory, cognition and/or movement. The major risk factors of neurodegenerative diseases include oxidative stress, genetics, and ageing, making it increasingly crucial for ageing populations of New Zealand and the general global population. In fact, the World Health Organization (WHO) predicts that in about 20 years, neurodegenerative diseases with major motor function influence will overtake cancer as the second-most prevalent cause of death (3).

The main pathways to neurodegenerative damage Include but is not limited to: Reactive Oxygen Species (ROS) generation, neurotoxic oligomers, mitochondrial dysfunction, metal accumulation, genetic factors, and deposition of amyloid fibrils (as shown on Figure 1.1). Some of these pathways are specific to some diseases; for example, amyloid fibril deposition is

directly related to AD progression. The amyloid cascade hypothesis suggests dysfunction and, by extension, cognitive defects in AD patients is triggered by the binding (and subsequent deposition) of amyloid-beta aggregates to both neuronal and non-neuronal membranes. Even though this is widely accepted as the main causative factor to the progression of AD, recent research has attributed many of the neurotoxic effects to small oligomeric species (2). In addition, the presence of ROS can result in significant oxidative stress that can damage glial and neuronal cells, which are particularly sensitive to ROS. Other causative factors include impaired mitochondrial function, which has been found to be a key factor in neurodegeneration. The excessive presence of metals like copper, zinc, lead or iron can create ROS and dysfunction in the mitochondria. Also, AD progression, specifically, is affected by impaired brain glucose metabolism (3). These all play a critical role in the pathophysiology of neurodegenerative diseases, particularly AD and PD. The multiple potential causative pathways for many of the neurodegenerative diseases makes it increasingly difficult to develop an effective therapy. This is further complicated by the difficulty of determining the onset of disease as significant damage could already have been done before the first signs of neurodegenerative symptoms even begin to appear (4).

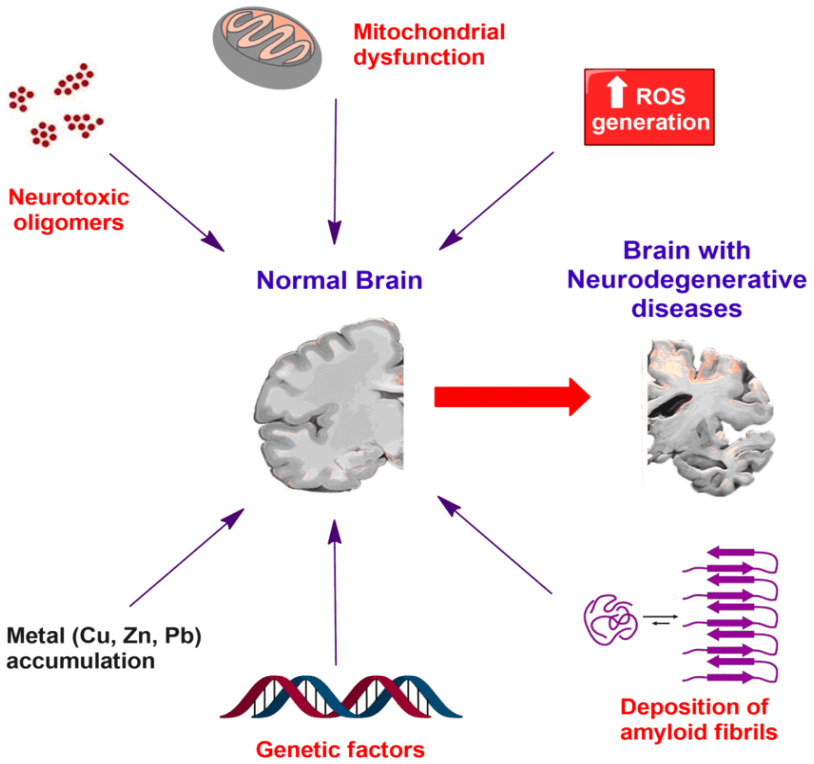

Figure 1.1. Demonstrates various mechanisms of neurodegeneration which lead to neurodegenerative diseases **(5)**.

Current treatments of neurodegenerative diseases can only manage symptoms or slow down disease progression. The treatment options for various neurodegenerative diseases are limited, often due to the requirement of the drug or treatment to reach the affected neuronal cells. There has been plenty of data published on various compounds or treatments that have successfully improved neuronal function or outright repaired neuronal cells, but many of these treatments have no practical pathway to the central nervous system (CNS). This typically means that invasive procedures such as intracranial injection must be used to deliver the drug, as even intravenous administration does not result in any appreciable amount of drug in the brain. Current treatments require consistent long-term dosing, and this means uncomfortable and invasive treatments would likely not be adhered to as well. The need for non-invasive treatment options is rising, and the most accepted of which is the oral route. A considerable amount of research has been done on compounds with neuroprotective effects so that they may attenuate neurodegenerative progression. The neuropeptide drugs glycine-proline-glutamate (GPE) and cyclic-glycine-proline (cGP) have demonstrated potent neuroprotective properties in many animal models of neurodegenerative diseases, including AD and PD models. Guan et al reported that cGP treatment not only reduced both caspase-3 mediated apoptosis and microglial activation but also enhanced astrocytic reactivity (6). Baker et al also reported that GPE could also reduce neuronal loss from hypoxic-ischemic brain injury following central administration and oral administration using microemulsion delivery system (7).

1.1.2. Peptides

Natural peptides are short amino acid monomer chains organically found in the environment that have gained a large amount of interest as therapeutic agents over the last decade. Peptides exert their pharmacological effect in various ways, but the process typically begins with binding to cell surface receptors or other proteins to trigger an intracellular or extracellular mechanism. Most natural peptides have predictable metabolism, high selectivity with good safety and efficacy. This means a shorter time to market, higher potency, and good patient tolerability. The main hurdle in the widespread adoption of peptides as drug candidates is their low bioavailability due to the chemical and physical instability of the peptide structure and low membrane permeability. This not only alters the peptide absorption and transport across the gastrointestinal tract (GIT) but also the BBB. These problems typically lead to a short half-life, fast elimination, and poor oral bioavailability (8).

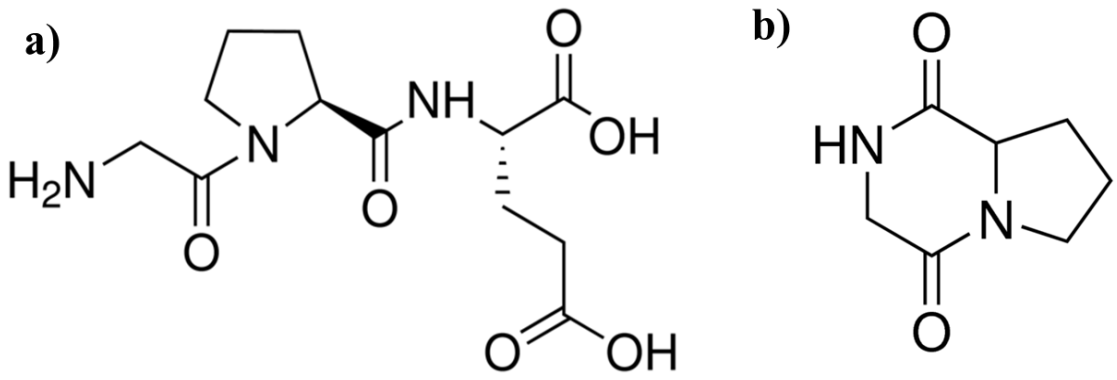

Figure 1.2. The chemical structure of a) GPE and b) cGP.

Insulin growth factor-1 (IGF-1) naturally forms bioactive metabolites, GPE and cGP as shown in Figure 1.2. Their neurotrophic functions are mediated by improving IGF-1 bioavailability through competitive binding to the IGF binding proteins represented in Figure 1.3 (9). IGF-1 is a neurotrophic hormone that has a vital role in CNS development, function, and homeostasis with significant neuroprotective effects on damaged cells in the brain. Unfortunately, the pharmaceutical application of IGF-1 has been problematic due to its high molecular weight and limited central uptake, caused by the physical and enzymatic barriers. GPE is a small, hydrophilic compound with poor enzymatic stability and limited penetration across the Blood-Brain-Barrier (BBB) (10). Alternatively, cGP is a small, stable, and orally bioavailable compound with the ability to cross the BBB. However, the effective dose of cGP is about 1000 times higher for the peripheral administration than that of central administration, due to the extensive protein binding issues in the peripherals and the BBB (8). Both GPE and cGP have powerful neuroprotective effects but cannot be significantly delivered to the brain through either oral or parenteral routes of administration (11).

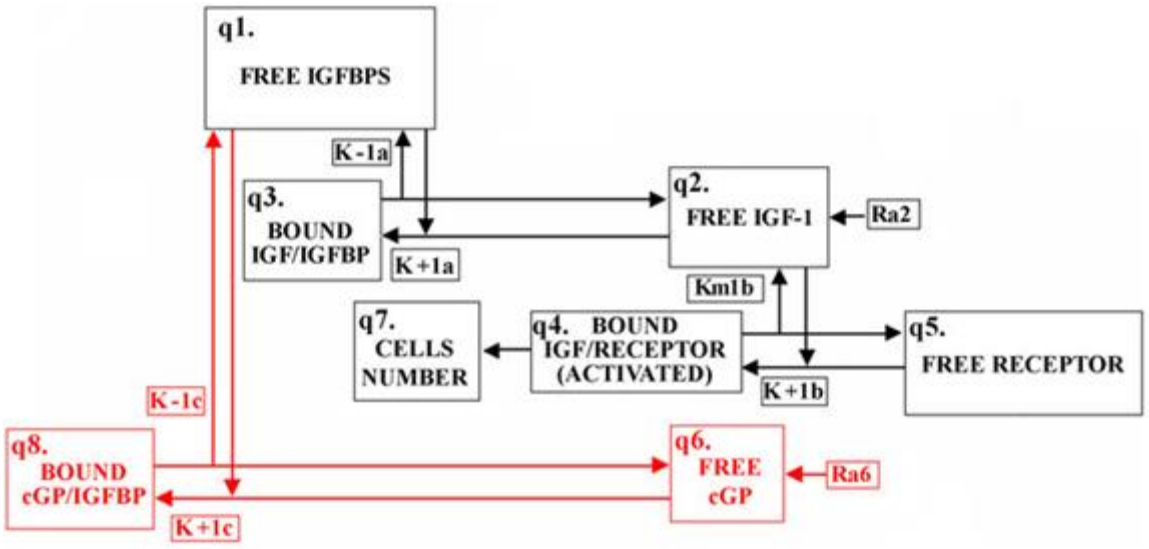

Figure 1.3. Schematic representation of the IGF-1 competitive inhibition with cGP, demonstrating the main mechanism by which the peptides exert their action **(12)**.

The two most common routes of administration to deliver peptides to their desired sites of action include oral and parenteral delivery. Unfortunately, many peptide drugs have insufficient oral delivery to the brain due to the low stability in the GIT and low membrane permeability across both the intestinal membranes and the BBB (13). The general oral bioavailability issues are mainly due to the physical and enzymatic barriers present on the GIT, drug metabolism and drug elimination (14). Due to peptides degradation in the GIT, parenteral delivery is often explored to avoid excessive degradation. Absorption after parenteral delivery is rapid, and, in general, blood levels attained are more predictable than those achieved by other routes. However, parenteral delivery is profoundly invasive, painful, and inconvenient, that places a significant burden on patients as injections are uncomfortable and difficult to be self-administered. This problem is only worsened by the fact that many neurological disorders are chronic in nature, meaning consistent and repeated doses are required to be administered over an extended period of time (15). Oral delivery is preferred over parenteral delivery as it is non-invasive, avoids pain and discomfort, eliminates the risk of infection, and has a high degree of patient compliance. For systemic absorption of neuropeptide drugs, it must pass from the site of administration across the intestinal epithelial cells to the peripheral bloodstream then to the BBB for brain uptake. The following section will focus on the main barriers to be overcome to successfully deliver the neuropeptides, highlighting the potential strategies utilising variable receptor pathways and formulation systems to improve the absorption and penetration via oral administration.

1.2. Gastrointestinal Barrier

The key role of the GIT is to digest and absorb nutrients while protecting the human body against harmful agents (16). To achieve this, the GIT has a few specialised routes of absorption and many protective mechanisms against potential pathogens, antigens, or toxins. The main pathways of drug absorption are paracellular, transcellular, and receptor-mediated transcytosis, as shown in Figure 1.4 (17). The paracellular pathway is the transport of molecules across the epithelium by their passage through the intercellular space between the cells. It is classified as a passive transport mechanism that is reliant on a concentration gradient and usually restricted to small (<100-200 Da) hydrophilic molecules (18). The transcellular pathways can either be an active or a passive process and is the transport of molecules through the cell across the apical and basolateral membranes (19). Receptor-mediated transcytosis is an active molecular transport process by which intestinal epithelial cells absorb various proteins, metabolites, or hormones by receptor recognition (20). The two main challenges of GIT absorption are physical and biochemical barriers, with drug metabolism and drug elimination being contributing factors as well.

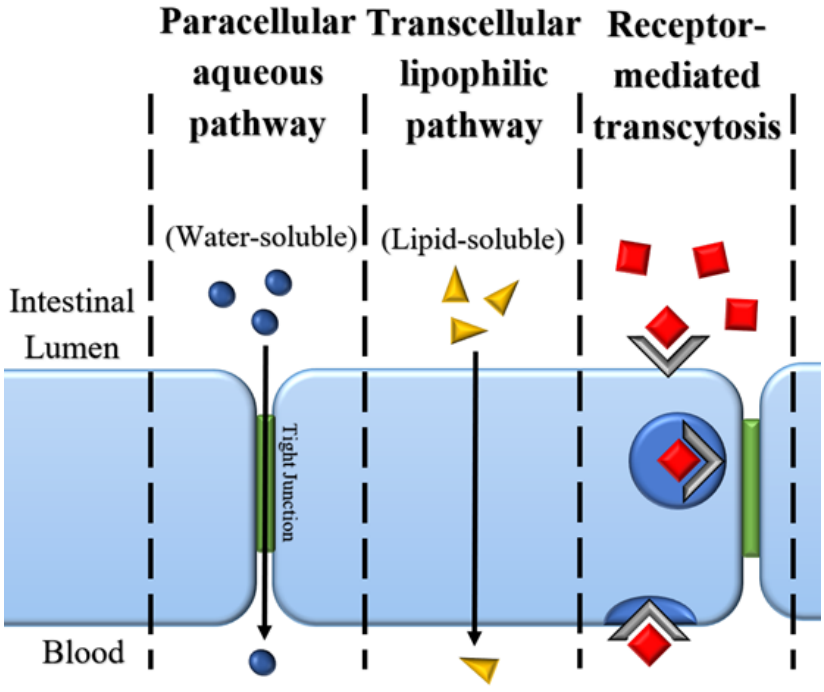

Figure 1.4. Schematic diagram of the various pathways of drug transport across the GIT.

Cell membranes and the tight junctions make up the cell lining, and along with the mucus layer and efflux systems, they create the GIT physical barrier (21). The presence of a stagnant aqueous layer consisting of water, mucus and glycocalyx inside the GIT creates the unstirred water layer. This layer can prevent large peptides from reaching the epithelium but is otherwise of limited significance in the absorption of molecules (22). A combination of enterocytes, goblet cells, endocrine cells and Paneth cells make up the single layer of intestinal epithelium (9,11). These cells are connected by tight junctions and create a rigid physical barrier that is semi-permeable due to the cellular phospholipid bilayer (23). The tight junctions, adherens junctions and desmosomes make up three parts of the intercellular junctional complexes (24). Tight junctions are the only occluding junctions and contain fenestrae of widths between 3 to 10 Å (23). These tight junctions are selectively permeable and are regulated by several compounds to alter their permeability (25). On the apical surface, there are also P-glycoprotein efflux pumps that actively pump molecules back into the GIT lumen, reducing overall absorption of specific drugs. Thus, efflux systems in combination with the physical barrier and intracellular metabolism can significantly alter the oral bioavailability of peptide drugs like GPE and cGP (26).

Biochemical barriers present in the GIT cause instability in peptides like GPE and cGP due to the presence of high pH, enzymes and/or microorganisms. Proteolytic enzymes are abundant throughout the body and can degrade unprotected peptides (27,28). The pH-dependent hydrolysis of drugs occurs throughout the GIT as the pH of the intestinal fluids varies significantly. Also, microorganisms found in the colon are capable of deglucuronidation, decarboxylation, reduction, hydrolysis, and dihydroxylation reactions, all of which can lead to the degradation of peptides. Specifically, there are a range of aminopeptidases and carboxypeptidases that facilitate the breakdown of the peptide at the terminal ends and endopeptidases can cleave peptides at specific sites within the peptide. After overcoming the GIT barriers, peptides need to be delivered across the BBB and target the brain (29,30).

1.3. Blood Brain Barrier (BBB)

The more important barrier for GPE and cGP delivery to the brain is the BBB (31,32). There are physical and enzymatic barriers present on the BBB that prevents many compounds from crossing, which includes many peptides (32,33). The BBB is composed of brain capillary endothelial cells, pericytes, astrocytes and neuronal cells. The key functions of the BBB include maintaining ion homeostasis, preserving neural connectivity, preventing neurotoxic molecules from crossing the BBB and transporting essential nutrients and molecules to the brain (32). The asymmetrical arrangement of the membrane-bound transport systems on the apical and basolateral surfaces of the endothelium is essential to its function. In particular, P-glycoprotein efflux pumps on apical surfaces can protect the brain from harmful or unwanted compounds (32,33).

Brain capillary endothelial cells are characterised by the continuous tight junctions connecting the cells together (32). These tight junctions as well as adherens junctions between adjacent endothelial cells on the apical side of the BBB create a physical barrier that prevents paracellular transport to the brain (32,33). The tight junctions between brain capillary endothelial cells have extremely high transendothelial electrical resistance and as such, these membranes are highly resistant to passive diffusion (3,33). Almost 100% of macromolecular drugs and 98% of the small lipophilic drug candidates are unable to cross the BBB, with small lipophilic (<500 Da) nutrient molecules being the exception (33,34). An additional metabolic barrier is present on the BBB due to the presence of various intracellular and extracellular proteolytic enzymes (3,32). This combination of characteristics makes the BBB very difficult to overcome. That is why researchers are utilising ligands to target specific transporters and carrier systems that can facilitate the uptake and transport of the drugs across the BBB (3,32).

The main pathways of drug transport across the BBB are the transcellular pathway, receptor-mediated transcytosis, adsorptive transcytosis, and the use of transporter proteins, as shown in Figure 1.5 (35). The enzymatic barrier makes it increasingly difficult to deliver certain drugs to the brain as there are many proteolytic enzymes on the surface. Some success has been seen when researchers delivered compounds across the BBB by utilising certain receptors that are overexpressed on the BBB (36). The most common receptors for brain delivery include transferrin receptors, insulin receptors, low-density lipoprotein receptor–related proteins, diphtheria toxin receptors, heparin-binding EGF-like growth factors and

leptin receptors (33). Glutathione and Choline transport proteins are also very prevalent on the BBB and have been used for drug delivery (33). Ligands that improve BBB penetration and can be divided into two categories: active targeting ligands and cell-penetrating peptides (CPP). To maximise brain uptake and targeting, various researchers have utilised multiple ligands in a single delivery system (36,37).

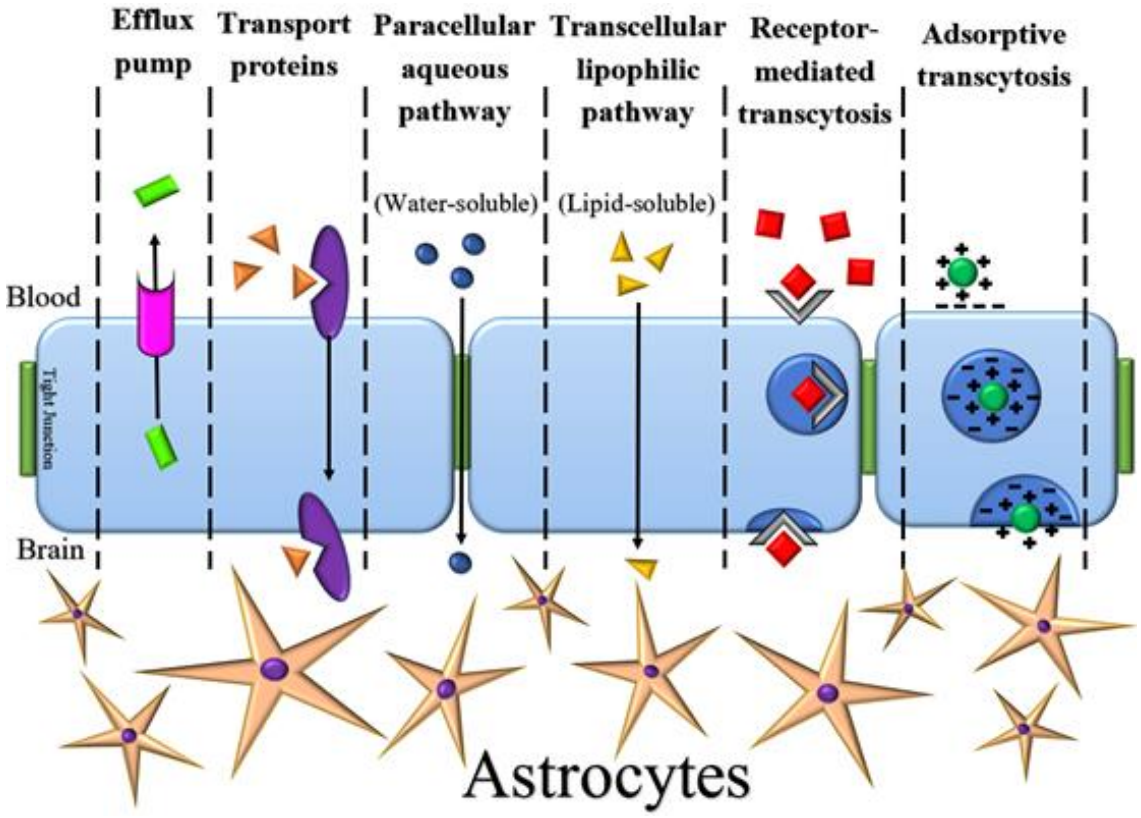

Figure 1.5. Schematic diagram of the various pathways of drug transport across the BBB.

1.3.1. Brain targeting ligands

One of the most promising ways to non-invasively improve oral drug delivery to the brain is to utilise active targeting ligands specific towards the BBB. These ligands have moieties that attach to and are complex with receptors on endothelial brain cells and assist with transport across the BBB. Various transport mechanisms can be employed, such as receptor mediated transport, carrier-mediated transport, or adsorptive mediated endocytosis (37). Previous studies demonstrated that dual ligand modification with a drug delivery system significantly increased penetration than with the use of just a single ligand (38,39). The use of a drug delivery system and hence protection of the peptide lessens the need for utilising

specific enzyme inhibitors that can potentially prevent the breakdown of peptides in the body. Only a few ligands with good potential and data have been selected to be discussed in this review.

1.3.2. Receptor-mediated transport

1.3.2.1. Transferrin receptor

The transferrin receptor is a transmembrane glycoprotein consisting of two linked 90 kDa subunits, which can bind to a transferrin molecule and transport iron via receptor-mediated transcytosis (33,40). Transferrin is an important molecule for cell proliferation and essential for iron homeostasis that strongly, but reversibly binds to iron on two high affinity Fe (III) binding sites. There are two isotopes of the transferrin receptor 1 (TfR1) and 2 (TfR2). TfR1 regulates intracellular iron levels with a greater affinity to iron than TfR2, which only maintains iron levels within the body. TfR1 delivers iron into the cells through an endocytic process known as the transferrin cycle, where after binding and releasing the iron into the cell, the iron-depleted TfR recycles itself to the cell surface.

The transferrin receptor is the most widely researched receptor for BBB targeting and is highly expressed in erythroid cells, placental tissue, and highly proliferating cells like brain endothelial cells. However, there are concerns about utilising transferrin as a ligand because of the high endogenous transferrin concentrations that nearly saturate the transferrin receptors, resulting in competition with endogenous transferrin (33). Nonetheless, success has been reported by Mishra *et al*., who use transferrin-PEGylated nanoparticles to deliver about 20% of an injected dose to the brain (40). Because of the size and competitive binding limitations of utilising transferrin, relatively smaller monoclonal antibodies (MAbs) with a higher affinity towards transferrin receptors than endogenous transferrin are utilised instead (41). MAbs basic structure consists of two heterodimeric transmembrane glycoproteins bound on a transferrin receptor, which is where transferrin binds to and transports iron via transcytosis. The most common MAbs with a high affinity to the transferrin receptors are OX26, 8D3 and RI7 (42,43). OX26 is the most well-known MAb and specifically binds to the rat transferrin receptor. It is thought to be only active in rat species (33,44). It was reported that in a mouse study, approximately 3.1% of the injected dose reached the brain when utilising the 8D3 MAb, and only 1.6% was achieved with RI7 whereas OX26 exhibited a negligible 0.06% uptake. Both 8D3 and RI7 MAbs are suitable for mouse brain uptake studies, but the RI7 MAb has

increased selectivity to the brain, as the liver and kidneys do not retain the ligand as much (33,44). Alata *et al*. confirmed the unidirectional and fully saturable mechanism of transferrin MAb, specifically RI7 across brain capillary endothelial cells in mice (44). Paris-Robidas *et al*. utilised quantum dots with the RI7 ligand showed that therapeutically relevant concentration of the target molecule can be transported inside brain capillary endothelial cells, indicating that the ligand is a good vector (45). The RI7 ligand seems the most promising as it has good penetration with the highest selectivity, to minimise the drug release of the neuropeptides in other parts of the body, potentially reducing any side effects (44,45).

1.3.2.2. Lactoferrin receptor

The Lactoferrin receptor consists of two identical transmembrane proteins (homodimer) that facilitate the transport of lactoferrin, which is found throughout the body, including the BBB (46). Lactoferrin is a single-chain cationic iron-binding glycoprotein belonging to the transferrin family with anti-inflammatory, antimicrobial and immunomodulatory functions (46,47). There are two binding sites on the lactoferrin receptor, where one is high affinity and the other is a low affinity binding site (48). Lactoferrin receptors have varying size and characteristics on different cell types, including the BBB, indicating the possibility to develop a selective lactoferrin receptor ligand (49). Transferrin and lactoferrin have similar qualities, with lactoferrin having two main advantages: the lower plasma concentration and the unidirectional uptake mechanism into the brain. Lower endogenous concentrations of lactoferrin lead to less competition and interference with the lactoferrin receptors in the body. Ji *et al*. compared lactoferrin to transferrin and OX26 MAb and found lactoferrin to have superior brain uptake (50). Huang *et al*. demonstrated that Lactoferrin modified nanoparticles are transported with both receptor and adsorptive mediated mechanisms that efficiently cross the BBB (51). Lactoferrin may be of interest in the treatment of neurodegenerative diseases as the expression of the lactoferrin receptor on the BBB is overexpressed in several neurological conditions like Alzheimer's disease, Parkinson's disease, and Huntington's disease (52,53).

1.3.2.3. Insulin receptor

The insulin receptor present on the BBB is a transmembrane receptor belonging to a large class of tyrosine kinase receptors, delivering insulin to the brain via transcytosis (52). The insulin receptor is about ~300 kDa and has 2 alpha-subunits and two beta subunits with a disulphide bond between alpha and beta, creating a cylindrical structure. When insulin binds, a conformational change occurs, enabling tyrosine kinase activity and receptor internalisation (42). Utilising insulin as a ligand has two significant problems, insulin degradation in the bloodstream with a half-life of 10 minutes and interference with natural insulin causing hypoglycaemia. These limitations can be addressed with utilisation of peptidomimetic MAb against the human insulin receptor, which has been investigated (42,54). Wu *et al*. reported the relatively high drug uptake utilising the human insulin receptor targeting ligand MAb 83-14, with about 4% of the injected dose being delivered to the brain (54). However, this MAb was not effective in rats and was only evaluated in old-world primates (rhesus monkeys). Due to the mouse origin of MAb 83-14, utilisation in humans could lead to various immunogenic responses. To overcome the immunogenicity, a chimeric antibody has been made with 85% human origin and 15% mouse origin and another being a fully humanised form. Humanisation of the antibody had about a 27% decreased affinity but can be directly applied to human patients, with lower side effects (55). Kuo *et al*. developed promising solid lipid nanoparticles modified with MAb 83-14, poloxamer 407 and tween 80, not only successfully enhanced BBB permeability but also promoted endocytosis function into human brain-microvascular endothelial cells (56). Utilisation of the insulin receptor may have decent potential in overcoming the BBB. The widespread expression of the insulin receptor on peripheral organs may limit its applicability with potential toxicity (57).

1.3.2.4. Low-Density Lipoprotein receptor-related protein

Lipoproteins bind to both the low-density lipoprotein receptors (LDL-R) and the low-density lipoprotein receptor-related proteins (LRP) to facilitate their transport via endocytosis (58,59). On the surface of the BBB endothelium, LDL-R are upregulated when compared to the peripheral endothelium, indicating a potential target for drug delivery. LDL's have a highly hydrophobic core with a hydrophilic shell exhibiting multimodal loading capacities with the ability to embed compounds of different affinities into the structure. Angiopep-2 is a 19-amino acid ligand for the LRP-1 receptor exhibiting high transcytosis capacity, able to bypass the P-glycoprotein efflux pump (33,57). Demeule *et al*. determined angiopep-2 to have superior

transcytosis capacity and parenchymal accumulation when compared to transferrin, lactoferrin and avidin (60). Current research suggests that utilisation of Angiopep-2 depends on the cargo as well because attachment on the drug molecule was found to have good penetration but attachment on a nanoparticular delivery system found little penetration (13,61). A comparative study carried out by van Rooy *et al*. showed that both angiopep-2 and COG133 conjugated to liposomes do not significantly target the mouse brain *in vivo* (62). Böckenhoff *et al*. found that TAT and angiopep-2 conjugated arylsulfatase A (ASA) showed insignificant transport to the basolateral membrane of the BBB whereas Apolipoprotein B and E significantly transported ASA across to the basolateral side. Both Apolipoprotein E (apoE) and Apolipoprotein B (ApoB) are proteins that facilitate the transport of lipids from the plasma to the CNS utilising LDL-R and LRP (63). Native low-density lipoproteins like ApoB are not suitable as they are difficult to isolate in large quantities and are variable in size and composition. ApoE and ApoB have proven efficacy but inherently experience protein instability and competition with LDL, and therefore, Laskowitz *et al*. developed COG133 as an apoE-mimetic peptide as an attractive smaller alternative (64). The lack of brain specificity and stability issues of these ligands are a major concern when attempting to orally deliver compounds to the brain.

1.3.2.5. Heparin-binding EGF-like growth factor

The heparin-binding epidermal growth factor-like growth factor (HB-EGF) is naturally found in the BBB, neurons, and glial cells to stimulate growth and differentiation (33,61,65). This transmembrane protein has no known endogenous ligands, but the diphtheria toxin can bind to it and enter the cell by endocytosis (33,66). Diphtheria toxin enzymatically blocks protein synthesis, causing cell death, so it cannot be directly used as a ligand (61). The Cross-reacting material-197 (CRM197) is a non-toxic mutated diphtheria toxin that lacks the enzymatic ability of diphtheria toxin but retains its binding capacity to HB-EGF (61). CRM197 has been extensively used as a carrier protein to deliver human vaccines safely and effectively Because of this, there is a large pool of information on this ligand including but not limited to its structure, transport receptor and mechanism of action (65). Gaillard *et al*. demonstrated *in vitro* targeting of CRM197 utilising a liposomal CRM197 (67). Wang *et al*. research group were able to successfully deliver microvascular endothelial cells to brain and determined that it can up-regulate caveolin-1 expression mediated by glucose transporters (GLUT)activity improving caveolae-mediated transcytosis that is possible to promote CRM197-targeted

delivery (68). The HB-EGF is upregulated in many inflammatory conditions caused by various brain diseases, meaning it may be a useful receptor for site-specific disease targeting. *In vivo* studies with the diphtheria toxin were successful with guinea pig models, but not rats or mice due to an amino-acid substitution in the receptor binding domain (65,66). Although transgenic mice expressing human HB-EGF are available for experimental purpose, A potential complication of utilising CRM197 is the individual antibodies against diphtheria toxin, which may reduce the efficacy of the drug delivery system with long-term application being unclear (57,65). CRM197 is still toxic, but with only about 100-fold less potency than the wild form of diphtheria toxin.

1.3.3. Transport-mediated transport

Many nutritive materials required by the brain are delivered by transport-mediated transporters, such as glutathione transporters, choline transporters, hexose transporters, and amino acid transporters (69,70). Both glutathione and choline transporters are highly expressed on the BBB and are the most widely researched transport-mediated transporters (69). The abundant endogenous tripeptide glutathione is delivered to the brain via glutathione transporters (69). To maintain cellular redox homeostasis and suppress oxidative stress, glutathione is an important cellular antioxidant (71,72). Rip *et al*. reported a 4-fold increase in drug brain accumulation comparing glutathione PEGylated liposomes to unmodified liposomes (73). Rotman *et al*. demonstrated the effectiveness of glutathione with their liposomal delivery system providing a 10-fold higher uptake into the brain, when compared to free drug. Rotman *et al*. also found significantly improved penetration of a single domain antibody in Alzheimer's disease mouse model utilising glutathione pegylated liposomes, when compared to free drug (74). Lindqvist *et al*. also utilised glutathione pegylated liposomes and reported double the drug uptake into the brain without using a specific brain targeting ligand (75). Geldenhuys *et al*. developed glutathione-coated nanoparticles that exhibited significantly higher brain uptake when compared to drug solution (76). Utilisation of glutathione as a ligand for brain delivery seems promising with its excellent long-term safety profile and biocompatibility but is relatively non-specific to brain delivery when compared to other ligand options (77).

An essential neurotransmitter, acetylcholine, requires choline which is transported to the brain via choline transporters to synthesise the neurotransmitter acetylcholine (69).

Choline itself is not suitable to modify into a ligand so Li *et al*. developed bis-quaternary ammonium compounds with a high affinity for the choline transporter (78,79). These bis-quaternary ammonium compounds effectively delivered across brain capillary endothelial cells and (exhibited both *in vitro* and *in vivo* difference) higher gene expression when delivering plasmid deoxyribonucleic acid (DNA), suggesting a targeted brain delivery (78,80). The choline derivative compounds seem promising, although the amount of research in improving brain delivery is limited (69,79).

Glucose is an essential fuel for the brain requiring its own transporters known as the GLUT transporters, which facilitate the transport of glucose from the blood to the brain (70). This is because neurons are unable to synthesise or store glucose, which is necessary for function. GLUT1 and GLUT3 are the main transporters in the mammalian brain, both being approximately equal in the brain. GLUT1 helps facilitate glucose from blood to the extracellular spaces in the brain while GLUT3 is the major neuronal GLUT that helps transport from the extracellular space to the neurons (81,82). Qin *et al*. prepared novel glycosyl derivatives of cholesterol that exhibited more than a 3-fold increase in drug concentration of the glycosyl liposomes compared to the base liposomes (82). Jiang *et al*. developed promising D-glucose functionalised nanoparticles that significantly improved the transport of nanoparticles across the BBB, both *in vitro* and *in vivo* (83). Gromnicova *et al*. developed glucose coated gold nanoparticles that had increased selectivity in the brain as there was three times higher transport of the drug in human brain endothelium rather than non-brain endothelium (84). Dufes *et al*. developed glucose-functionalised niosomes and demonstrated 86% drug uptake into the brain after 5 minutes of treatment (85). There are a few concerns with different pathologies like Alzheimer's and hyperglycaemia where the number of GLUT receptors may change, but overall, these glucose-targeting ligands may be an effective method for brain delivery (81).

1.4. Cell-penetrating peptides

CPPs are a broad and diverse set of peptides that are usually small (~30 amino acid residues) peptide chains that can ubiquitously cross cellular membranes without needing receptors (33,86,87). Back in 1988 the first evidence for CPP's originated from Green *et al*. demonstrating that the viral protein TAT can rapidly translocate over the cellular membrane into the cytoplasm (88,89). The mechanism of action is not completely known, but two pathways are suggested with drastically different internalisation efficiency. The two pathways are the direct penetration (energy-independent) and endocytosis (energy-dependent) pathways. The direct penetration pathway utilises the electrostatic interactions between the CPP and hydrogen bonds on the cell membranes for the direct transduction of small molecules across the lipid bilayer. The primary endocytic pathway is pinocytosis which can get large molecules and nanoparticulates across the cell. Depending on the CPP or the CPP-cargo conjugate, it is able to enter the cells via single or even multiple endocytic methods leading to different deposition into the cell (33,86,87).

1.4.1. TAT Peptide

Transactivator of transcription (TAT) derived peptides originate from the human immunodeficiency virus transcriptional activator with the ability to facilitate the transport of large proteins (~480kDa) across the BBB (33,79). It has been suggested that part of the mechanism of entry is due to adsorptive-related endocytosis, direct penetration, and pore formation (86). Cao *et al*. showed when they utilised the death-suppressing molecule Bcl-xl and created a Fusion protein with TAT, it was able to significantly decrease neuronal cell death following ischaemic damage (90). Malhotra *et al*. developed TAT PEG chitosan nanoparticles, which successfully transfected siRNA in an *in vitro* model after 48 hours (91). Gregori *et al*. demonstrated a 3-fold increase in uptake of their nanoliposomes across human brain capillary endothelial cells after attaching the TAT peptide with no difference in the cell viability (92). TAT has also been conjugated with many drug delivery systems with mostly positive results, although its lack of specificity can be a concern (90,93,94).

1.4.2. Penetratin

Derived from the drosophila species Penetratin is capable of facilitating internalisation across epithelial cells in a two-step mechanism (87,95). Penetratin binds to the cell surface lipids by electrostatic interactions and translocated across via tryptophan-induced destabilisation (87,95). In one study by Kamei *et al*., they exhibited a bioavailability increase of insulin from 35% to 50% when co-administered with Penetratin (96). A comparison study on the effects between 3 different CPPs TAT, Penetratin and Mastoparan, on doxorubicin-loaded transferrin liposomes were carried out by Sharma *et al*. (97). They determined that Matoparan had higher cytotoxicity and haemolytic problems while Penetratin and TAT had great biocompatibility. The Transferrin-Penetratin liposomes had more than 90% cellular internalisation of drug with maximum translocation of drug across brain endothelial cells (97). Tseng *et al*. concluded that attaching either Penetratin or TAT to a liposome increased the intracellular accumulation of the liposomes but did not produce any significantly improved drug activity, due to low unloading efficiency (98). There are mixed conclusions on the final outcomes of penetration, so it should be considered with caution.

1.4.3. Poly-L-arginine

Poly-l-arginine is a synthetic peptide consisting of 8 or more arginine residues as shown in Figure 1.6 and it is the most readily available and widely used peptide in various drug delivery systems (78,99). It was determined that nonamers of arginine have improved penetration when compared to their truncated analogues and lysine counterparts (78,100). Cationic amino acids like arginine adsorb onto the phospholipid membrane of the cell not only by electrostatic interaction but also by polarisation forces causing surface rearrangements (78). An early study by Westergen and Johansson studied three compounds Poly-L-arginine, Poly-L-lysine and protamine comparatively, and Poly-L-arginine had the greatest permeability across the BBB (101). Poly-l-arginine has also been utilised in gene delivery and has been largely successful in improving transfection, but only on certain cell types (102,103). Sharma *et al*. developed a bi-ligand liposomal system that investigated the distribution of the liposomes in different organs in rats. It was found that the addition of Poly-l-arginine significantly improved uptake into highly perfused organs and the brain (15). Poly-l-arginine seems like a promising CPP, although it is not specific to the BBB but does improve penetration across.

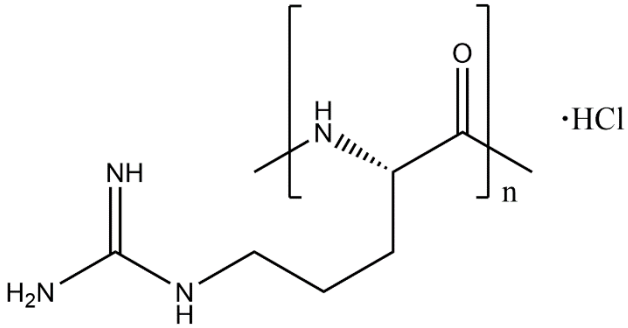

Figure 1.6. The chemical structure of Poly-L-arginine.

1.5. Drug Delivery Systems

Encapsulating the neuropeptides (GPE or cGP) into a drug delivery system like niosome can overcome protein binding issues and improve their stability and permeability across the BBB. We need to consider the drug delivery systems (DDS) with respect to the application in oral brain delivery. These include polymeric nanoparticles, solid-lipid nanoparticles, liposomes, niosomes, and nanogels. All DDS are with their own advantages and limitations but should be able to be modified for effective brain delivery. These ideal characteristics for brain delivery are a particle size of <100 nm, good stability in the GIT and blood, BBB targeting, nonimmunogenic, nonthrombogenic, scalable, cost-effective and able to incorporate a wide variety of molecules (104). This review is summarised in Table 1.1 by comparing all the drug delivery systems discussed. Other drug delivery systems were not included here either due to their inability to be functionalised by ligands and/or lack of literature for brain delivery.

Table 1.1 Comparison between different drug delivery systems, highlighting the advantages and limitations.

Drug delivery system	Basic components	Advantages	Limitations
Polymeric nanoparticles	Natural or synthetic Polymers.	• Low cost • Easy preparation methods • High stability when compared to their lipid counterparts • High drug release flexibility	• Particle aggregation • Polymer chemical stability • Rapidly cleared by the body
Solid lipid nanoparticles	Solid Lipid, emulsifier, and solvent.	• Increased scope of drug targeting • Long shelf-life • Incorporation of both hydrophilic and hydrophobic drugs • Controlled release	• Rapidly cleared by the body • Particle growth • Unpredictable gelation tendency and unexpected dynamics of polymeric transitions
Liposomes	Phospholipid, cholesterol, and charge stabiliser.	• Biocompatible • Incorporation of both hydrophilic and hydrophobic drugs • Controlled release • Can be functionalised with multiple ligands	• High cost • Phospholipid degradation • Leakage and fusion of encapsulated molecules • Some time-consuming formulation methods

Niosomes	Non-ionic surfactant, Cholesterol, and charge stabiliser.	• Biocompatible • Incorporation of both hydrophilic and hydrophobic drugs • Controlled release • Can be functionalised with multiple ligands • Lower cost than liposomes	• Leakage and fusion of encapsulated molecules • Potential incomplete hydration of surfactants • Some time-consuming formulation methods
Microemulsions	Water, water-insoluble organic compound, and surfactant.	• Incorporation of both hydrophilic and hydrophobic drugs • Long shelf life • High drug loading potential	• High concentrations of surfactants, resulting in incompatibility issues • Limited solubilizing capacity for high melting substances
Nanogels	Hydrogel and cross-linked hydrophilic polymer.	• Biocompatible • High drug loading potential • Tunable swelling, degradation and chemical functionality	• Expensive methodology • Toxicity with trace amount of surfactants or monomers from methodology

1.5.1. Polymeric nanoparticles

Polymeric nanoparticles (shown on Figure 1.7) consist of biocompatible and biodegradable polymers loaded with drugs, within the size range of 10-1000 nm (105,106). Depending on the preparation method, the drug is either dissolved, entrapped, encapsulated or attached to the nanoparticle matrix (107,108). Polymeric nanoparticles are advantageous due to their low cost and easy preparation methods, increased stability of the drug, high flexibility in the drug release parameters, improved efficacy and reduced toxicity of the drug (105,108). The Mononuclear Phagocyte System rapidly clears polymeric nanoparticles from the blood, limiting its distribution in the body; this however is alleviated by size manipulation and surface modification. The most common natural polymers used are chitosan, gelatin, sodium alginate and albumin (105,108). Synthetic polymers are plentiful ranging from Poly-lactide co-glycolides to poly-vinyl alcohol and poly-ethylene glycol (107,108). All polymers suggested for fabrication are non-toxic, biodegradable, and biocompatible. Some common methods of preparation include nanoprecipitation method, solvent evaporation, salting out, emulsion diffusion, and emulsion evaporation (107,108). Calvo *et al*. demonstrated the effectiveness of surface modification on polymeric nanoparticles to increase the half-life and therefore, penetration of the drug delivery system to the brain (109). Cheng *et al*. significantly improved the brain transport of a centrally active peptide utilising polylactic acid nanoparticles (110). Polymeric nanoparticles are easily tuned, with many options in materials and methods, resulting in an effective scalable DDS.

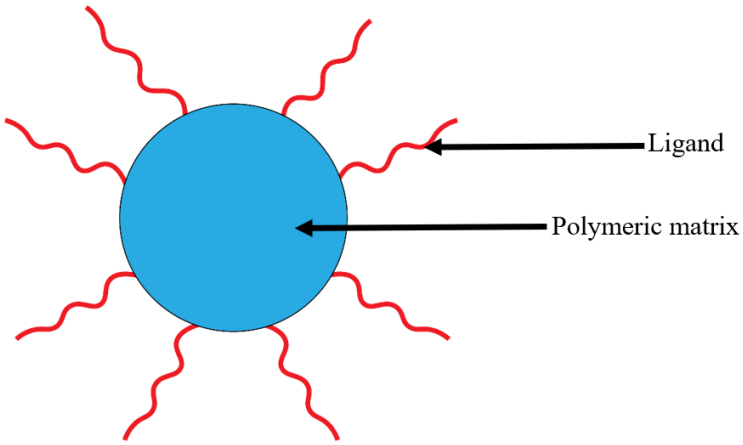

Figure 1.7. Diagram showing the structure of Polymeric Nanoparticles.

1.5.2. Solid lipid nanoparticles

Solid lipid nanoparticles (SLN) (shown on Figure 1.8) are a colloidal drug delivery system with a spherical solid lipid matrix between 10- 1000 nm which are dispersed in an aqueous solution (111,112). The main advantages of SLN are the increased scope of drug targeting, long shelf-life, being able to incorporate both hydrophilic and hydrophobic drugs and controlled release of the incorporated drug for up to several weeks (111,113,114). Similar to the polymeric nanoparticles, a main concern of solid lipid nanoparticles is the uptake into the Mononuclear phagocyte system, which can lead to therapeutic failure. The nanoparticles can be formulated to have a small particle size and with surface modification to avoid the Mononuclear Phagocyte System and improve absorption across both the GIT and BBB (111,113,114). Some challenges of the SLN include the possibility of particle growth, unpredictable gelation tendency and unexpected dynamics of polymeric transitions (111,112). Various preparation methods include, high pressure homogenisation, ultra-sonication/high speed homogenization, solvent evaporation method, solvent emulsification-diffusion method, supercritical fluid method, microemulsion method, spray drying method, emulsion method, precipitation technique and film ultrasound dispersion (111,113,114). Dhawan *et al*. utilised Tween 80 in the quercetin-loaded SLNs to demonstrate the great neuroprotective effects in a mouse Alzheimer's model (115). Mulik *et al*. conjugated transferrin to SLNs and was found effective *in vitro* for the delivery of curcumin (116). Ramalingam & Ko showed that trimethyl chitosan coated SLNs improved the oral bioavailability, brain distribution and stability of curcumin (117). SLNs are suitable for brain delivery as it generally has lower cytotoxicity, higher loading capacity and best production scalability than most other drug delivery systems (111,113,114).

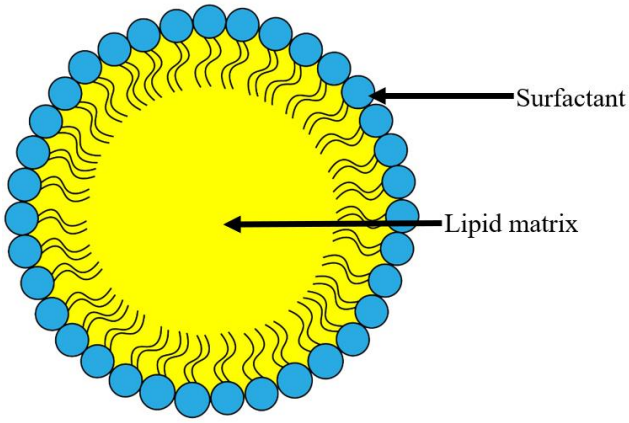

Figure 1.8. Diagram showing the structure of Solid-Lipid Nanoparticles.

1.5.3. Liposomes and Niosomes

Liposomes and niosomes (shown on Figure 1.9) are vesicular drug delivery systems, made up of amphiphilic molecules and cholesterol. Structurally, liposomes and niosomes have a sealed spherical structure typically ranging within the nanometre to micrometre size range (108,118). The amphiphilic molecules are capable of enclosing the surrounding solution to create a bilayer, due to the water-soluble head and hydrophobic tail (119,120). Liposomes and niosomes are similar, except liposomes utilise phospholipids (like phosphatidylcholine and dipalmitoylphosphatidylcholine) as the amphiphilic molecule, and niosomes typically utilise non-ionic surfactants (Tween, Span, Brij etc.). The common method of preparations for both liposome and niosomes are thin film hydration, ether injection, reverse phase evaporation, heating method, homogenisation, freeze-thaw, sonication and extrusion (108,118). Liposomes and niosomes have modifiable characteristics to optimise them for their use, such as the particle size, zeta potential and stability (108,120,121). Vesicular delivery systems of less than 100 nm diameter are ideal for brain delivery although larger sizes have demonstrated good efficacy. There is also focus on optimising the zeta potential to +/- 30 mV as it improves overall formulation stability. Liposomes and niosomes have favourable stability characteristics and can protect the encapsulated drug from the harsh environment. Further optimisation with cholesterol, antioxidants or coatings like chitosan, pectin or Eudragit can improve the stability of the delivery system *in vivo* (120,122,123). Qin *et al*. formulated liposomes with TAT-modified cholesterol and exhibited promising uptake into brain glioma in animals (94,122,123). Utilising *in vivo* mouse models Chen *et al*. found a 2-fold increase in brain penetration when comparing lactoferrin conjugated procationic liposomes against conventional liposomes (124). Dufes *et al*. research proposed that glucose-targeted niosomes are a promising carrier for any neuroactive peptide that was previously unable to cross the BBB by itself (85). Bragagni *et al*. reported a significantly higher antinociceptive effect when they intravenously delivered dynorphin-B in a N-palmitoyl glucosamine functionalised niosome compared to just dynorphin-B in saline (125). There have been many successful attempts at brain delivery utilising both niosomes and liposomes, the main advantages are biocompatibility, the ability to encapsulate any drug and the possibility to incorporate various ligands and/or peptides to the surface. Niosomes are generally preferred over liposomes due to their longer half-life, cheaper fabrication materials and improved stability (120,122).

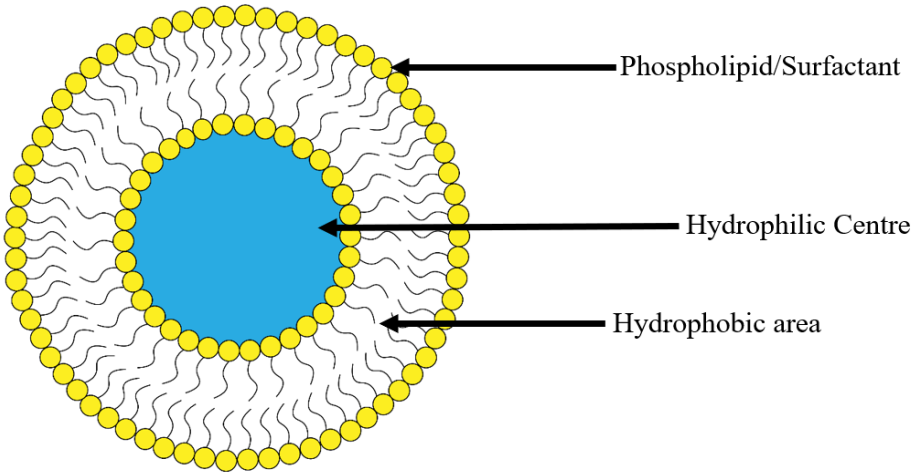

Figure 1.9. Diagram showing the structure of a Liposome/Niosome.

1.5.4. Microemulsions

Microemulsions (shown on Figure 1.10) are thermodynamically stable systems of water and oil, typically transparent, isotropic, low viscosity and stabilised with a surfactant and a cosurfactant (126). The stability of microemulsions is usually the product of the ultralow interfacial tension between the water and oil phases. In addition to improving oral bioavailability and enhancing absorption, the main advantage of microemulsions is the spontaneous formation of stable systems with a long shelf life and able to load large quantities of lipophilic and/or hydrophilic drugs. Both oil-in-water and water-in-oil microemulsions can be used to enhance the oral bioavailability of drugs, although oil-in-water emulsions are favoured for the treatment of brain disorders (126). The main limitation of microemulsion application in the pharmaceutical field is the compatibility of each individual component with high concentrations of surfactants and cosurfactants. Microemulsions have a dispersed domain diameter from approximately 1 to 200 nm, more commonly between 10 to 50 nm (126,127). The conventional high energy emulsification methods for emulsions, cannot be used to create microemulsions, as those methods do not readily produce the required micro droplet sizes (127,128). Low-energy methods are able to form microemulsions including phase inversion temperature, phase inversion composition and emulsion inversion point (128,129). Another method for microemulsion fabrication is the emulsion titration or dilution method that utilises both ‘high energy’ and ‘low energy’ techniques. Typically, ‘low energy’ methods are limited to non-ionic small molecule surfactants in high concentrations as their

emulsifiers and require non-triglyceride oils with very low viscosity (130,131). In order to maximise drug delivery to the brain, microemulsions can be functionalised with various excipients that typically improve circulation time or improve brain uptake (126). Valduga *et al*. found that formulation of etoposide oleate with the cholesterol-rich microemulsion not only reduced toxicity but can potentially enhance brain uptake because of cholesterol's strong affinity to low density lipoprotein receptors (126,132). Kang *et al*. developed a microemulsion containing PLGA that exhibited controlled drug release characteristics with improved therapeutic efficacy (126,133). There are many examples of functionalised microemulsions that can include different ligands, polymers, lipids or more, to further improve drug delivery to the brain. Microemulsions for brain delivery are typically designed for intranasal delivery as a non-invasive and rapid-acting treatment (134,135). Although, oral drug delivery of a microemulsion for brain targeting is an underexplored area with some potential in the form of functionalised microemulsions.

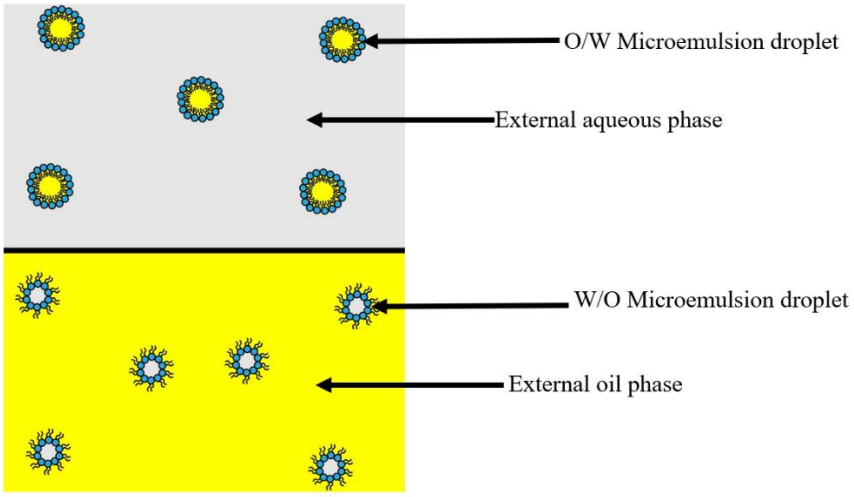

Figure 1.10. Diagram showing the structure of Microemulsions.

1.5.5. Nanogels

Nanogels are nanoparticles composed of physically or chemically cross-linked hydrophilic polymers within the nanoscale size range (136). Nanogels are fabricated with natural polymers, synthetic polymers, or a combination of the two (136,137). Similar to hydrogels, nanogels can encapsulate small molecules or macromolecules, with tuneable swelling, degradation and chemical functionality (136). Nanogel preparation can be made from polymer precursors and utilise methods such as disulphide cross-linking, amine-based cross-linking, clock chemistry-based cross-linking, photo-induced cross-linking, and physical cross-linking. Alternatively, nanogels can be prepared from a heterogeneous polymerisation of monomers via emulsion or inverse emulsion polymerisation. Azadi *et al*. prepared surface-treated methotrexate-loaded chitosan nanogels and demonstrated a considerable increase in brain concentration when compared to administering free drug alone (137). Blackburn *et al*. successfully produced maleimide-functionalised nanogel, that improved siRNA activity by effective protection during the endosomal uptake and escape in the cells (138). Soni *et al*. showed nanogels have significant penetration into the brain, further improved with polysorbate 80 ligand (139). Nanogels are favourable delivery systems due to their high drug loading which can reach up to 50%, and their flexibility to incorporate different ligands into the structure (140).

1.6. Thesis aims and structure

This chapter has provided background information on the current research around peptide delivery science, focusing on the challenges and the related strategies. Neurodegenerative disorders require long-term and consistent dosing of medicine to manage the symptoms and disease progression. This makes invasive techniques unfavourable, which increases the need to develop oral drugs for the brain. Delivery of large neuropeptides across the BBB comes with many challenges. The specialised structure and properties of the BBB make it highly selective on what is allowed to pass through it. After reviewing all the delivery systems, niosomes have been determined to be the most promising for this project. This is mainly due to its stability, capacity to entrap hydrophilic and lipophilic drugs, and ability to be functionalised by ligands. Utilisation of a niosomal delivery system will protect the peptides and enable BBB transport via specialised ligands. If successful, this will provide the groundwork to deliver virtually any compound across the BBB via a bi-ligand niosomal

delivery system. The first ligand used is the non-specific cell penetrating peptide PLR and the second ligand is the BBB specific RI7 ligand. Both ligands are used together to improve uptake, transport, and specificity across the BBB for brain delivery.

The aim of this thesis is to develop, formulate and characterise a bi-ligand niosomal delivery system to orally deliver neuropeptides across the BBB. Both GPE and cGP are small neuropeptides that have been shown to be effective in reducing brain inflammation. These two endogenous peptides were chosen as drug candidates because they are effective but require protected transport to the BBB. GPE has poor enzymatic stability and cGP has extensive peripheral protein binding issues preventing passage across the BBB. The utilisation of these two ligands together into a niosomal delivery system has not been attempted before. The innovative applications of this drug delivery system for oral delivery targeted towards the brain is ambitious. These points alongside the ability of this delivery system to entrap both hydrophilic and lipophilic drugs all contribute to this projects novelty and potential disruption to brain medicine. To achieve this aim, the structure of this thesis was established by exploring the following objectives:

Chapter 1: To introduce the background information and the current research around peptide delivery across GIT and BBB.

Chapter 2: To develop and validate an HPLC analytical method for qualifying and quantifying GPE and cGP.

Chapter 3: To develop, formulate and characterise the bi-ligand niosomal delivery system:

a. Preparation of GPE-loaded and cGP-loaded niosomes and optimisation of the formulation by changing various parameters using factorial design
b. Characterisation of the physical and chemical properties of the optimised niosomes.

Chapter 4: To evaluate free and loaded GPE and cGP niosomal cellular uptake and penetration on human colorectal adenocarcinoma cells (Caco-2) cells mimicking the GIT tract.

Chapter 5: To evaluate free and loaded GPE and cGP niosomal cellular uptake and penetration on RBMVEC mimicking the BBB.

Chapter 6: To conclude this research and discuss the future perspective.

Chapter 2
Analytical method development for GPE and cGP

2.1 Introduction

All pharmaceutical projects must develop an accurate and reliable analytical method to quantitatively determine drug content in both formulations and biological samples. Various analytical techniques are currently available, including but not limited to: spectrofluorimetry, spectrophotometry, voltammetry, flow injection analysis, and high performance liquid chromatography (HPLC). HPLC is a widely used technique for the separation, identification, and quantification of chemical compounds in a mixture (141). It relies on a high-pressure pump to pass a solvent containing the sample mixture through a column filled with a solid adsorbent material such as silicon (142). The compounds in the sample interact differently with the adsorbent material and lead to the separation of the components as they flow out of the column (143). An HPLC instrument typically consists of an auto-sampler, pump, and detector. The auto-sampler brings the sample mixture into the mobile phase, which carries it into the stationary phase. The pumps deliver the mobile phase through the stationary phase (144). The detector generates a signal that is proportional to the amount of sample components emerging from the column hence allowing for quantitative analysis of the sample components (145). However, only few pieces of literatures were found to use HPLC to separate and quantify GPE and cGP (146). There is a tendency for base-line shifting, long retention time, or complicated preparation procedures in other analytical methods of GPE and cGP, indicating the necessity of developing a new HPLC method to quantify GPE and cGP (147).

Therefore, in this chapter, a sensitive, rapid, and reliable HPLC method was developed and validated to quantify both GPE and cGP. Forced degradation studies have been extensively studied under six different stress conditions (pure water, acidic solution, basic solution, oxidative, lights, and high temperature) for up to seven days. These fundamental analytical methods and degradation kinetics will be helpful in future work on the development of a stable and effective formulation of both GPE and cGP.

2.2 Chapter Aims

To successfully develop and evaluate novel formulations, the compounds of interest must be able to be accurately quantified under various conditions. This chapter aims to develop and validate a gradient HPLC assay for the analysis of both GPE and cGP in an aqueous medium with and without potential formulation components and degradation products. The specific objectives are:

- Development of HPLC analytical method of both GPE and cGP.
- Validation of HPLC analytical method of both GPE and cGP, including specificity, linearity, repeatability, intermediate precision, sensitivity, recovery, and robustness.
- Investigation of the factors influencing drug stability (Forced degradation studies).

2.3. Experimental methods

2.3.1. Materials

Glycine-proline-glutamate (GPE), Cyclic-Glycine-proline (cGP), Span 80, Tween 20, cholesterol (CH) and dihexadecyl phosphate (DCP) were purchased from Sigma-Aldrich (Sigma, USA). Methanol and acetonitrile (ACN) of analytical reagent grade were purchased from Merck (Merck, Germany). Trifluoroacetic acid (TFA) was purchased from Fluka (Fluka, Germany). Milli-Q water was available from the Pharmaceutics Laboratory at University of Auckland (Auckland, New Zealand). All other reagents and chemicals were of analytical grade.

2.3.2. HPLC method development and validation

2.3.2.1. Chromatographic conditions

The assay to quantify both GPE and cGP has been developed and tested to run on an Agilent 1260, using a C18 HPLC column of Synergi™ Polar-RP C18 Column (250 x 4.6 mm; 80 Å pore size; Phenomenex, Torrance, CA, USA) fitted with a guard column. The mobile phase consisted of 3% acetonitrile with 0.025% trifluoroacetic acid and 97% Milli-Q water with 0.025% trifluoroacetic acid to quantify both GPE and cGP. A constant flow rate of 1 ml/min was used. The injection sample volume was 50 µl and the column temperature was

maintained at 25°C. The absorbance was determined at 220 nm (the maximum absorption wavelength). All mobile phases were filtered and degassed prior to use.

2.3.2.2. Stock Solution Preparation

A stock solution containing GPE or cGP was prepared by dissolving a known amount of drug in Milli-Q water. The stock solution was 100 µg/ml for both GPE and cGP. Different concentrations of standard solutions were made ranging from 5-100 µg/ml were prepared by dilution of the stock solution using the same solvent. Samples were stored at 4℃ and protected from light before use.

2.3.2.3. Mobile phase optimisation

An optimised mobile phase is to achieve acceptable resolution of the target drug. The mobile phases were varied with different Milli-Q:ACN ratios between 90:10 and 99:1 in the absence or the presence of TFA were investigated in this study. The mobile phases were filtered through a 0.45 µm membrane and degassed before use. The retention time of the drug candidates was set to be below 10 minutes, but above 2 minutes, peak resolution (R_s) also needed to be greater than 2, where R_s is defined as:

$$R_S = \frac{2(R_{ta} - R_{tb})}{(W_a - W_b)} \quad \textbf{Equation 2.1}$$

In equation 2.1, W_a and W_b are the widths of the two peaks measured at the baseline, obtained from the chromatograms, whereas R_{ta} and R_{tb} are the retention times.

2.3.2.4. Method Validation

According to British Pharmacopeia (BP) and International Conference on Harmonisation (ICH) guidelines, the modified HPLC analytical method was validated in terms of specificity, linearity, repeatability, intermediate precision, sensitivity, recovery, and robustness (148,149).

Linearity:

A calibration curve was made by plotting the peak area against each GPE or cGP concentration. Nine standard solutions (1, 5, 10, 25, 50, 75, and 100 μg/mL) were prepared and tested from a stock solution with serial dilution. Linear regression was used to determine the slope, y-intercept, and linearity of the curve.

Specificity:

The specificity of the HPLC method was determined by spiking the analytical run with both GPE, cGP and their degraded products as well as all the individual components of the niosomal formulation dissolved in methanol. The mixtures were filtered through a 0.45 μm syringe filter before being analysed by the HPLC machine. The specificity was investigated by comparing the UV chromatograms of niosome components and both GPE and cGP.

Repeatability:

Repeatability analysis was carried out by evaluating both instrumental precision and intra-assay precision. Instrumental precision (system precision) was determined by analysing three different concentrations for both GPE and cGP in five replicate injections. Intra-assay precision (method precision) was determined by analysis of five independent standard solutions of three different concentrations for both GPE and cGP.

Intermediate precision:

Three different concentrations of both GPE and cGP were analysed four times in one day to test the intra-day repeatability. Three different concentrations of both GPE and cGP were tested over three consecutive days to test the inter-day repeatability. All injections were carried out in triplicate. The precision of the assays was calculated as the percentage of coefficient of variation (% C.V).

Sensitivity:

The limit of detection (LOD) and limit of quantification (LOQ) must also be determined to ascertain the sensitivity of the HPLC method. This was estimated by calculating the standard deviation of the response (σ, based on the regression of the calibration curve via Excel®

calculations) and the slope (S) of the standard curve using the following equations (International Conference on Harmonisation 1994):

$$\mathbf{LOD} = \mathbf{3.3} \times \frac{\boldsymbol{\sigma}}{\mathbf{S}} \quad \textbf{Equation 2.2}$$

$$\mathbf{LOQ} = \mathbf{10} \times \frac{\boldsymbol{\sigma}}{\mathbf{S}} \quad \textbf{Equation 2.3}$$

Recovery:

To determine if GPE and cGP can be recovered in the presence of niosome components, blank niosomes were prepared and spiked with GPE and cGP, respectively. The recoveries of each drug at three concentrations levels were determined by measuring the percentages of detected concentrations over added initial concentrations.

Robustness study:

A robustness study was carried out to determine the reliability of the analytical method during normal usage. The peak areas and retention times of GPE and cGP were determined and compared at three different conditions for each variable: changes in mobile phase, pH, injection volume, flow rate, and temperature.

2.3.3. Forced degradation studies

Forced degradation studies were carried out for both GPE and cGP, so it may be considered for the formulation and quantification of the drug. Based on the ICH guidelines, both GPE and cGP was exposed to five different stress conditions (148). However, the conditions used in this study were modified because of the fragile nature of both GPE and cGP. The optimised stress conditions used in forced degradation studies were modified on the premise of acquiring more than 10% degradation in the allocated time of 7 days (150). The final optimised stress conditions used were the heat (60℃), UV (1000 lux), base hydrolysis (0.1M NaOH), acid hydrolysis (0.1M HCl), and oxidation (0.01% v/v H_2O_2). Only one factor was changed at a time and the rest were kept constant when testing for the different conditions i.e., temperature was controlled at room temperature, pH was neutral and in the absence of any oxidising compounds or exposure to any light source. Samples were analysed by comparing with the initial concentrations at different time intervals (0.1, 1, 2, 3, 4, 5, 6, and 7 days) (150). The peak purity analysis was conducted by analysing the similarity between the five different UV spectra acquired from HPLC-PDA detector.

2.4. Results and discussion

2.4.1. HPLC method development and validation

2.4.1.1. Mobile phase optimisation

A gradient HPLC method was developed and validated to quantitatively analyse GPE and cGP (Table 2.1). Various isocratic and gradient methods were utilised under different conditions of Milli-Q water, Acetonitrile and Methanol guided by specific literature. The flow rate was 1 ml/min over 15 minutes and found the ideal UV detection wavelength at 220 nm. Each compound was independently tested and individually run. Desirable peaks were obtained utilising the same method for both compounds, and this makes sense considering all their structural similarities. GPE has a sharp symmetric peak at approximately 4.7 minutes whereas cGP has a sharp, symmetrical peak at 8.1 minutes. This significant separation of elution time of the 2 compounds is also desirable for the future work if we need to quantify both compounds in a single solution, it is now possible with this HPLC method.

Table 2.1 Gradient HPLC method for both GPE and cGP.

Time (min)	**Mobile phase ratio** (Milli-Q water:ACN)
0.00	97:3
7.00	97:3
7.01	60:40
12.00	60:40
12.01	97:3
15.00	97:3

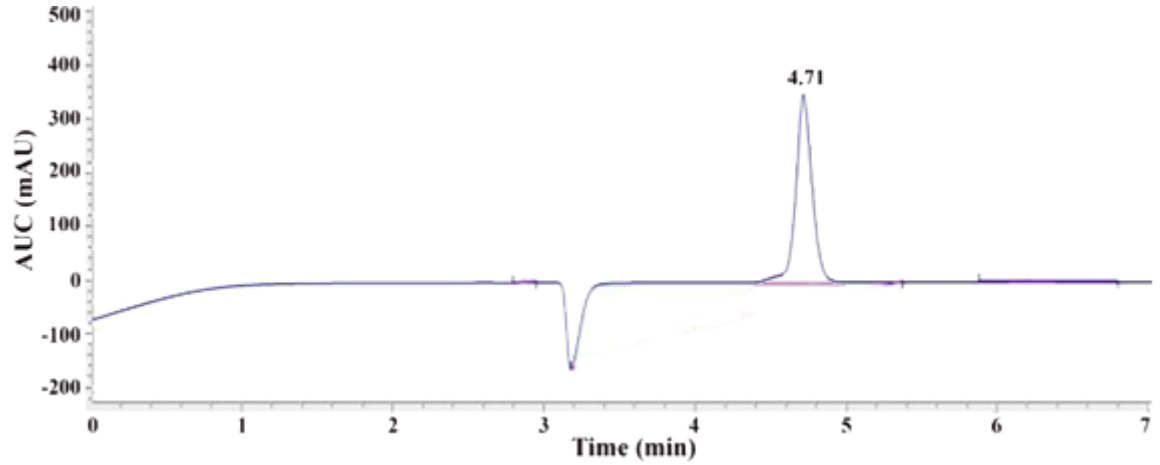

Figure 2.1. HPLC peak for GPE eluting at 4.71 minutes.

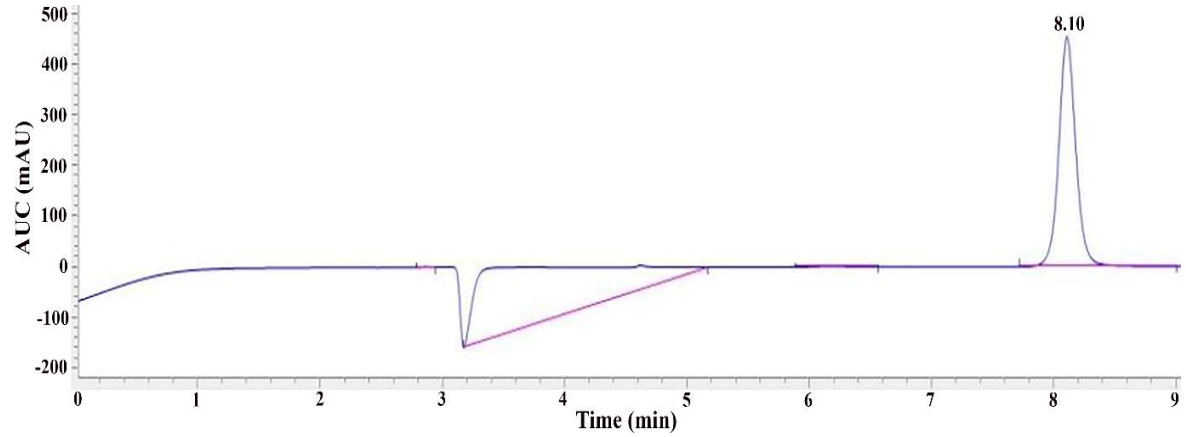

Figure 2.2. HPLC peak for cGP eluting at 8.10 minutes.

2.4.1.2. Method Validation

Following the ICH guidelines, method validation is a process that evaluates whether the system, in this case the HPLC method for both GPE and cGP, have acceptable limits within the parameters of the analytical method.

Linearity:

The calibration curves were obtained by plotting peak areas against concentrations. The results of the regression analysis are shown in Table 2.2. The y-axis is the peak area under the curve, and the x-axis is the concentration of the drug, the equation in the tables demonstrate the connection between the peak area and concentration. The two drugs showed good linearity over the range tested with the correlation coefficients (R^2) all above 0.999 as shown in Figure 2.3.

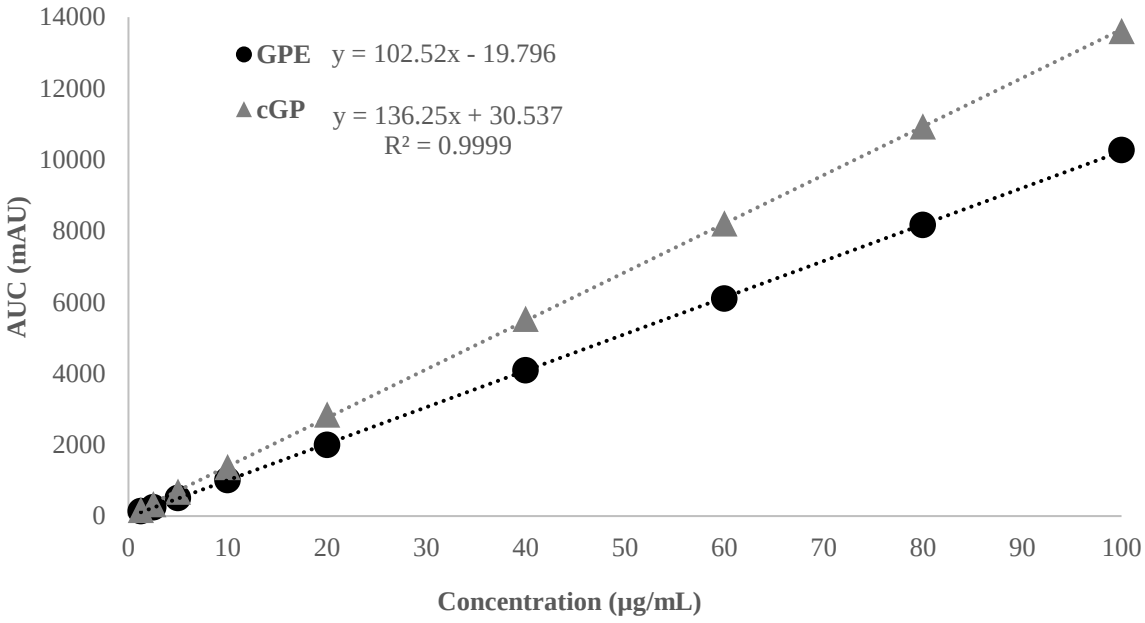

Figure 2.3. Calibration curves of GPE and cGP in the concentration range from 1.25 to 100 **µ**g/ml (n=3).

Table 2.2. Regression analysis of linearity for the calibration curves of GPE and cGP

Compounds	**Concentration range (µg/ml)**	**Standard curve equation [a]**	**Correlation coefficient**
GPE	1.25 - 100	y = 102.12x - 13.086	> 0.9999
cGP	1.25 - 100	y = 136.25x + 30.537	> 0.9999

[a] y is the peak area (mAU*min), and x is the concentration of drug (µg/mL) (n=3).

Specificity:

In the presence of known or suspected compounds, the analytical method is meant to be specific to the analyte in question. When niosome components and degradation products of GPE and cGP were tested it was shown the peaks to be sufficiently separated from the interferences with resolution all above 2, indicating satisfactory specificity. The mixture of niosome components gave no response, and GPE and cGP were completely separated.

Repeatability:

Instrumental precision was measured by repetitive injection of the same sample of three concentrations. The relative standard deviation (R.S.D.) or the coefficient of variation (CV) was determined to assess instrumental precision. Intra-assay precision was determined by preparing five independent standard solutions, which were at three different concentrations and measuring the CV values shown in Table 2.3. The CV values of both instrumental precision and intra-assay precision were below 2.0%, indicating the HPLC analytical method was precise according to ICH guidelines.

Table 2.3. Instrumental and intra-day precision studies.

Concentration (µg/ml)		**Instrumental Precision**		**Intra-day precision**	
		Peak area (mAU*s) (Mean ±SD, n=5)	**%CV**	**Peak area** (mAU*s) (Mean ±SD, n=5)	**%CV**
GPE	**5.0**	501.67 ± 0.98	0.20	492.11 ± 10.45	2.12
	20.0	1994.23 ± 2.36	0.12	1976 ± 38.88	1.97
	80.0	8169.43 ± 7.19	0.09	7942 ± 143.85	1.81
cGP	**17.5**	2671.04 ± 11.42	0.43	2661.87 ± 62.89	2.36
	35.0	5296.33 ± 9.42	0.18	5241.15 ± 81.89	1.56
	70.0	10034.37 ± 15.20	0.15	10305.21 ± 172.78	1.68

Intermediate precision:

Intermediate precision for GPE and cGP were determined by assessing intra-day and inter-day repeatability. The results of intra-day and inter-day repeatability studies for both compounds are shown in Table 2.4. According to the ICH guidelines, the CV values in three concentration groups for both compounds were approximately or below 3%, which is acceptable.

Table 2.4. Intra-day and inter-day repeatability studies.

Concentration (µg/ml)		**Intra-day repeatability**		**Inter-day repeatability**	
		Peak area (mAU*s) (Mean ±SD, n=5)	**%CV**	**Peak area** (mAU*s) (Mean ±SD, n=5)	**%CV**
GPE	**5**	1763.35 ± 5.42	0.31	513.47 ± 12.21	2.38
	30	3466.80 ± 27.49	0.79	2005.17 ± 35.96	1.79
	70	6877.93 ± 54.01	0.79	8034.53 ± 84.04	1.05
cGP	**17.5**	2590.12 ± 14.22	0.55	2502.45 ± 22.13	0.88
	35	2590.12 ± 9.74	0.19	5000.35 ± 62.13	1.24
	70	10223.15 ± 9.56	0.09	10216.64 ± 47.13	0.46

Sensitivity:

The sensitivity of HPLC method was determined by the lower limit of detection (LOD) and lower limit of quantification (LOQ). LOD is the lowest concentration of the analyte the method can detect and LOQ is the lowest concentration that can be quantified accurately by the HPLC method. The LOD and LOQ of GPE and cGP are shown in Table 2.5, indicating the sensitivity of the method.

Table 2.5. Sensitivity of GPE and cGP (Mean, n=3).

Drug	**LOD** (µg/ml)	**LOQ** (µg/ml)
GPE	0.1038	0.3463
cGP	0.108	0.360

Recovery:

The recovery measures the closeness between the theoretically added drug amount at initial and the experimental value, which was determined by spiking the empty niosomes with a known amount of GPE and cGP, respectively. The recovery of GPE and cGP at three different concentrations was above 95% with CV values below 3% (Table 2.6.). The results indicate that GPE and cGP can be fully recovered in the presence of niosome components.

Table 2.6. Recovery of peptides from niosomes (Mean ±SD, n=3).

Sample concentration (µg/ml)		**Concentration found**(µg/ml)	**Recovery** (%)	**CV** (%)
GPE	20	20.577 ± 0.47	102.83	2.30
	40	41.32 ± 0.53	103.29	1.28
	80	81.93 ± 0.71	102.42	0.87
cGP	17.5	18.47 ± 0.35	105.52	1.90
	35	38.73 ± 0.47	110.67	1.22
	70	72.51 ± 0.46	103.57	0.63

Robustness study:

There are no significant changes in peak areas, and the retention time were observed for cGP, with the %CV of the individual runs being less than 2% (Table 2.7). However, for GPE, there are large discrepancies when the change mobile phase ratio is from 99:5 to 99:1

(MilliQ:ACN) or the change pH is from 1.6 to 3.6. Therefore, mobile phase composition and pH could affect the GPE quantification as shown in Table 2.8.

Table 2.7. Robustness experiments for cGP by varying 5 conditions (Mean ±SD, n=3).

Conditions	**Optimized parameters**	**Screening parameters**	**Average Area**	**SD**	**CV%**
Mobile phase	Milli-Q:ACN	95:01	10284.7	20.61	0.0020
	97:3	97:03	10547.6	29.04	0.0027
		99:01	10485.1	47.28	0.0045
pH	2.6	1.6	9291.3	65.93	0.0070
		2.6	10547.6	29.04	0.0027
		3.6	10349.8	21.70	0.0020
Injection volume	50 µl	40 µl	8450.2	35.52	0.0042
		50 µl	10547.6	29.04	0.0027
		60 µl	12518.7	51.16	0.0040
Flow rate	1 ml/min	0.8	10410.1	12.78	0.0012
		1	10547.6	29.04	0.0027
		1.2	10596.9	26.41	0.0024
Temperature	45°C	40°C	10469.1	18.40	0.0017
		45°C	10547.6	29.04	0.0027
		50°C	10559.1	19.90	0.0018

Table 2.8. Robustness experiments for GPE by varying 5 conditions (Mean ±SD, n=3).

Conditions	**Optimized parameters**	**Screening parameters**	**Average Area**	**SD**	**CV%**
Mobile phase	Milli-Q:ACN	95:01	5618.7	55.69	0.0099
	97:3	97:03	6865.5	7.45	0.0011
		99:01	6866.8	2.00	0.0003
pH	2.6	1.6	5353.2	54.96	0.0102
		2.6	6865.5	7.45	0.0011
		3.6	7509.6	91.73	0.0122
Injection volume	50 mcl	40 µl	5565.3	5.08	0.0009
		50 µl	6865.5	7.45	0.0011
		60 µl	8236.7	52.80	0.0064
Flow rate	1 ml/min	0.8	7266.8	12.50	0.0017
		1	6865.5	7.45	0.0011
		1.2	6305.3	8.17	0.0013
Temperature	45°C	40°C	6946.9	9.34	0.0013
		45°C	6865.5	7.45	0.0011
		50°C	6955.8	18.14	0.0026

2.4.2. Forced degradation studies

A key consideration in formulation development is to examine drug stability. GPE solution is susceptible to heat, base hydrolysis, and oxidation, where the powder is comparatively very resilient. As shown in the Table 2.9 and 2.10, the results indicate that base hydrolysis and oxidation were a real issue for GPE solution as only after one day it experienced a 55% degradation in the presence of NaOH and about 30% degradation with hydrogen peroxide. cGP is relatively stable in heat and light illumination exposure, with consistent results from the powder form as well. cGP is particularly susceptible to basic condition as after only one day, there was no significant amount detected (100% degraded). For both acid and oxidation parameters, only ~30% and ~35% respectively of cGP were degraded. Therefore, both GPE and cGP are extremely fragile in basic and oxidative conditions. Stability within the niosomes were studied in the recovery section above in the HPLC validation.

Table 2.9. Data of forced degradation studies of GPE by varying different conditions (Mean ±SD, n=3).

Compound	**Conditions**	**Time till > 10% degradation** (days)	**Drug remaining** (%)
GPE	Heat (60°C)	5	79.27 ± 2.06
	UV light (1000 lux)	N/A (>7 days)	93.21 ± 2.66
	Acid hydrolysis (0.1M HCl)	N/A (>7 days)	98.46 ± 0.66
	Base hydrolysis (0.1M NaOH)	1	46.81 ± 1.55
	Oxidation (0.01% v/v H_2O_2).	1	70.24 ± 3.20
	Powder heat (60°C)	N/A (>7 days)	95.51 ± 1.33
	Powder UV light (1000 lux)	N/A (>7 days)	96.37 ± 1.71

Table 2.10. Data of forced degradation studies of cGP by varying different conditions (Mean ±SD, n=3).

Compound	**Conditions**	**Time till > 10% degradation** (days)	**Drug remaining** (%)
cGP	Heat (60°C)	N/A (>7 days)	96.63 ± 4.66
	UV light (1000 lux)	N/A (>7 days)	97.02 ± 1.61
	Acid hydrolysis (0.1M HCl)	1	70.30 ± 1.23
	Base hydrolysis (0.1M NaOH)	1	Undetectable
	Oxidation (0.01% v/v H_2O_2).	1	63.37 ± 3.84
	Powder heat (60°C)	N/A (>7 days)	93.84 ± 1.37
	Powder UV light (1000 lux)	N/A (>7 days)	93.96 ± 2.22

2.5. Conclusion

A rapid, precise, and sensitive HPLC method to separate GPE and cGP have been developed and validated in terms of their linearity, specificity, repeatability, sensitivity, recovery, robustness, and intra- and inter- day validation studies. All the results indicate that it is a reliable method to quantify the peptide drugs with variations within acceptable ranges, according to ICH guidelines. External stressors like heat, oxidation, acid and base hydrolysis must be considered in formulation development and future experiments. In particular, the peptides need to avoid any acidic or basic conditions as well as any oxidative environments. These small and susceptible neuropeptides like GPE and cGP need to be protected for their brain delivery journey. Therefore, formulation into a niosomal formulation can both protect and target the neuropeptides to the BBB so that they may exert their action in the brain.

Chapter 3

Formulation Development, Optimisation and Characterisation

3.1. Introduction

Nanocarrier development for drug delivery has received considerable attention due to their potential for targeted delivery to the central nervous system (CNS) to treat neurological disorders. Efficient, safe, and sustained CNS drug delivery systems have always been a significant challenge for scientists globally. Niosomes and liposome are vesicular biodegradable delivery systems that have offered a great potential to enhance drug delivery and have had a significant impact on pharmaceutical, cosmetical, food and biological sciences over the past 30 years (151). Niosomes are structurally similar to liposomes with a bilayer of amphiphilic molecules, capable of enclosing the surrounding solution/agents, as shown in Figure 3.1. (151-154).

Niosomes have attracted many pharmaceuticals, nutraceuticals, and cosmetics community attention, and this is mainly due to their ability to possess the same advantages as liposomes, like, biodegradability, biocompatibility, non-immunogenicity, and the ability to incorporate both hydrophilic and lipophilic compounds. Compared to liposomes, niosomes have exhibited outstanding advantages such as increased long-term stability, cheaper production costs and improved penetration. Consequently, niosomes were used as an alternative delivery system to liposomes, utilising only non-ionic surfactants instead of phospholipids (151). Phospholipids and non-ionic surfactants are amphiphilic molecules generally connected by an ether, amide, or ester bond (153,155).

Niosomes are self-assembled nano-vesicular delivery systems, which is typically formed via thin film hydration in the presence of non-ionic surfactant, cholesterol, or other amphiphilic molecules. This structure enables hydrophilic drugs to be entrapped in the hydrophilic centre and lipophilic drugs trapped in between the hydrophobic bilayers (156). This makes niosomes a promising drug carrier with the ability to incorporate a wide range of drugs. An important consideration for utilising niosomes is their drawbacks, such as leakage, drug fusion and aggregation (157,158). A valuable benefit for niosomes is the ability to add various and multiple ligands or coatings to the vesicle surface (159-161). This allows niosomes to be increasingly accurate when targeting to the brain. There is a lot of potential for niosomes application in brain delivery as niosomal encapsulation can protect the drug from degradation, improve drug penetration and prevent large proteins from binding to the drug (162,163). Several researchers have reported that the niosome carriers provides many benefits to deliver

antioxidants, protein, and peptide drugs via many routes of administration like oral, transdermal, or parenteral routes (164-167).

In this chapter, neuropeptides GPE and cGP will be loaded into niosomes, which was modified using two ligands and delivered to the brain via oral administration. The bi-ligand niosomal delivery system can protect the peptide drugs from degradation, improve drug permeation and prevent large serum proteins from binding to the neuropeptide. Therefore, encapsulating the neuropeptides into a drug delivery system like a niosome can overcome protein binding and improve their stability and permeability across the BBB, resulting in increased concentration in the brain (18). To formulate an optimum carrier system, it is required to understand the carrier components, formation theory, and processing methods. A factorial design was implemented to further elucidate the most influential factors for encapsulation efficiency and niosomal size. The factorial design method can screen a large range of parameters with utilising an efficient number of trials to examine trends.

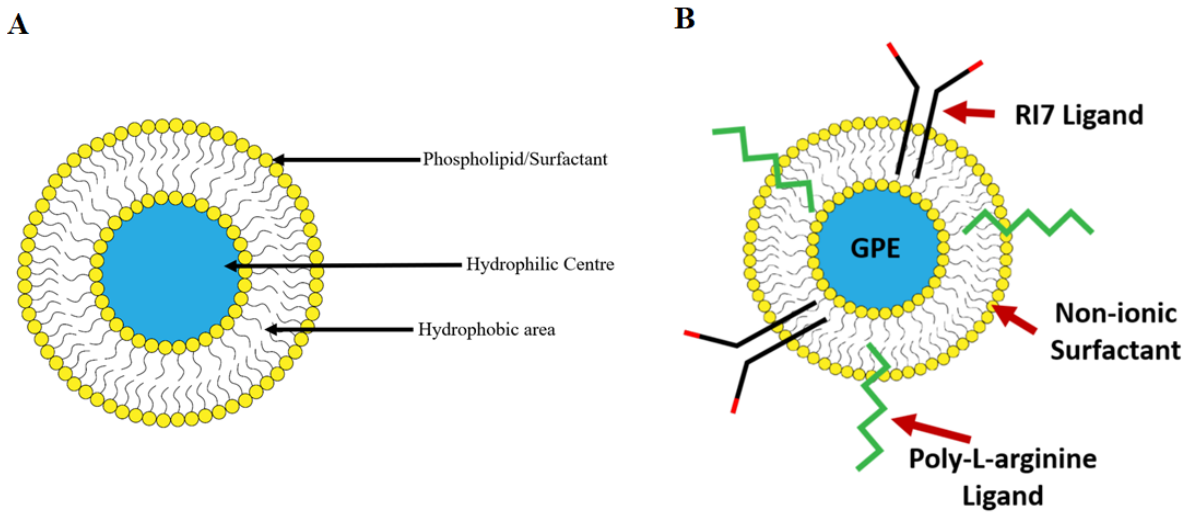

Figure 3.1. Diagram A shows the structure of a niosome and diagram B shows the structure of the niosome after functionalising with the 2 ligands, RI7 and PLR.

3.2. Chapter Aims

The aim of this chapter is to determine an optimal condition to prepare a novel bi-ligand niosomal delivery system for the encapsulation of GPE and cGP and to characterise the niosomal formulation. The specific objectives of this chapter were:

1. To investigate the effect of several parameters on the niosome formulation and to determine an optimal condition by factorial design.

2. To characterize drug-loaded niosomes in terms of entrapment efficiency (EE), particle size, zeta-potential, FTIR and *in vitro* release profiles.

3.3. Experimental

3.3.1. Materials

Glycine-Proline-Glutamate (GPE), cyclic Glycine-Proline (cGP), Span® 80, Tween® 20, hydroxylamine hydrochloride, tris(2-carboxyethyl)phosphine (TCEP), Hank's Balanced Salt Solution (HBSS), Sodium tetraborate Succinimidyl-S-acetylthioacetate (SATA), cholesterol (CH) and dihexadecyl phosphate (DCP) were purchased from Sigma-Aldrich (Sigma, USA). Trifluoroacetic acid was purchased from Fluka (Fluka, Germany). Analytical reagent grade methanol and acetonitrile were purchased from Merck (Merck, Germany). DSPE-PEG (1,2-distearoyl-sn-glycero-3-phosphoethanolamine-N-amino(polyethylene glycol)) was purchased from Avanti Polar Lipids (Avanti, USA), CD71 monoclonal antibody (RI7) was purchased from ThermoFisher scientific (Thermofisher, USA), Poly-L-arginine (PLR) was purchased from Alamanda Polymers (Alamanda, USA), Milli-Q water and deionized water was available from the Pharmaceutics Laboratory at the University of Auckland (Auckland, New Zealand). All other reagents and chemicals were of analytical grade.

3.3.2. Bi-ligand conjugated niosome development and optimisation

3.3.2.1. Couple R17 ligand on the niosome vesicle

RI7 was diluted to 60 µM in HBS buffer and incubated with SATA (Succinimidyl-S-acetylthioacetate) in a 1:8 ratio for 40 minutes at room temperature. Followed by filter Centrifugation that removed the free SATA. The SATA groups were deacetylated in HBS containing 0.5 M hydroxylamine.HCl and 0.02 mM TCEP, pH 7.4, for 90 min at room temperature (Sulfhydryl group/Protein ratio is 3.0). RI7 ligand can be incorporated into the niosomal structure after the initial formation of the liganded niosomes.

3.3.2.2. Poly-L-arginine with polyethylene glycol (PLR-PEG) preparation

First, 50 mM of Sodium tetraborate buffer was made and adjusted to pH 8.5 with 0.1 mol/L of HCl. Poly-L-arginine (PLR) was dissolved in the sodium tetraborate buffer and stirred vigorously for approximately 30 min and subsequently filtered through a 0.22 m Durapore® membrane. The appropriate stoichiometric amount of DSPE-PEG (1,2-distearoyl-sn-glycero-3-phosphoethanolamine-N-amino(polyethylene glycol)) powder was then slowly added to the solution while it was continuously stirred. After another 6 hours of vigorous stirring at room temperature, the solution was transferred to a dialysis tube. The synthesized product was dialyzed out for 24 hours in 10 mM phosphate buffered saline (PBS) adjusted to pH 7.0, followed by an additional 24 hours of dialysis in deionized water. The product was then freeze-dried for 48 hours at −70°C with a pressure of 0.2 mbar.

3.3.2.3. Bi-ligand niosome preparation

The surfactant, DCP, cholesterol and PLR-PEG was mixed and dissolved in a 4:1 mixture of chloroform and in a round bottom flask. The resultant solution was rotary evaporated (Laborota 4000, Buchi, Switzerland)) to form a thin, dry film, which was then purged by nitrogen gas for 5 minutes. Then the drug solution dissolved in PBS was added to hydrate the dry film to create the drug-loaded niosomes. Hydration was carried out for up to 2 hours under 58°C with constant stirring. The niosomes were left at room temperature for 30 minutes to anneal. The previously prepared RI7 conjugate is then incubated with niosomes in a ratio of 0.4 nmol peptide/µmol total lipid overnight at 4°C. This will result in the niosomes being coupled to both the RI7 ligand and PLR. Various surfactants and ratios will be utilized to optimize the formulation for the neuropeptide. Niosome optimizations are carried out with

a 2-level and 5 factors, factorial design examining different factors like drug amount, pH of hydration medium, hydration time, surfactant to cholesterol ratio and the surfactant type to evaluate the optimum entrapment efficiency through variable screening by 2^{5-2} fractional factorial design.

3.3.2.4. Size optimization via sonication

Sonication and extrusion are both considered the best approaches to reduce particle size in niosomes. Compared to both methods, sonication was selected for this study due to its convenience and ability to create niosomes of a desirable size. The UPS200 probe-sonicator (200W, 26kHz) was used to reduce the niosome particle size with variable parameters.

3.3.2.5. Factorial design to optimize entrapment efficiency

Due to the large number of factors that have the potential to significantly alter the most important parameters (e.g., entrapment efficiency) of the niosomal delivery system a factorial design method was implemented. The simpler method for formulation optimisation involves a step-by-step process where a single factor at a time is altered and is justified with prior knowledge and results. This method when compared with factorial design will require significantly more runs and batches with the advantage of potentially having a clearer interpretation of how each factor influences the outcome. A factorial design can be used to screen for the most influential factors with an efficient number of trails as reported by many other researchers (168-170). This can then be double checked with a central composite design and checkpoint analysis. Due to time and resource constraints, we settled on utilising a factorial design as it will still elucidate the most influential factors and optimise the outcome within the limits initially set.

Five independent variables have been chosen based on preliminary experiments and literature. The variables were surfactant type (Span 80 or Tween 20) (X_1), surfactant to cholesterol ratio (X_2), hydration time (X_3), pH of hydration medium (X_4) and Drug amount (X_5) to determine their effect on the entrapment efficiency (Y). These factors were chosen based on preliminary experiments and used to make the factorial design more efficient. There is a small limitation of only two surfactants used, both were found to have decent entrapment efficiency and have a significant difference in the hydrophilic-lipophilic balance (HLB) with Span 80 having 4.3 and Tween 20 having 16.7. Different surfactants and/or a mixture of

surfactants are also possible to be used here, with specific HLB values providing more desirable results (171-173). The factors were described on two-levels, either low or high with the corresponding transform codes to be -1 and +1, respectively. 28 runs in the one-half two level 5 factor fractional factorial design were carried out. Design Expert® 11.0 was used to test the statistical significance by analysis of variance (ANOVA) with a high level of significance with a p-value being less than 0.05. A central composite design was also carried out to further optimize the formulation. A central composite design is a full-factorial design with a centre point and start points that fit within a second-order polynomial design. Drug amount (X_1) and the surfactant to cholesterol ratio (X_2) were chosen as the independent variables, entrapment efficiency as the dependent variable and all the other factors stayed constant based on the initial fractional factorial design. A total of 13 runs were executed, which included 5 replicates on the centre point. Checkpoint analysis was carried out to establish the reliability of the regression model on the effect of the variables on entrapment efficiency. An optimum point was chosen and triplicated to compare. The actual and predicted values of the entrapment efficiency of bi-ligand niosome were determined, and their predicted and actual values were compared.

3.3.3. Characterisation of the optimal bi-ligand niosomes

The optimized GPE and cGP loaded bi-ligand niosomes were fully studied in terms of their particle size, zeta-potential, entrapment efficiency percentage (EE%), Morphology, Differential scanning calorimetry (DSC) and Fourier transform infrared spectroscopy (FTIR) spectrum and *in vitro* release profiles.

3.3.3.1. Entrapment efficiency

The bi-ligand niosomes were dispersed in the medium and vortexed for a few seconds and were subjected to ultracentrifugation (WX80, Sorvall, USA) at 41000 rpm for 1 hour at 4°C. The supernatant was withdrawn, and the drug content was quantitatively assayed using the HPLC method (developed and validated in Chapter 2).The niosome pellets were then washed thoroughly and put into 10% Triton-100 solution to disrupt the niosome carrier. This process was taken place in a water-bath sonicator for 10 mins. The resultant mixture was filtered and diluted before carrying out sample analysis by HPLC. The following equation 3.1 was used to calculate the entrapment efficiency of the GPE or cGP, respectively.

$$\boldsymbol{EE}\ (\%) = \frac{\boldsymbol{amount\ of\ drug\ entrapped}}{\boldsymbol{total\ amount\ added}} \times \mathbf{100} \quad \text{Equation 3.1}$$

3.3.3.2. Particle size and zeta-potential determination

Dynamic Light Scattering (DLS) is an accurate and precise technique for measuring particle size in suspensions and emulsions. It is based on the Brownian motion of particles (i.e., small particles move fast, while larger particles move slower).] Particle size and size distribution of nanoparticles are regularly determined using this DLS technique. The bi-ligand niosomal samples were diluted with Milli-Q water and measured its particle size and size distribution using the Zetasizer instrument(Malvern Instruments, UK). The bi-ligand niosomes particle size was measured in triplicates for each sample, and the average of volume diameter and polydispersity index (PDI) were calculated.

3.3.3.3. Fourier transform infrared spectroscopy

FTIR was used to confirm the encapsulation of GPE and cGP within niosome vesicles in an amorphous state. FTIR was conducted on the samples using a Tensor 37 FTIR Spectrometer (Bruker Optics, Ettlingen, Germany) equipped with an attenuated total reflection Germanium crystal cell in the reflection model. A background spectrum was collected first, followed by the samples under the same conditions. The interaction between the drug and each individual excipient was investigated using FTIR spectroscopy. The spectra were obtained with a resolution of 4 cm^{-1} in the region of 4000 cm^{-1} to 500 cm^{-1}. The absorption intensities under the spectra were integrated at variable wavenumbers, which represent the different regions to help the identification, respectively.

3.3.3.4. *In vitro* drug release studies

In vitro release studies were conducted on Franz (vertical) diffusion cells (VTC 200, Logan Instruments Corporation, USA). Cellulose membranes (12000-14000 weight cut-off) were prepared by pre-soaking the membrane in the release medium overnight. The cellulose membranes were sandwiched between the donor and receptor compartments. Hanks balanced salt solution (HBSS, pH 7.4) was used to fill the receptor compartment, and GPE or cGP loaded niosomal suspension was added to fill the donor compartment. All niosomes used in the release studies were created 24 hours (or less) prior and stored at -20 ºC overnight. Niosomes were

not extruded in these release studies, but they were subjected to a single wash cycle of centrifuging, removing the supernatant, followed by resuspension with HBSS. Caution was taken to remove all air bubbles between the underside of the membrane and the receptor medium. The receptor cells were maintained at 37 ± 0.5 ºC and stirred by a magnetic bar at 600 rpm. Samples were taken at predetermined time intervals and replaced with the same amount of fresh medium. The resulting samples were then analysed using the validated HPLC method (reported in chapter 2). The cumulative amount of drug released (Q_n) was plotted as a function of time and was calculated based on the following equation 3.2:

$$\boldsymbol{Q_n = C_n \times V0 + \sum_{i=1}^{n=1} C_i \times V_i} \quad \text{Equation 3.2}$$

Where C_n was the drug concentration in the receptor medium at each sampling time, C_i was the drug concentration of the sample and V_0 and V_i were the volume of dissolution medium and the sample, respectively. The percentage of drug release was obtained by comparing the total amount of drug in the donor chamber and the concentration measured in the receptor chamber.

In order to elucidate the drug release mechanism from the bi-ligand niosomes, the release data has been fit through various mathematical models, and the Korsmeyer-Peppas was selected as the best fit model for our peptide drug release from the bi-ligand niosomal delivery system. The Korsmeyer-Peppas model was used to analyse the drug release from the niosomal vesicles. Log cumulative percentage of drug released from the niosomes versus log time was calculated using the Korsmeyer-Peppas model equation 3.3 (174).

$$\boldsymbol{Q_t = k_k t^n} \quad \text{Equation 3.3}$$

(*t* is the release time, Q_t is percentage cumulative amount of drug release from niosomes at time *t*, and *n* is an exponent that correlates to the drug release mechanism. k_k is a kinetic constant of the drug/niosomal system.)

3.4. Results and discussion

3.4.1. Factorial design development of the bi-ligand niosomes

The results of preliminary screening for the development of the GPE bi-ligand niosomes are shown in Table 3.1 and the central composite design (CCD) on Table 3.2.

Table 3.1. Screening design of GPE bi-ligand niosome with 5 factors and response EE (%).

Run	**Factor 1** Surfactant (Type)	**Factor 2** Surf:Chol (Ratio)	**Factor 3** Hydration Time (min)	**Factor 4** Hydration Medium (pH)	**Factor 5** Drug Amount (mg)	**Response** Entrapment Efficiency (%)
1	Tween 20	0.8	30	11	2.5	14.35
2	Span 80	0.8	120	11	2.5	9.93
3	Tween 20	0.65	75	7	1.5	17.33
4	Span 80	0.65	75	7	1.5	16.84
5	Span 80	0.8	30	11	0.5	29.20
6	Tween 20	0.65	75	7	1.5	16.19
7	Span 80	0.65	75	7	1.5	13.53
8	Span 80	0.5	120	11	0.5	31.51
9	Tween 20	0.65	75	7	1.5	16.20
10	Span 80	0.65	75	7	1.5	17.46
11	Tween 20	0.8	120	3	2.5	9.93
12	Tween 20	0.5	120	3	0.5	25.90
13	Tween 20	0.65	75	7	1.5	12.83
14	Tween 20	0.5	30	11	0.5	29.98
15	Span 80	0.5	30	3	0.5	24.76
16	Span 80	0.65	75	7	1.5	12.30
17	Span 80	0.8	30	3	2.5	10.98
18	Span 80	0.65	75	7	1.5	13.30
19	Tween 20	0.5	30	3	2.5	27.55
20	Tween 20	0.65	75	7	1.5	14.23
21	Tween 20	0.8	120	11	0.5	25.80
22	Span 80	0.5	30	11	2.5	28.09
23	Span 80	0.5	120	3	2.5	23.64
24	Tween 20	0.8	30	3	0.5	26.20
25	Tween 20	0.5	120	11	2.5	23.22
26	Span 80	0.65	75	7	1.5	12.34
27	Tween 20	0.65	75	7	1.5	12.82
28	Span 80	0.8	120	3	0.5	26.38

Table 3.2. CCD of GPE bi-ligand niosome with 2 factors and response EE (%).

Run	Factor 1 Drug Amount (mg)	Factor 2 Surf:Chol (Ratio)	Response Entrapment Efficiency (%)
1	2.5	0.8	15.94
2	1.5	0.65	23.22
3	2.5	0.5	16.75
4	0.5	0.5	27.31
5	1.5	0.437868	22.12
6	1.5	0.65	21.58
7	1.5	0.65	21.44
8	1.5	0.65	22.17
9	0.5	0.8	21.82
10	0.0858	0.65	24.66
11	1.5	0.65	22.09
12	2.9142	0.65	12.21
13	1.5	0.862132	17.74

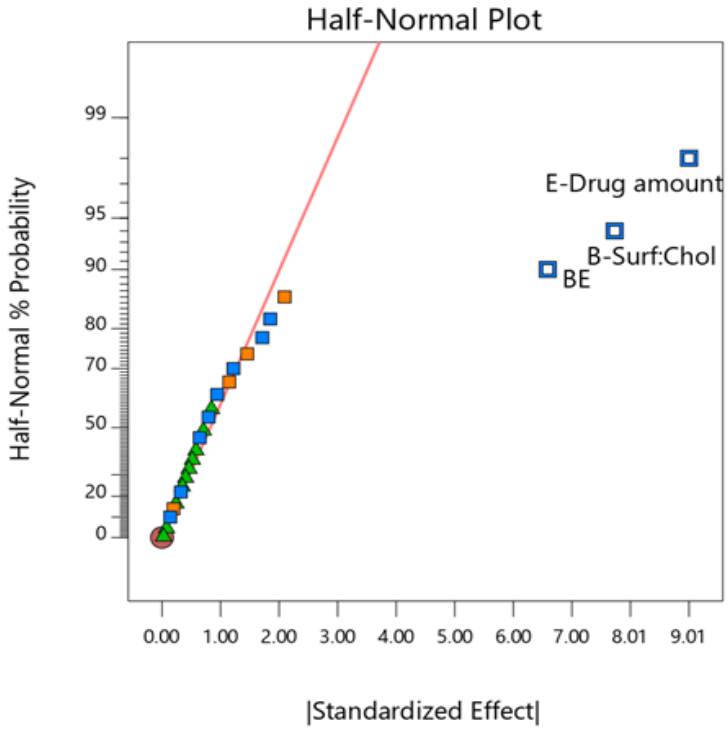

Figure 3.2. Half-normal plot of the Factorial design, produced by Design Expert® 11 indicating the 3 most significant factors.

A total of 13 runs were executed on the centre point study (5 replicates). The final polynomial equation to calculate the entrapment efficiency of GPE is:

$$\boldsymbol{Y\,(EE) = 25.04 - 4.78X_1 + 22.22X_2 + 7.81X_1X_2 - 1.52X_1 - 34.11X_2}$$ Equation 3.4

The p-value of less than 0.05 indicates that this model is also statistically significant. Figures 3.2 shows the half-normal plot of the factorial design which is used to determine which factors have the most effect on the response. Any factor or combination of factors that do not lie on the standard line reveals them as the factors with the most effect, in this case it was drug amount, surfactant to cholesterol ratio and the combination of both. Figure 3.3 shows the graphical representations of the second-order model as a contour plot and a three-dimensional surface plot to examine trends. The two factors are drug amount (X_1) and the surfactant to cholesterol ratio (X_2). The contour plot shows contour lines of entrapment efficiency on the X_1 and X_2 plane. The three-dimensional surface plot graph is a plane of entrapment efficiency values generated through various combinations of X_1 and X_2. It can be predicted that the lower the surfactant to cholesterol ratio and drug amount, the higher the entrapment efficiency. The limits set for the factors both the factorial design and the central composite design appears to have restricted the optimisation. Going beyond these limits resulted in either failed formation of the niosome or significantly decreased entrapment of the drug. So, it may seem that we should further reduce the surfactant to cholesterol ratio to maximise entrapment efficiency but that results in failure to form niosomal vesicles.

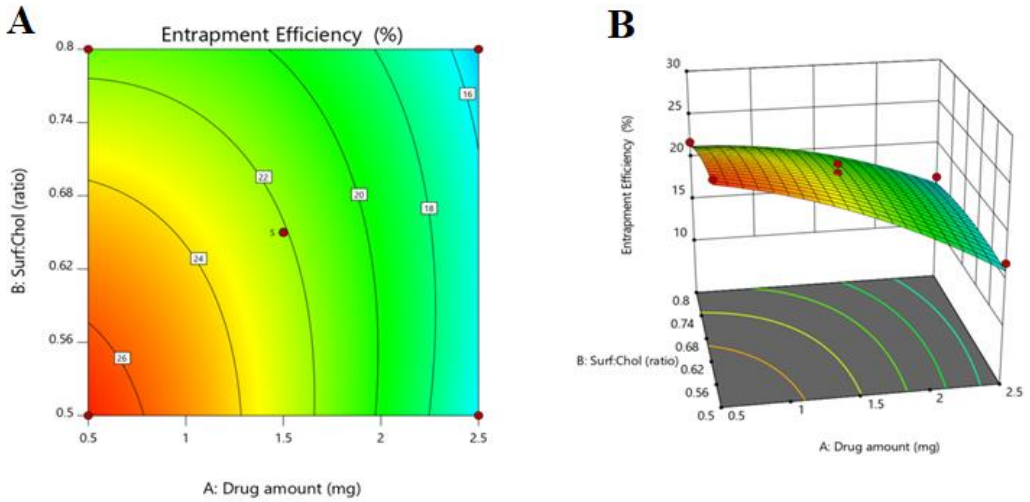

Figure 3.3. (A) Contour plot for the entrapment efficiency as a function of the independent variables. (B) Three-dimensional surface plot for entrapment efficiency as a function of the independent variables.

Table 3.3 shows the optimum checkpoint analysis results for GPE loaded niosomes. The predicted and actual values of the GPE entrapment efficiency were found to be very close with the margin of error being within the predicted response, and the bias was only 0.11%.

Table 3.3. Check point analyses of GPE-niosomes (Mean ± SD, n=3).

	Factor 1 Drug amount (mg)	**Factor 2** Surf:Chol (Ratio)	**Actual** (%)	**Predicted** (%)	**Bias** (%)
Niosome	0.5	1:1	28.34 ± 2.21	28.04	0.11

3.4.2. Sonication optimization

To deliver the niosomal delivery system across the BBB, it is recommended in the literature that the particle size is better to be close to 100 nm (or at least less than 200 nm). From our preliminary study, the particle size of the niosome formed in our study was around 400 nm, so size reduction is necessary. Extrusion and sonication are both methods that can be used to reduce the particle size, but sonication seemed promising because the process is more convenient and creates the niosomal vesicles of appropriate size. A UPS200 probe-sonicator was used at variable conditions was used to reduce the particle size and PDI. Table 3.4 showed the preliminary study using sonication to reduce the particles size. The result showed that utilising the same batch of niosomes, the high amplitude and duration did not necessarily create the smallest niosomes (Table 3.4). The duration of sonication appeared to have the most significant impact on the PDI, with longer times used resulted in a smaller PDI. Interestingly, a pulse of 1 and amplitude of 0.6 seemed to achieve an ideal particle size with acceptable PDI.

Table 3.4. Particle size comparison with various sonication conditions (Mean, n=3)

Trial	Time (min)	Amplitude	Pulse	Size (nm)	PDI
1	30	0.6	0.5	230.7	0.063
2	30	1.0	1.0	222.6	0.049
3	30	0.6	1.0	173.5	0.031
4	3	0.6	1.0	170.9	0.134

Table 3.5 showed the results that compare the particle's size under variable conditions. The RI7-ligand GPE-loaded niosomes had a larger size than the niosomes created with the same conditions but without RI7 ligand. This may be attributed to the RI7 ligand could have the effect of enlarging the particle size. The particle size from sonicated niosome was much smaller than the other two groups and the particle size was less than 200 nm with a smaller PDI value (0.088). One phenomenon that was observed during trials is that the sonication time would influence the drug encapsulation efficiency as it would heat the solution to speed up the drug release. Therefore, the method with good results but the shortest amount of time exposed to sonication was chosen and this consideration was applied in future experiments.

Table 3.5. Particle size comparison between different states of GPE niosomes (Mean, n=3).

	Size (nm)	PDI
RI7-Ligand GPE niosome	544	0.487
GPE niosome	463	0.475
Sonicated GPE niosome	170	0.008

3.4.3. Optimised formulation

Table 3.6 showed the summary of the final optimised formulation for GPE and cGP niosomes. The entrapment efficiency for GPE was much lower compared to cGP niosome (28% vs 68%). This is likely due to the significant difference in lipophilicity between GPE and cGP, with cGP having a higher log P value. Other factors such as method parameters or molecular weight of the peptide are unlikely to have significantly contributed to the difference in entrapment efficiency.

Table 3.6. Optimised GPE and cGP formulation.

Parameter	**GPE niosome**	**cGP niosome**
Surfactant (X_1)	Span 80	Span 80
Drug amount (mg) (X_2)	0.5	0.5
Molar ratio of CH to surfactant (X_3)	1:1	1:1
DCP amount (μmol) (X_4)	5	5
Hydration medium volume (mL) (X_5)	10	10
Hydration time (h) (X_6)	0.5	0.5
EE (%)	28.3	68.1

3.4.4. Characterisation study

3.4.4.1. Particle size and zeta-potential

The niosomes particle size in the absence or presence of ligands were measured and the results were summarized in Table 3.7. The R17 ligand niosome particle size for GPE was 263.1 ± 5.9 nm and for cGP was 255.8 ± 4.3 nm. The GPE niosome without ligand had a vesicle size of 189.8 ± 6.4 nm and cGP niosome without ligand had a vesicle size of 183.4 ± 3.1 nm. The PDI values for both GPE and cGP niosomes are both below 0.2. PDI values lower than 0.5 indicate a relatively narrow size distribution and is generally accepted by the scientific community. Particle size has been reported to play a crucial role in pharmaceutical drug delivery. Large vesicles with a size of >500 nm was found not to be able to deliver the drug across the gastrointestinal epithelial membrane. The ideal particle size to facilitate drug uptake and transport across the gastrointestinal epithelial membrane and BBB should be less than 200 nm. The niosomes produced were in the range of approximately 250 nm which may not be ideal but acceptable to deliver the neuropeptides across the gastrointestinal epithelial membrane and BBB (33-35).

The zeta potential is defined as the average electrostatic potential existing at the hydrodynamic plane of shear, and it provides essential information in determining the physical stability of niosomes (166). It has been reported that niosomes with a zeta potential higher than +30 mV or lower than −30 mV is considered to have acceptable physical stability. The zeta-potential values for GPE niosome and its bi-ligand niosome were determined to be -50.7 ± 2.1 and -54.2 ± 1.6, respectively (Table 3.7). The zeta-potential values for cGP niosome and its bi-ligand niosome were determined to be -48.1 ± 0.8 and -54.5 ± 0.8, respectively (Table 3.7). Current results indicated that the inclusion of DCP imparted sufficient negative potential to the particle, to improve formulation stability (175).

Table 3.7. GPE and cGP niosomal particle size and zeta-potential (Mean ± SD; n=3).

Niosome Type	Size (nm)	PDI	Zeta-potential (mV)
Bi- ligand GPE niosome	263.1 ± 5.9	0.164 ± 0.009	-54.2 ± 1.6
Bi- ligand cGP niosome	255.8 ± 4.3	0.175 ± 0.004	-54.5 ± 0.8
GPE niosome	189.8 ± 6.4	0.139 ± 0.008	-50.7 ± 2.1
cGP niosome	183.4 ± 3.1	0.150 ± 0.007	-48.1 ± 0.8

3.3.4.2. Fourier transform infrared spectroscopy characterisation

FTIR spectroscopy is a particularly useful analytical method able to determine the presence of a wide range of compounds and whether they are aqueous, organic or a solid [170]. These FTIR results shows transmittance peaks (%) along specific wavenumbers denoting to a functional group on each of the materials tested. Our studies ran tests between 500-4000 cm^{-1}, which covers all the main functional groups present in our compounds [170, 171]. Each compound has a unique spectrum due to the different transmittance of its functional groups. DCP only had one important peak at 2917 cm^{-1} which showed a C-H alkane bond. Cholesterol had two distinctive peaks at 3414 cm^{-1} and 1671 cm^{-1}, denoting to an alcoholic O-H group and a C=C alkene bond, respectively. GPE had two distinctive peaks at 1712 cm^{-1} showing a C=O (carboxylic acid) and an N-H (amide) group at 3340 cm^{-1}. Whereas cGP spectra showed N-H stretch at 3149 cm^{-1} and C=O (carboxylic acid) stretch at 1712 cm^{-1}. The spectra of the Span 80 niosome and all its individual components closely resemble the Span 80 with peaks at the 1742 cm^{-1} indicating an ester C=O and an aromatic C-H at 2928 cm^{-1}. There were no similar drug peaks observed in the niosome formulation from the FTIR spectra of Figure 3.4, 3.5, 3.6, 3.7, and 3.8, which indicated that the drug had been encapsulated and was protected from degradation. Another potential explanation for this absence of spectra is when the drug forms complexes with the ingredients present. These complexes may exhibit or hide certain spectra peaks which can make it difficult to be certain of what is occurring with the current results

only. This is a possible explanation although the same findings were also reported by Wang *et al*, Basha *et al.* and Kumbhar *et al.* indicating drug encapsulation (176,177).

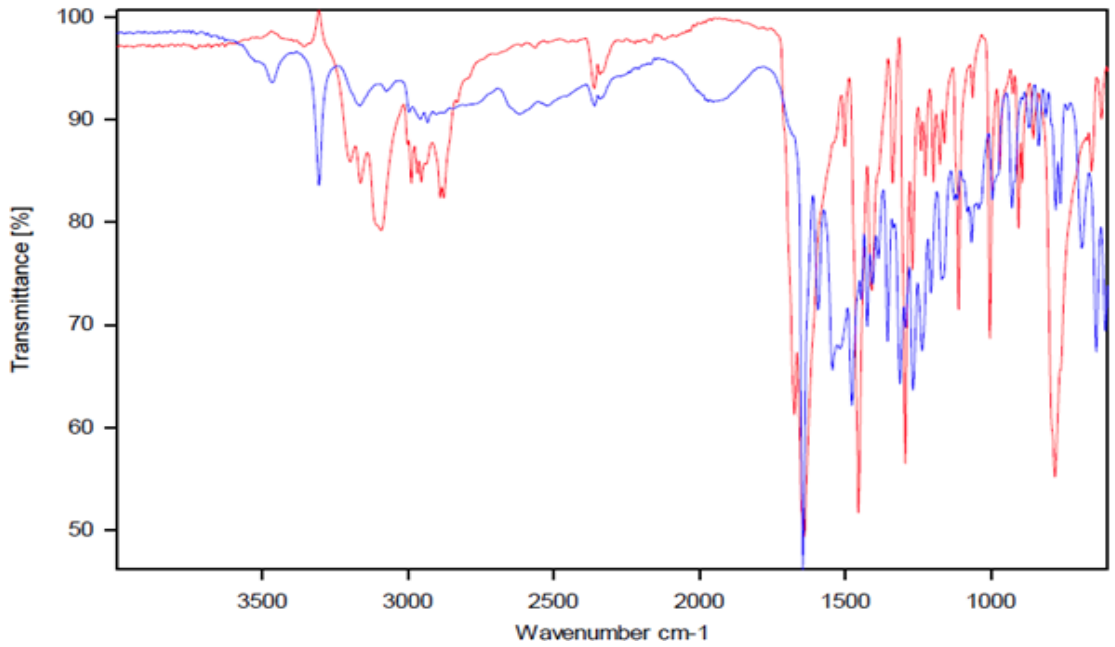

Figure 3.4. FTIR infrared spectra for GPE (blue) and cGP (red).

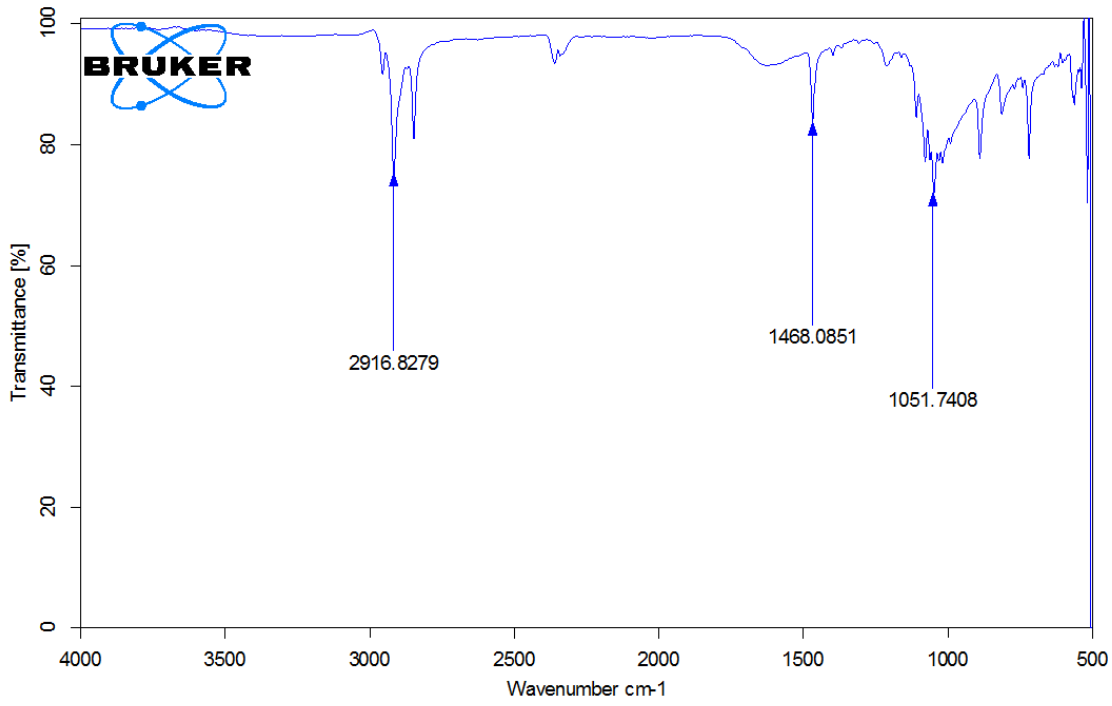

Figure 3.5. FTIR infrared spectra for DCP.

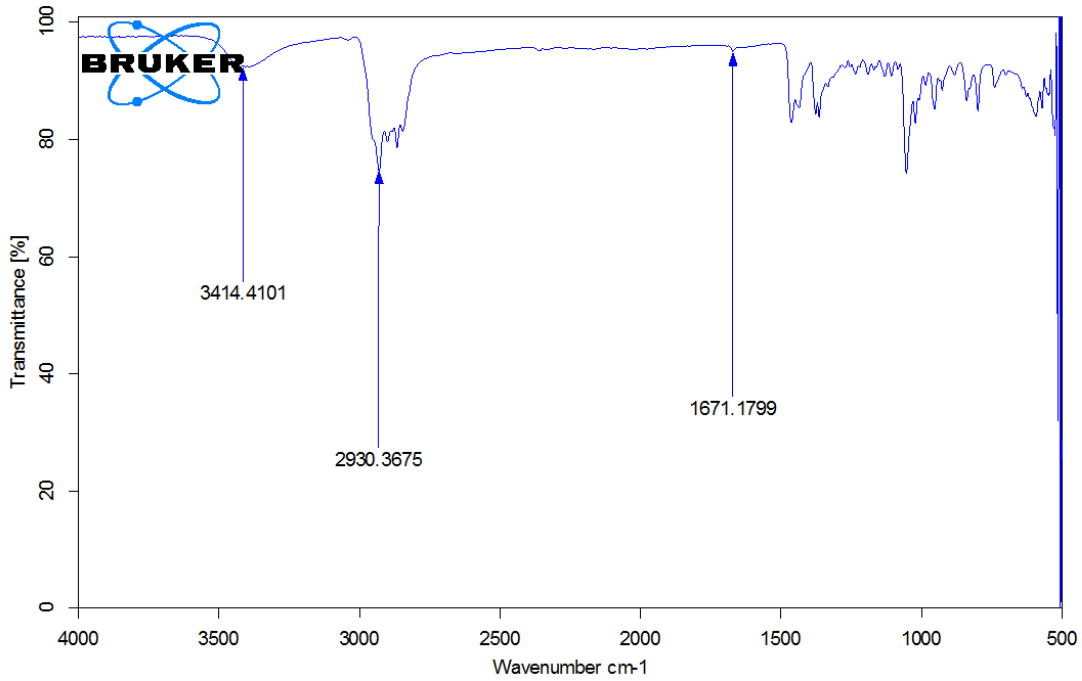

Figure 3.6. FTIR infrared spectra for Cholesterol.

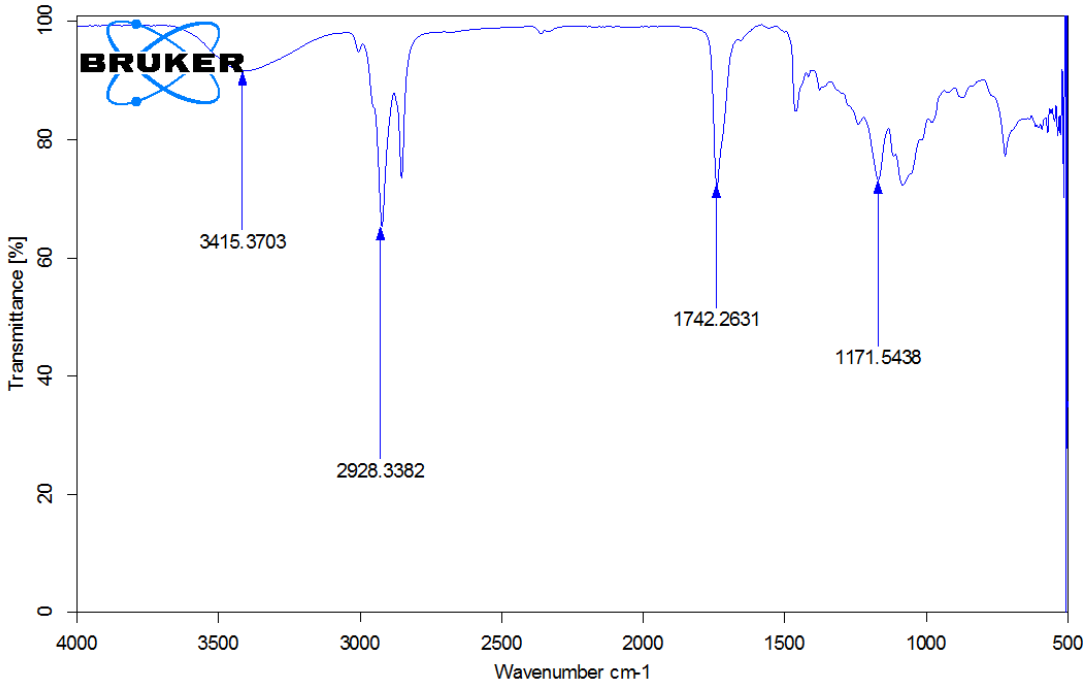

Figure 3.7. FTIR infrared spectra for Span 80.

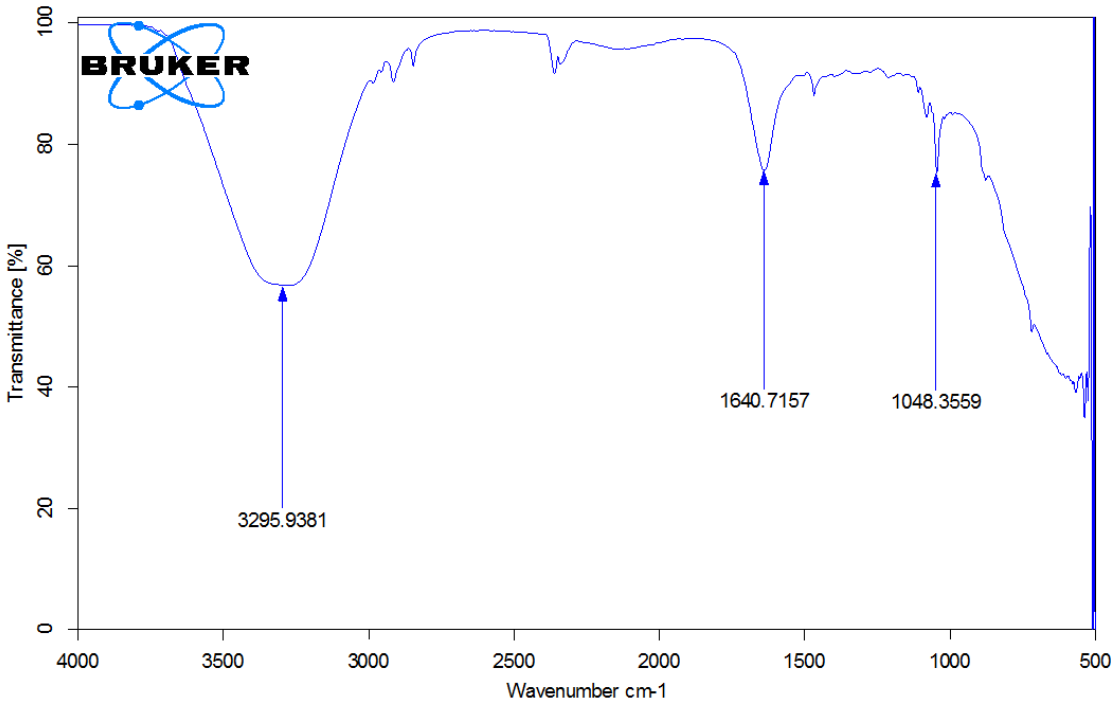

Figure 3.8. FTIR infrared spectra for drug loaded niosome.

3.3.4.3. *In vitro* release studies

In vitro release behaviour from niosomal vesicles is one of the fundamental parameters to determine the safety and efficacy of the delivery system. It is also extremely important for both regulatory and quality control requirements in pharmaceutical and cosmetical industry. The drug release can be affected by many factors such as hydration volume, drug concentration, and the nature of the membrane. The drug release profile of GPE from niosomes was illustrated in Figure 3.9, representing a biphasic release. There was an initial burst release of 50% in the first hour then, another 16% sustained release over the following 40 hours. The release data was modelled into 4 different mathematical models; Zero order, First order, Higuchi model and Korsmeyer-Peppas model. The Korsmeyer-Peppas model had the best fit with an R^2 value of 0.92. This model indicates there is a complicated release mechanism likely to include both diffusion and erosion release processes. From the release profiles, it showed that the diffusion of free drug (either GPE or cGP) from solution was fast and nearly complete (> 90%) within 2 hours (data not shown). Compared to the free drug solution, drug release from the niosomal formulation was biphasic, including an initial fast release phase followed by a sustained release phase. About 50% drug was released from the niosomal vesicle over 3 hours. In both cases, the initial rapid release phase was followed by a prolonged release up to

48 hours, and around 70% cumulative release of GPE was observed at the end of 48 hours (a very similar result was observed for cGP). The Korsmeyer-Peppas model is used to analyse the drug release from polymeric dosage form, such as drug release from nanoparticles (174,178,179). Even though this is of course not a polymeric system it would seem other researchers like Ghafelehbashi, and Kumar have also seen a similar release profile and reached similar conclusions (180,181) Sink conditions were met and maintained throughout the experiment. A partial explanation of this phenomena might be attributed to some of the drug being attached to the outside of the niosomal vesicle exhibited by some other researchers as well (182,183). No detectable amounts of degradation were found in the raw data which might indicate that approximately 30% of the niosomes had not released the GPE contents after 48 hours. Future *in vitro* release experiments might benefit from intentionally lysing the leftover niosomes in the compartments to verify the leftover GPE that was not released. Log of the cumulative percentage of drug released from niosomes versus log time was calculated using Korsmeyer-Peppas model equation.

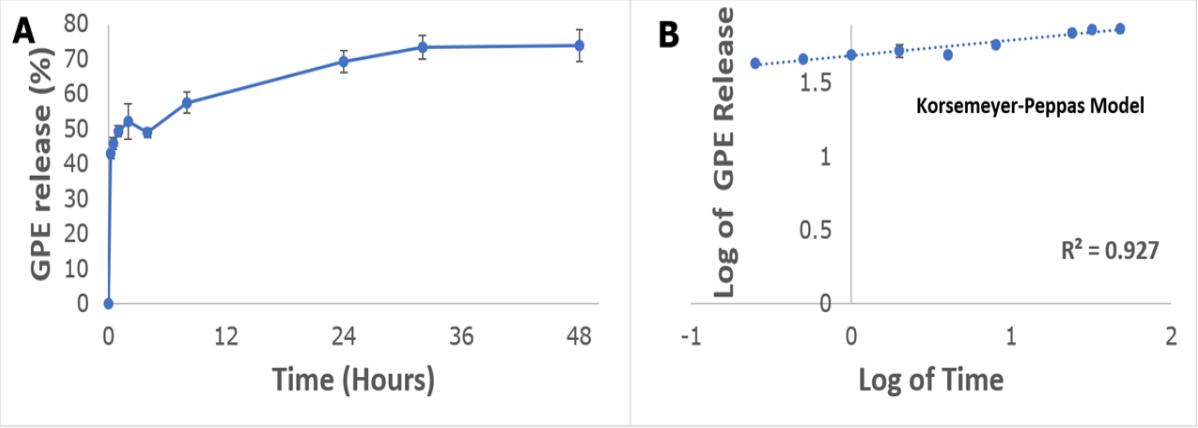

Figure 3.9. Graph A shows the cumulative GPE release (%) from optimised niosomes as a function of time (hours). Graph B shows the log of GPE release against log of time with a linear trendline and an R^2 value of 0.92. (Mean ± SD, n=3).

3.4. Conclusion

In this chapter, GPE and cGP bi-ligand niosomes were developed and optimized via factorial design. Five different variables focusing on drug entrapment efficiency were evaluated and two leading factors were identified and isolated for further optimization by central composite design. Drug-loaded niosomes with the highest entrapment efficiency were created by use of a design of experiments (DOE) strategy. The optimal formulation was Span 80 and CH (total 150 µM) at a molar ratio of 1:1 was used as vesicle components; with DCP at 5 µM as a charge inducer, 10 ml hydration medium containing 0.5 mg of GPE or cGP and hydrated for 30 minutes. After sonication the niosomes created were of suitable size for brain delivery (~250 nm) with decent entrapment efficiency 28.3% for GPE and 68.1% for cGP. *In vitro* release of the optimised formulation showed that the release followed a Korsmeyer-Peppas trend. The release exhibited a biphasic profile with a rapid release followed by slow release over a longer period, making it suitable for sustained drug release. This shows that the formulation exhibits a similar release profile as polymeric systems although this has been seen with niosomal carriers before as well.

In summary, the author found that niosome formulated is a suitable carrier for peptides and optimized the encapsulation strategy. The factorial design was utilised as it enabled the screening of multiple factors with a relatively smaller number of trails, compared with testing each individual factor. Our parameters that were set in both the initial factorial design and central composite design appears limited in nature and this resulted in the relatively low entrapment efficiency for GPE. Although with the instruments and parameters that were available to us this is the optimised formulation that will be used in future experiments. The next chapter of this thesis will evaluate the effectiveness of uptake and transport of the niosomal delivery system in a Caco-2/E12 cell model mimicking GIT transport conditions.

Chapter 4
Evaluation of drug loaded bi-ligand niosomes using GIT Model

4.1. Introduction

Despite enormous advances in brain research, brain and central nervous system disorders remain the world's leading cause of disability and account for more hospitalization and prolonged care than almost all other diseases combined. Individuals over the age of 65 have a one to three percent risk of developing Parkinson's disease (184). Although peptide drugs such as GPE and cGP were reported to have the therapeutic effect of treating stroke, Parkinson's disease, and other neurological disorders. However, their poor stability, poor membrane permeability, and limited oral bioavailability present a significant gap or limitation for research. Scientists have undertaken the challenge of stabilising and delivering protein and peptide drugs via non-invasive and somewhat novel routes such as intranasal, buccal, sublingual, rectal, oral, or ocular delivery. However, the oral route of the administration still prevails as the most popular due to the convenience, cost-effectiveness, patient acceptability, and all correlating with improved patient compliance (185-187). Thus, the scientific challenges for protein and peptide drug delivery are to overcome their inherent weaknesses of large molecular weight, low permeability through biological membranes and mucus layers (physical barrier), surface activity, and susceptibility to degradation by the enzymes in the gastrointestinal tract (a biological barrier) together with short plasma half-life and the tendency to undergo denaturation upon storage. There are many approaches that are used to improve protein and peptide oral bioavailability, such as penetration enhancers, enzymatic inhibitors, and chemical modification methods. Formulation scientists use drug delivery systems as suitable carriers to bypass obstacles and carry them and target delivery to specific locations. Such delivery systems include the use of liposomes, microemulsion, polymeric hydrogels, polymer-based nanoparticles such as chitosan, alginate, hyaluronic acid, poly-alkyl cyanoacrylate, and poly(lactic-co-glycolic acid) (PLGA) nanoparticles (188-190). Compared to all these delivery systems, niosome could offer more potential as the delivery system to deliver protein and peptide drugs orally due to its excellent biodegradability, biosafety, biocompatibility, enhanced cellular penetration, ability to include ligands and providing sustained delivery for the drug candidates (187).

In this chapter, GPE or cGP-loaded niosome was conjugated with both poly-L-arginine (PLR, the cell-penetrating peptides) and RI7 (high-affinity binding to transferrin receptor on the brain). These ligands were chosen to facilitate the endocytosis of the delivery systems

across the intestinal epithelial membrane and actively target drug delivery to the brain. The bi-ligands conjugated niosomes for GPE and cGP were evaluated using human colorectal adenocarcinoma (Caco-2) and HT29-MTX-E12 (E12) co-cultured cells. Caco-2/E12 co-cultured cells show biochemical and morphological similarities to mimic the normal intestinal epithelium. Caco-2/E12 cell model was used over the Caco-2 cell model as it is a more reliable intestinal absorption model which is routinely used to estimate intestinal permeability and cellular uptake mechanism by many other researchers (191-193). They contain several active transporters and metabolic enzymes (194). Specifically, the E12 cells can produce the mucus to create the mucus layer (as one of the physical barriers) that can influence drug transport (195). Therefore, we hypothesized that the niosome carrier, after being conjugated with poly-L-arginine (cell penetrating peptides) will expect not only to protect the neuropeptides from the enzymatical degradation in the gastrointestinal (GI) tract, but also to facilitate them across the epithelial membranes to overcome the physical barrier.

4.2. Chapter Aims

The aims of this chapter are to evaluate the cellular uptake and transport of free and loaded GPE and cGP bi-ligand niosomes towards Caco-2/E12 monolayers and maximize the permeability of the drug candidates.

The specific objectives of this chapter were:

1. To investigate the cellular uptake and transport mechanism of free and loaded GPE bi-ligand niosome in the absence or presence of variable transport inhibitors.
2. To investigate the cellular uptake and transport mechanism of free and loaded cGP bi-ligand niosome in the absence or presence of variable transport inhibitors.

4.3. Experimental Methods

4.3.1. Materials

Dulbecco's Modified Eagle Medium (DMEM) with high glucose, Non-Essential Amino Acid Solution (NEAA), Phosphate-Buffered Saline (PBS), Hank's Balanced Salt Solution (HBSS), Heat-inactivated Fetal Bovine Serum (FBS), trypsin-

ethylenediaminetetraacetic acid (EDTA), penicillin-streptomycin were purchased from Invitrogen (Auckland, New Zealand). Glycine-Proline-Glutamate (GPE), cyclic Glycine-Proline (cGP), Span 80, Tween 20, dimethyl sulfoxide (DMSO), hydroxylamine hydrochloride, tris(2-carboxyethyl)phosphine (TCEP), sodium azide, 3-(4, 5-dimethyl-thiazol-2-yl)-2, 5-diphenyl tetrazolium bromide (MTT), (Sodium tetraborate Succinimidyl-S-acetylthioacetate (SATA), cholesterol (CH) and dihexadecyl phosphate (DCP) were purchased from Sigma-Aldrich (Sigma, USA). Trifluoroacetic acid was purchased from Fluka (Fluka, Germany). Analytical reagent grade methanol and acetonitrile were purchased from Merck (Merck, Germany). DSPE-PEG (1,2-distearoyl-sn-glycero-3-phosphoethanolamine-N-amino(polyethylene glycol)) was purchased from Avanti Polar Lipids (Avanti, USA), CD71 monoclonal antibody (RI7) was purchased from ThermoFisher scientific (Thermofisher, USA), Poly-L-arginine (PLR) was purchased from Alamanda Polymers (Alamanda, USA), Milli-Q water and deionized water was available from the Pharmaceutics Laboratory at the University of Auckland (Auckland, New Zealand). All other reagents and chemicals were of analytical grade.

4.3.2. Analysis of GPE and cGP

GPE and cGP were quantified using a previously developed and validated HPLC method described in Chapter 2. Briefly, both peptides were separated on the C18 HPLC column of Synergi™ Polar-RP C18 Column (250 x 4.6 mm; 4.0 µm particle size) fitted with a guard column. The mobile phase consisted of 3% acetonitrile and 97% Milli-Q water containing 0.025% trifluoroacetic acid to quantify GPE and cGP. A constant flow rate of 1 ml/min was used. The injection sample volume was 50 µl, and the column temperature was maintained at 25°C. The absorbance was determined at 220 nm. All mobile phases were filtered and degassed before use.

4.3.3. Preparation of GPE and cGP loaded bi-ligand niosomes

The fabrication method for GPE and cGP loaded bi-ligand niosomes was described in chapter 3. Briefly, the surfactant, DCP, cholesterol and PLR-PEG will be mixed and dissolved in a 4:1 mixture of chloroform in a round bottom flask. The resultant solution will be rotary evaporated (Laborota 4000, Buchi, Switzerland)) to form a thin, dry film. Then the drug

solution dissolved in PBS will be added to hydrate the dry film to create the drug-loaded niosomes. Hydration was carried out for up to 2 hours under 58°C with constant stirring. The niosomes were left at room temperature for 30 minutes to anneal. The previously prepared RI7 conjugated is then incubated with niosomes in a ratio of 1:2.5 (peptide:lipid) overnight at 4°C. This will result in the niosomes conjugated with both the RI7 and PLR ligands.

4.3.4. Cell culture

Caco-2 cell line was originally obtained from the American Type Culture Collection (ATCC, Rockville, USA). During growth, Caco-2 cells go through processes of proliferation, confluency, and differentiation. They can grow under standard conditions (5% CO_2/95% air) at 37°C, and fully differentiated Caco-2 cells are very similar to normal human enterocytes. Cells of passage number 45-55 were used. Caco-2 cells were cultured in DMEM medium supplemented with 10% FBS, 1% penicillin-streptomycin), 1% NEAA and 2 mM L-glutamine. The Caco-2 cells were grown in cell culture flasks in the incubator (5% CO_2/95% air) at 37°C and exchanged for fresh medium every 2-3 days. Viable cells can be determined by the trypan blue exclusion method. For subculturing, the cells were dissociated with 0.25% trypsin-EDTA, split in a ratio of 1:3. The E12 cell line was purchased from Sigma Aldrich (St. Louis, MO, USA). E12 cells were differentiated into mature goblet cells using methotrexate. They were cultured using the same medium as culturing the Caco-2/E12 cells (see information above). They were also used in the same culture condition (i.e., 5% CO2, 95% relative humidity, at 37°C) and exchanged fresh medium every 2-3 days. When Caco-2 cells and E12 cells grew up to 80-90% confluency, Caco-2 and E12 cells with a ratio of 3:1 were transferred to a new flask for co-culturing to carry out the cellular uptake and transport experiments. The co-cultured cells reach 90% confluence in about 21 days (194,195).

4.3.4.1. GIT co-culture cell model

To carry out the transport studies, Caco-2/E12 cells with a density of 1×10^5 cells/cm^2 were seeded on the apical side of the Transwell® inserts (0.4 μm pore diameter, 1.13 cm^2 area) to allow cell attachment and proliferation, as shown on Figure 4.1. The apical chamber of the insert could hold 0.5 ml cell culture medium, and the basolateral chamber could hold 1.5 ml medium. The cells were grown in DMEM until cell confluency is reached and TEER values

were taken before initiating experiment. Figure 4.1 is a schematic diagram of a completed Transwell® insert with Caco-2/E12 cells seeded on the apical side of the Transwell® membrane.

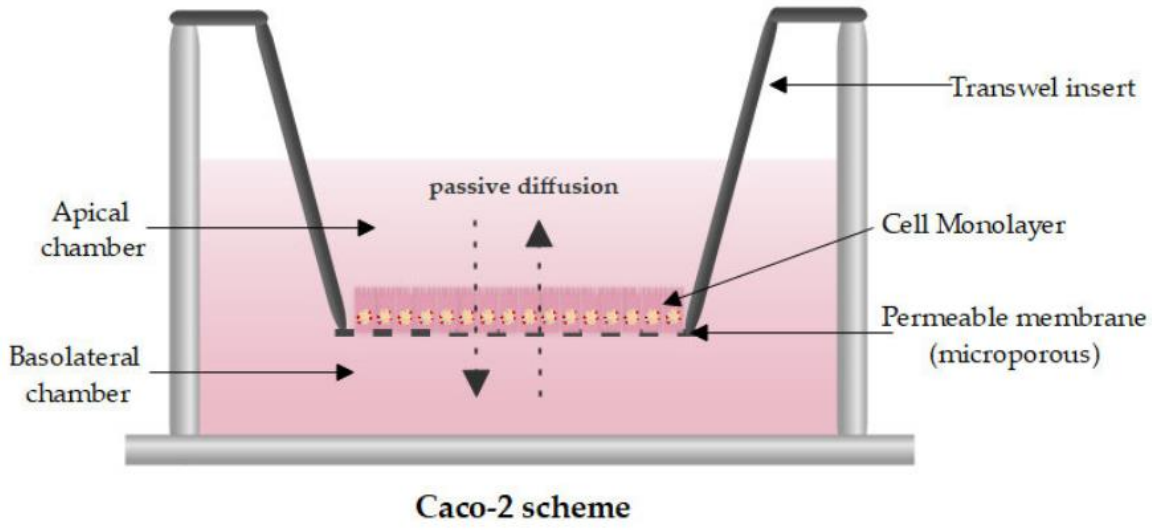

Figure 4.1. Diagram of a Transwell® insert indicating where Caco-2/E12 cells will be seeded.

4.3.4.2. TEER Measurement

Transepithelial/endothelial electrical resistance (TEER) measured with epithelial Volt/Ohm (TEER) Meter (World Precision Instruments, USA) is a useful method for assaying *in vitro* tissue barrier integrity (such as BBB integrity) in a non-invasive manner. TEER measurements can be performed by applying the electrodes on both sides of a cellular monolayer to measure the voltage and current and calculate the electrical resistance of the barrier in $\Omega.cm^2$. TEER was checked routinely throughout the experiments specifically before and after any trails to maintain consistency and repeatability.

4.3.5. Cytotoxicity studies

Before carrying out the drug cellular uptake and transport studies, the concentrations of the drug candidate must be within the safe dosage range for the cells. Therefore, the cytotoxicity of the drug and drug-loaded formulations on the cells should be investigated. The cytotoxicity of free and loaded GPE and cGP niosomes toward the Caco-2/E12 co-cultured cells were examined using a 3-(4, 5-dimethyl-thiazol-2-yl)-2, 5-diphenyl tetrazolium bromide (MTT) assay for the assessment of cell viability. Briefly, 10^4 cells/cm^2 per well were

subcultured into 96-well plates (Corning, New York, USA). After cells were confluent, the medium was replaced with a serum-free medium containing various concentrations of GPE, cGP, and the corresponding drug-loaded niosome formulations. In contrast, cells were treated with the serum-free medium as a control group. After the 8 hours incubation, 20μL of MTT (5 mg/mL in the serum-free medium) was added to each well, and then the cells were incubated for another 4 hours at 37°C. The supernatants were removed, and the precipitates were solubilised using a small amount of dimethyl sulfoxide (DMSO), then shaking for 15 minutes. The MTT assay assessed cell viability by measuring the enzymatic reduction of yellow tetrazolium MTT to a purple formazan at 570 nm using a SpectraMax Plus 384. The percentage of cell viability was then calculated and compared with positive and negative controls on the same plate. Concentrations within the safe range of cell viability for the specific drug or formulation were applied in all future cell experiments.

4.3.6. Cellular uptake studies for GPE or cGP loaded bi-ligand niosomes

To carry out the cellular uptake study, Caco-2/E12 cell suspension at a density of 1×10^5 cells/cm^2 were seeded onto Petri dishes (60 mm diameter, Corning, New York, USA) to allow cell attachment and proliferation. To promote cell growth, the DMEM was changed every three days. When the cells reached about 90% confluence, the culture medium was replaced with HBSS and incubated for 30 minutes before the uptake experiment. Then, the medium was replaced with a range of concentrations for GPE, cGP solution, or drug-loaded niosomal suspension and incubated up to 2 hours at 37°C to investigate the effect of temperature and drug concentrations on the cellular uptake.

For the time-dependent uptake experiments, the fresh HBSS medium was replaced by solution of GPE, cGP or drug-loaded niosomal suspension, which contained variable drug concentrations. The drug-loaded Petri dishes were incubated for a large range of time points (5, 15, 30, 45, 60, 90 and 120 minutes) at 37°C. To determine the effect of temperature, uptake studies were also carried out in a 4°C environment for 120 minutes. To terminate the cellular uptake the HBSS medium that contained the drug was promptly removed, which means in the system the only drug left is the amount that has already been taken into the cells. After medium removal, the cells were immediately washed with PBS buffer five times and the cells were physically removed using a cell scraper (BD Biosciences, USA). The cell mixture was then

transferred to an Eppendorf tube, containing lysis medium. The resulting suspension was centrifuged for 15 minutes to separate the supernatants and the heavy cell pellets. The supernatant was quantified via HPLC (as described in Chapter 2) to determine the amount of drug which has not been uptaken by the cells. To establish the protein concentration involved in the cells, sodium hydroxide was used to dissolve the cell pellets. The solution was then subjected to a bicinchoninic acid (BCA) protein assay (Thermo Scientific, Waltham, USA) to determine the amount of protein in the cells. This is important as the amount of protein is directly related to the number of cells and even when the Petri dishes are accurately seeded with the same number of cells, variations can and do occur. Assessing the amount of protein allows us to accurately express cell uptake as amount of drug (µg) uptake per mg cell protein, which is the more applicable method of presenting the data. This is all summarised in Figure 4.2.

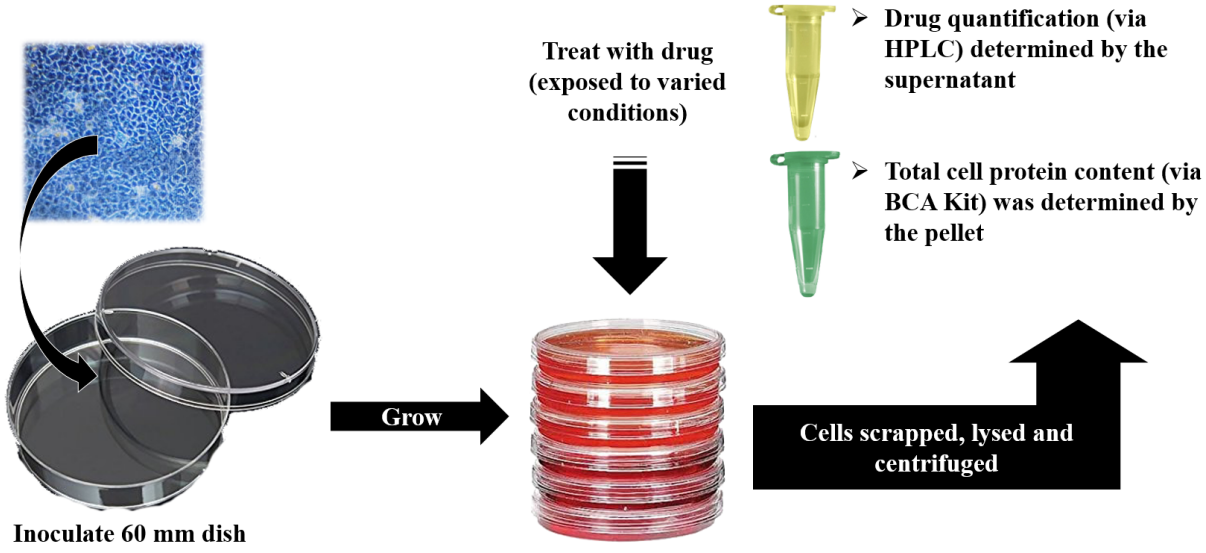

Figure 4.2. Summary diagram of the steps required to carry out the cellular uptake experiments.

4.3.7. Cellular uptake mechanism studies for GPE or cGP loaded bi-ligand niosomes

To investigate the cellular uptake mechanism of GPE or cGP bi-ligand niosomes, the Caco-2/E12 co-culture cells were incubated into Petri dishes and exposed to various conditions. To evaluate the effect of concentration on cellular uptake, cells were incubated with solution of GPE, cGP or drug-loaded niosomal suspension at 37°C for 120 minutes with GPE or cGP.

To evaluate the effect of temperature on cellular uptake, cells were incubated with solution of GPE, cGP or drug-loaded niosomal suspension at 4°C and 37°C for 0, 5, 15, 30, 45, 60, 90 and 120 minutes. To determine the uptake mechanism variable inhibitors (sodium azide, chlorpromazine, protamine sulfate and filipin) were dissolved in the niosomal suspension before adding to the cells and incubating for 120 mins at 37°C. Both positive (GPE or cGP solution, with no inhibitor) and negative (solution with no drug) controls were also used for comparison, incubated with the same conditions.

4.3.8. Cellular transport studies for GPE and cGP bi-ligand niosomes

Transport experiments were performed on in vitro co-culture GIT model (i.e., Caco-2/E12 co-cultured cells) in 12-well Transwell® inserts (detailed in section 4.3.4.1). The Caco-2/E12 cells were cultured for about 14 days at 37°C in an atmosphere of 5% CO_2 and 95% relative humidity before starting the transport study. Every 3 days, the DMEM medium was replaced in both the apical and basolateral chamber and the TEER was measured using a Millicell®-ERS system to monitor the Cell membrane integrity. The monolayers with TEER values higher than 400 $\Omega.cm^2$ were used for the transport study. The medium in the apical and basolateral chambers were replaced with pre-warmed HBSS buffer, and the cells were allowed to equilibrate at 37°C for 30 min before the study. The apical chamber medium was then replaced with solution of GPE, cGP or drug-loaded niosomal suspension at a 100 µg/mL concentration and maintained at 37°C. At 0.5, 1, 1.5, 2 and 3 hours, an aliquot of the sample was removed from the basolateral chamber, and an equal volume of HBSS buffer was filled back in. Niosomes not loaded with any drug (unloaded niosomes) were used as a negative control to assess any significant HPLC result interference. There is a chance that the niosome components (without any drug) can interact with the cells/cell media and interfere with the HPLC results, so we had a negative control to check for this. The amount of GPE or cGP that was transported is determined using HPLC (developed and validated in Chapter 2). The cumulative amount of GPE and cGP transported across the cell membrane was determined, and the transport rate flux and the permeability coefficient (P_{app}) were also calculated (196). The Flux was expressed in µg/min/cm^2 and calculated using the equation:

$$\boldsymbol{Flux = (dM/dt) - A}$$ Equation 4.1

The dM/dt is the cumulative amount of drug in the basolateral side per unit time (μg/min), and A is the surface area of the insert membrane used (1.13 cm^2). The P_{app} was expressed in cm/s and C_i is the initial concentration and is calculated by:

$$\boldsymbol{P_{app} = (dM/dt)/\,(60 \times A \times C_i)}$$ Equation 4.2

4.4. Statistical analysis

All results from cellular uptake and transport are presented as mean ± SD with at least three replicates. A statistical analysis of one-way ANOVA followed by Turkey-test were used to evaluate any significant differences between the treatment and the control groups (SigmaStat 3.5, Systat Software, USA), with the level of significance of $p < 0.05$.

4.5. Results and discussion

4.5.1. *In vitro* cytotoxicity studies towards Caco-2 cells

To determine the cytotoxicity of a drug, in vitro cytotoxicity studies are carried out and expressed as a percentage of viable cells when compared to the control with no drug added (i.e., no potential toxicity), a negative control is also taken into consideration with no cells present. Figure 4.4 showed the percentage of cell viability of Caco-2 cells retained was around 100% for both GPE and cGP for concentrations up to 15 mM. This phenomenon of having more than 100% viability has been seen in other studies and is attributed to the fact that drugs used promoted cell growth and division (e.g., antioxidants) (197,198). Both GPE and cGP appear to increase cell viability due to their neurotrophic functions associated with IGF-1. When the cells were exposed to the corresponding niosomal formulations cell viability decreased to about 60% at 10 mM concentration. There was no significant difference ($p > 0.05$) compared to both GPE and cGP solution and its niosome suspension after 24 hours incubation with Caco-2 cells at the corresponding drug concentration of 5 mM. This shows that as long as we keep the niosome concentrations below 5 mM, no significant toxicity will be experienced after 24 hour incubation. This shows that both the peptide drugs and the niosomal components are biocompatible at these acceptable concentrations.

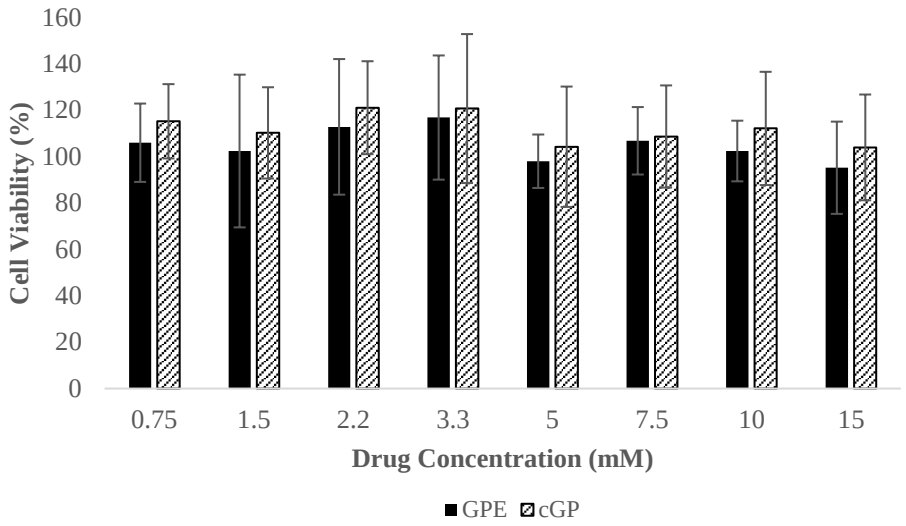

Figure 4.3. Cytotoxicity of GPE or cGP on Caco-2/E12 cells for 8 hours. (Mean ± SD, n=5)

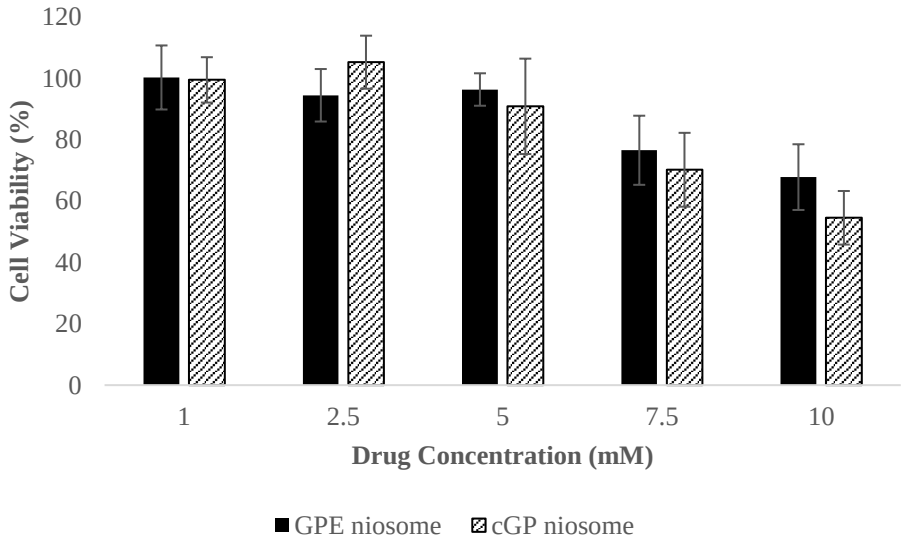

Figure 4.4. Cytotoxicity of GPE or cGP loaded bi-ligand niosomes on Caco-2/E12 cells for 8 hours (Mean ± SD, n = 5).

4.5.2. *In vitro* cellular uptake studies towards Caco-2 cells

The cellular uptake experiments were investigated and quantified by both HPLC and BCA assay methods. The uptake was evaluated on whether the mechanism is concentration-dependent, time dependent and/or temperature dependent.

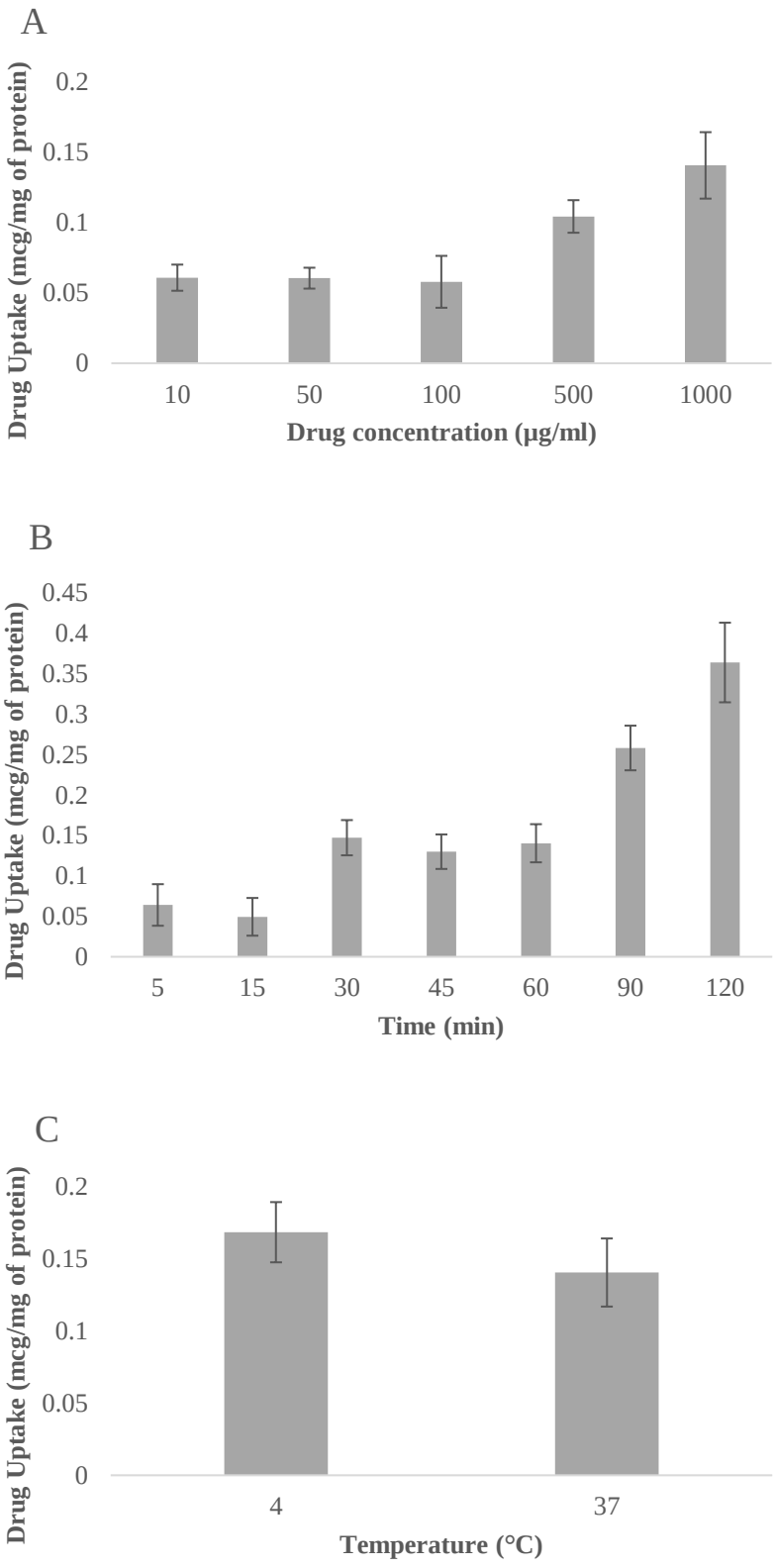

Figure 4.5. GPE uptake study at variable conditions on Caco-2 cells. **A** shows the concentration dependent effect on uptake, **B** shows the time dependent effect on uptake, **C** shows the temperature dependent effect on uptake (Mean ± SD, n = 3).

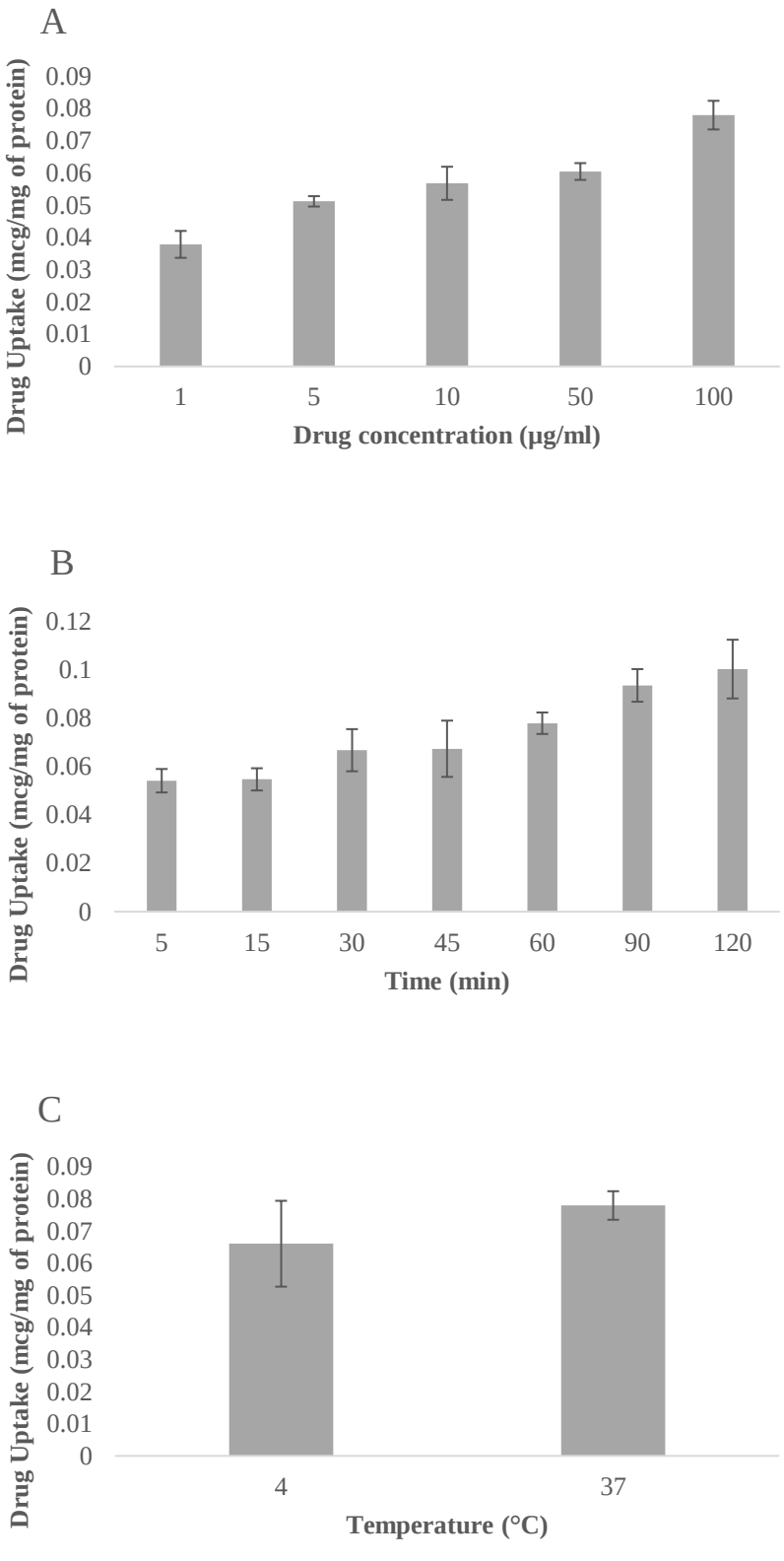

Figure 4.6. cGP uptake study at variable conditions on Caco-2 cells. **A** shows the concentration dependent effect on uptake, **B** shows the time dependent effect on uptake, **C** shows the temperature dependent effect on uptake (Mean ± SD, n = 3).

The highest amount of GPE or cGP present within the cells was when the highest concentration of GPE (1000 µg /ml) or cGP (100 µg/ml) was used. Figure 4.5A and 4.6A showed the uptake of GPE and cGP were proportional to the concentration, therefore the uptake of GPE and cGP was concentration dependent. With the current results we cannot definitively conclude that the highest concentration used the uptake has become saturated. Figure 4.5B and 4.6B showed the uptake of GPE or cGP were also proportional to incubation time. A time-dependent manner was observed for the uptake with longer incubation time the larger amount of drug was uptaken. Figures 4.5 and 4.6 both revealed that drug uptake had not been saturated after 120 mins of incubation. There seem to be no linear increase in uptake between 30 minutes and 60 minutes, this is most likely due to statistical error in the results. Figure 4.5C and 4.6C both showed there was no significant influence of the cellular uptake by either GPE or cGP by temperature, indicating that uptake mechanism is not temperature dependent likely due to no significant energy requirements in this specific uptake process.

Figure 4.7 showed the cellular uptake comparison between GPE or cGP and the corresponding niosomal suspension (with no additional ligands), niosomal suspension with one ligand attached and niosomal suspension with both ligands attached. The rank order of the most effective GPE cellular uptake is bi-ligand niosome ≈ poly-L-arginine (PLR) niosome > niosome (no ligand) ≈ RI7 niosome> free GPE (not encapsulated in niosome). The rank order of the most effective cGP cellular uptake is bi-ligand niosome > niosome (no ligand) > free GPE. More than two fold amount of drug was uptaken in bi-ligand niosome group when compared with free drug, with a very high statistical significance in the difference ($p < 0.01$). These results exhibited that the main driver from GPE uptake into Caco-2/E12 cells is the PLR ligand as there was no statistical significance between the PLR ligand and both ligands. Encapsulating GPE into a niosomal delivery system also significantly improved the uptake when compared with free GPE. As expected, the RI7 ligand seems to have had no effect on the Caco-2/E12 cells as its purpose is specific to the blood brain barrier unlike the nonspecific nature of PLR. Therefore, the bi-ligand niosome has proven to significantly improve drug uptake into the Caco-2/E12 cell lines, of which has significant *in vivo* correlation to have improved absorption in the gastrointestinal tract when compared to free drug not encapsulated into niosomes.

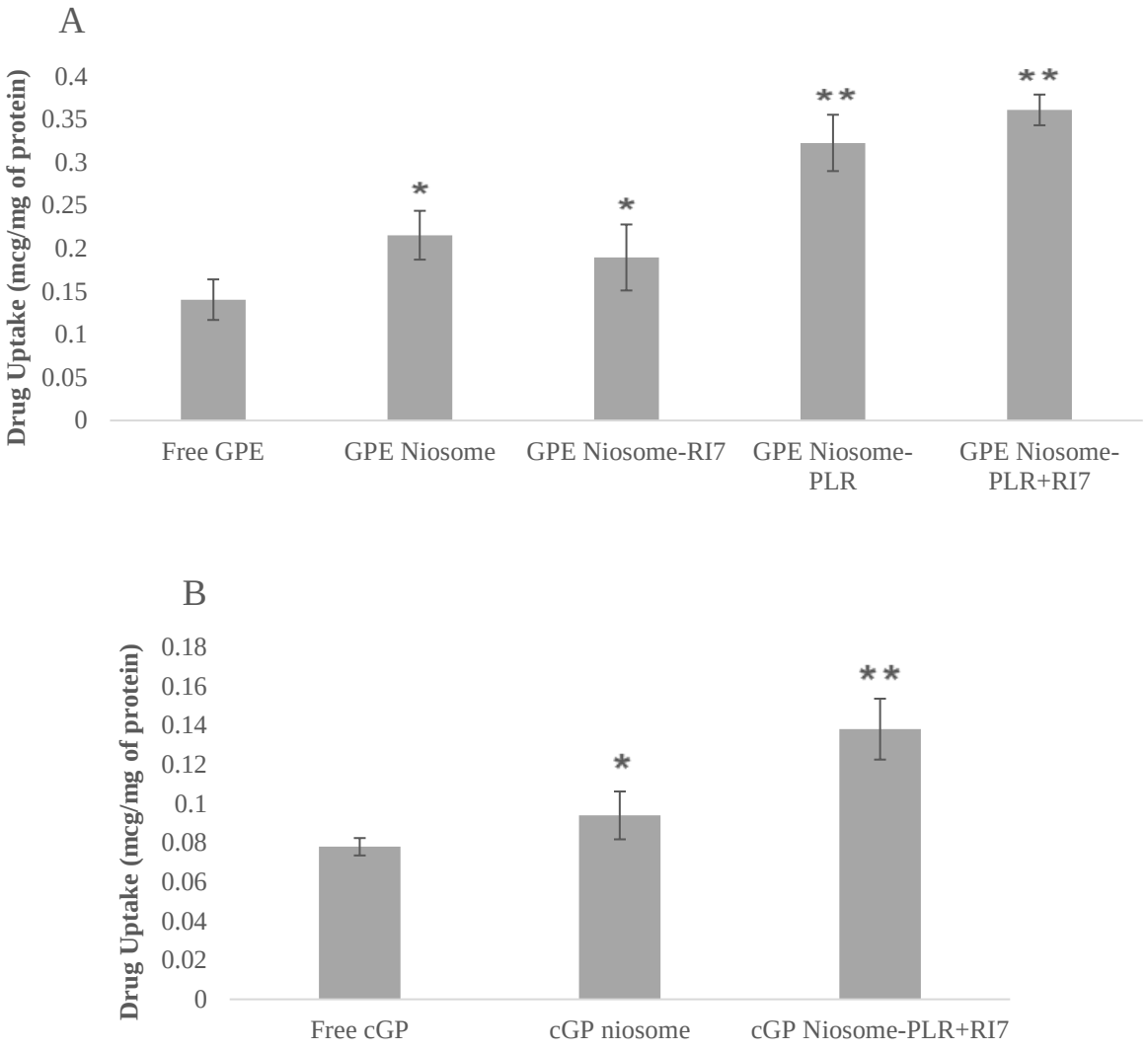

Figure 4.7. Cellular uptake of free and niosomal GPE or cGP niosomes on Caco-2 cells. **A** shows the effect of different ligands on GPE niosomes and Free GPE. **B** shows the effect of different ligands on cGP niosomes and Free cGP. (Mean ± SD, n = 3, *p < 0.05, **p < 0.01)

This model can decently predict future *in vivo* results as shown by previous research including studies by Bettencourt and Gleeson (199,200). The cGP uptake experiments had the same trend as the GPE experiments and proved that this niosomal delivery system was effective in delivering both drugs. Figure 4.8 showed that the uptake mechanism of the niosomal formulation into the Caco-2/E12 cells is time dependent, concentration dependent and temperature dependent. Higher concentrations (up to 100 µg/ml for GPE) and longer time (up to 120 minutes) resulted in larger uptake of drug. It was also observed that a higher temperature (37°C) had a larger amount of drug uptake when compared to colder temperatures (4°C), indicating energy dependent mechanism of uptake.

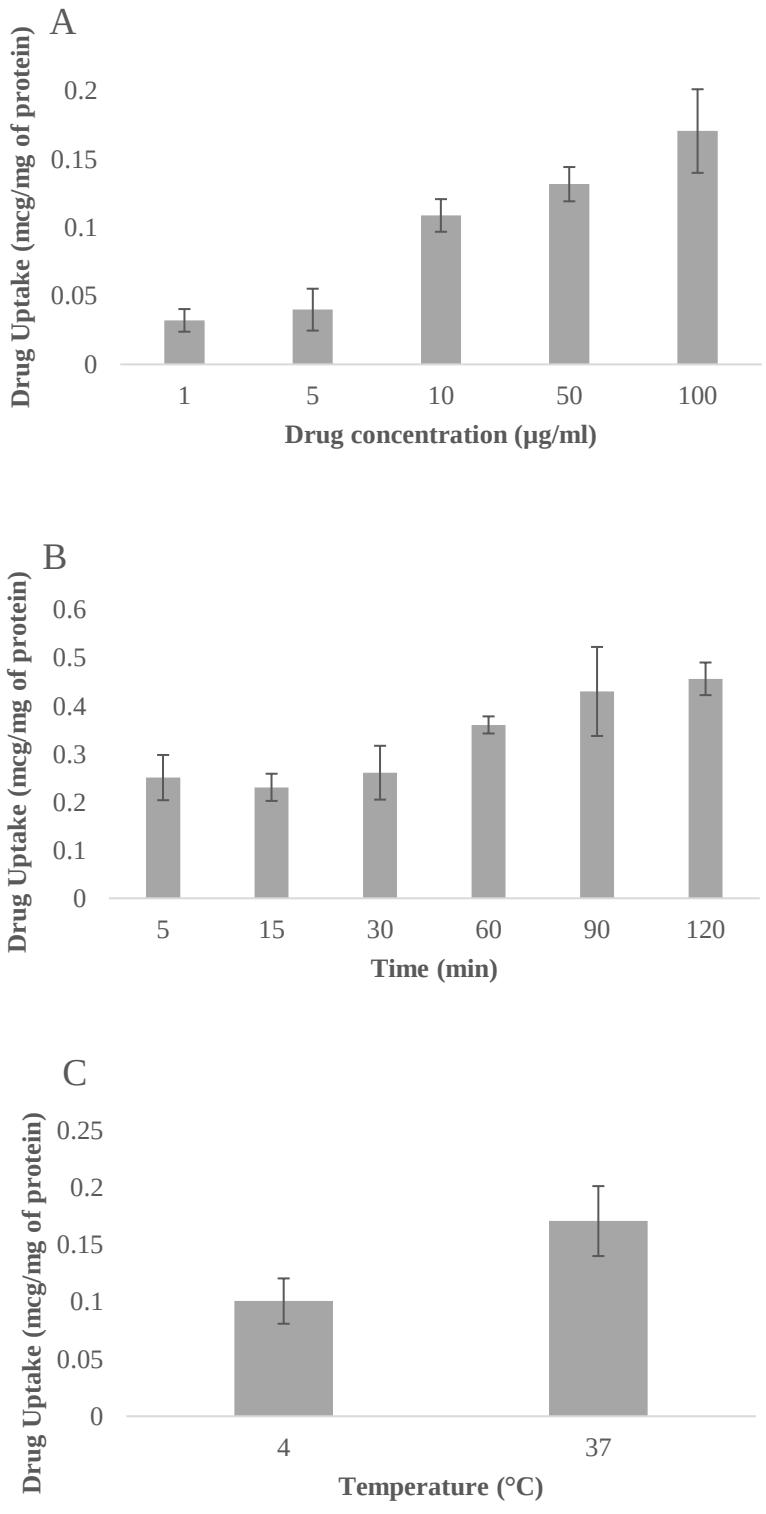

Figure 4.8. GPE niosome uptake study at variable conditions on Caco-2 cells. **A** shows the concentration dependent effect on uptake, **B** shows the time dependent effect on uptake, **C** shows the temperature dependent effect on uptake (Mean ± SD, n = 3).

4.5.3. *In vitro* cellular uptake mechanism studies towards Caco-2 Cells

Figure 4.9 showed the uptake mechanism studies for the free and loaded GPE bi-ligand niosomes in the absence or presence of variable inhibitors. The cellular uptake experiment was carried out at 37ºC for up to 120 minutes of incubation. After adding sodium azide, the active transport inhibitor, the uptake amount of GPE experienced a 3-fold increase when compared to the control group ($p < 0.05$). This result is unexpected but suggests that GPE transport mainly goes through a paracellular pathway that depends on the drug molecular weight and lipophilicity rather than going through the energy dependent active transport pathway. However, cGP uptake is energy-dependent with the addition of sodium azide, the cellular uptake was significantly decreased ($p < 0.05$). Similar results were also seen with sodium azide in the bi-ligand niosomal group, which follow that niosomal uptake is an energy dependent pathway. With separate addition of chlorpromazine (clathrin mediated endocytosis) inhibitor and filipin (caveolae endocytosis inhibitor), the cGP uptake did not significantly change when compared to the control group ($p > 0.05$), whereas the GPE uptake showed significant increase. This indicates that both cGP and GPE uptake is not correlated to the clathrin or caveolae mediated endocytosis pathways (201,202). However, after adding protamine sulfate (adsorptive-mediated endocytosis inhibitor) the GPE uptake was significantly decreased when compared to the control group ($p < 0.05$), but cGP uptake had no statistical significance with the control. This was also seen with the GPE loaded niosome group, as with the addition of protamine sulfate, chlorpromazine, and sodium azide, the cellular uptake amount of GPE was significantly decreased. This demonstrated that the uptake mechanism of the GPE niosomes is at least partially governed by adsorptive mediated, clathrin mediated endocytosis and active transport pathways. The uptake mechanism for GPE is mostly governed by adsorptive mediated endocytosis pathway and mechanism for cGP is mostly governed by active transport pathway.

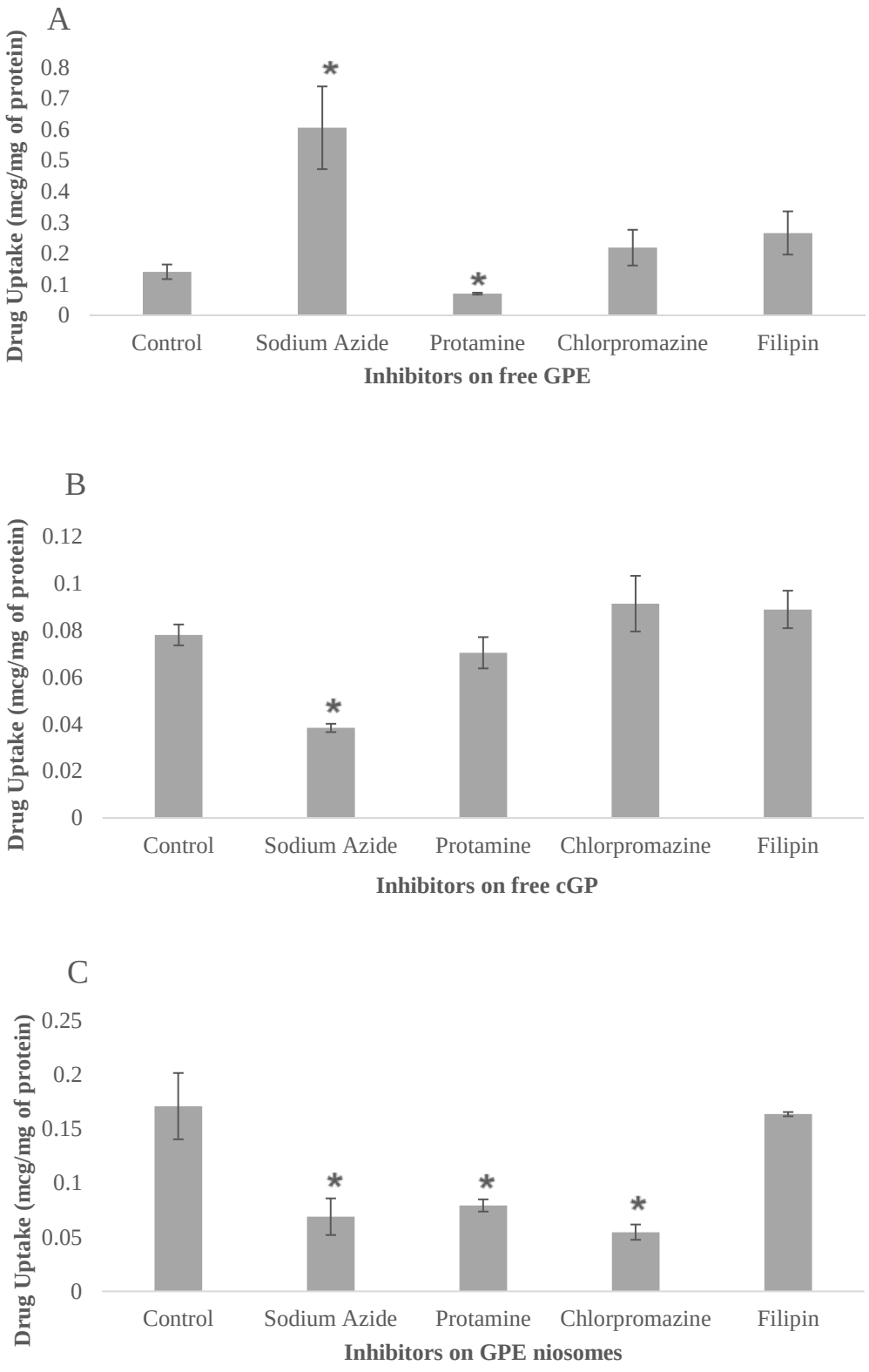

Figure 4.9. Mechanism uptake study with variable inhibitors on Caco-2 cells. **A** shows the inhibitors effect on GPE, **B** shows the inhibitors effect on cGP, **C** shows the inhibitors effect on GPE niosomes (Mean ± SD, n = 3, *p < 0.05).

4.5.4. *In vitro* cellular transport studies towards Caco-2 cells

Transport studies were carried out for both GPE and cGP niosomes (and their corresponding variables) to transport across a GIT model comprising of Caco-2/E12 cells. Unfortunately, no drug was able to be quantified in the basolateral chamber of both the free GPE and cGP and the niosome versions as well. This is quite peculiar as it means that the drug was able to be uptaken into the cell but due to various reasons like degradation, intracellular lysosomal destruction and/or unable to exit the cells, as no drug was able to be found on the basolateral side. We suspect it is a mixture of multiple reasons including but not limited to the sensitivity of our quantification method.

4.6. Conclusion

The cytotoxicity study was carried out using an MTT assay. The results showed whether GPE and cGP drug solution or their drug-loaded bi-ligand niosome counterparts towards Caco-2/E12 cells were a threat to cell viability. At all concentrations tested with both peptides GPE and cGP they showed no statistically significant cytotoxic effects at all. At the higher concentrations of niosome formulation there was a statistically significant decrease in cell viability, but concentrations below 5 mM showed no cytotoxic effects. The range tested did not give enough information to calculate the half-maximal inhibitory concentration (IC_{50}) of the niosome preparation but did give us a range to carry out future experiments effectively with cytotoxicity in mind.

The cellular uptake study showed GPE and cGP uptake was a time- and concentration-dependent mechanism in Caco-2/E12 cells. Furthermore, GPE and cGP loaded bi-ligand niosomes had a 3-fold increase in drug uptake when compared to control group. The active transport, adsorptive-mediated and clathrin mediated endocytosis pathways were the main mechanism of uptake for GPE loaded bi-ligand niosomes. As expected after encapsulation the results showed that the bi-ligand niosomes have altered the uptake process for both GPE and cGP. No detectable amounts of the drug were seen present in the basolateral chamber of the attempted transport studies. The combined results suggests that the niosomes were successfully uptaken by the cells but not fully transported across the cells. The reasons could be plentiful but are likely due to degradation of GPE/cGP and/or the niosomes within the cells.

Chapter 5
Evaluation of drug loaded bi-ligand niosomes using BBB Model

5.1. Introduction

Stroke is a major health issue worldwide. It is also the third greatest cause of death in New Zealand. It contributes to long-term hospitalization or permanent disability for more than 60,000 New Zealanders. A novel neuropeptide, GPE and its analogue (cGP) has shown great potential for the treatment of stroke and improvement of functional recovery in animal models (203). There is also some evidence of attenuating neurological conditions like Alzheimer's and Parkinson's disease. However, being a peptide (as discussed in chapter 4) its oral bioavailability is less than 1% as it is susceptible to the degradation in the gastrointestinal tract and so currently, the parenteral route is the only effective route of administration. Once administered it must then overcome the BBB to reach its site of action, which can be difficult due to degradation and protein binding issues. A formulation that can overcome the limitations of oral delivery and aid transport across the BBB would significantly enhance the utility of this peptide. This provides a means for the drug to be easily administered either as a prophylactic treatment for chronic neurological diseases or long-term aid for post-stroke recovery.

Nevertheless, the major problem for delivering a drug to the brain is the BBB. The BBB can be considered a system of layers of cells connected continuous tight junctions at the level of the cerebral capillary, the choroids plexus, and the arachnoid membrane. These collectively segregate the brain and cerebrospinal fluid (CSF) from the blood and limit foreign substances, including many valuable therapeutic agents to gain access into the brain. In addition to forming the structural elements of the barrier, numerous enzymes present in the BBB have high metabolic activity that make up the enzymatic barrier. These enzymes can rapidly metabolize therapeutic agents or related drugs, decreasing their efficacy. Nanoparticular delivery systems have received great attention to target drug candidates (such as peptide drugs) across the BBB via oral administration (204). These systems serve as novel carriers to the brain by masking the BBB and facilitating drug candidates transport through the epithelial membrane while simultaneously protecting the drug against enzymatic degradation (104).

Drug loaded nanoparticular delivery systems (Nps) can cross the BBB by binding to the inner endothelial cells of brain capillaries and the subsequent transport via passive diffusion driven by a concentration gradient. On the other hand, drug-loaded Nps could enter the brain via phagocytosis through various endothelial uptake methods (205). Drug loaded niosomal delivery systems can offer great potential for both hydrophilic (peptide drugs) and lipophilic

(vitamins) drugs that could be entrapped into niosomes and transported through the BBB by enhancing drug stability and permeability (206). As reported in Chapter 1 there are various methods that can be implemented into a niosomal delivery system to improve drug targeting to the brain. The transferrin receptor is the most widely researched receptor for BBB targeting and is highly expressed in brain endothelial cells. However, the main concern about utilising transferrin as a ligand is the high endogenous transferrin concentrations that nearly saturate the transferrin receptors, potentially limiting efficacy (33). Nonetheless, the RI7 ligand was reported to overcome this concern due to its higher affinity towards transferrin receptors than endogenous transferrin (33). Therefore, utilising a RI7 coupled nanocarrier could enhance the drug concentration in the brain as it specifically can target the BBB. Another ligand is also used in this project the PLR ligand which is a highly effective but nonspecific cell penetrating peptide, to further enhance brain delivery across the BBB. The RI7 and PLR conjugated bi-ligand niosomes have been developed and characterised in chapter 3. In chapter 4, we evaluated the cellular uptake and transport of GPE and cGP in Caco-2/E12 cells as a gastrointestinal model mimicking oral delivery. In this chapter, we attempt to develop an *in vitro* BBB model based on co-culture rat brain microvascular endothelial cells (RBMVECs) and astrocytes and evaluate GPE and cGP cellular uptake and transport.

5.2. Chapter Aims

The aims of this chapter are to evaluate the cellular uptake and transport of free and loaded GPE and cGP the bi-ligand niosomes towards RBMVECs/astrocytes co-cultured cells to maximize the cellular uptake and transport of the GPE or cGP.

The specific objectives of this chapter were to:

1. To investigate the cellular uptake and transport mechanism of free and loaded GPE bi-ligand niosome towards RBMVECs/astrocytes co-cultured cells in the absence or presence of variable transport inhibitors.

2. To investigate the cellular uptake and transport mechanism of free and loaded cGP bi-ligand niosome towards RBMVECs/astrocytes co-cultured cells in the absence or presence of variable transport inhibitors.

5.3. Experimental Methods

5.3.1. Materials

Dulbecco's Modified Eagle Medium (DMEM) with high glucose, Non-Essential Amino Acid Solution (NEAA), Phosphate-Buffered Saline (PBS), Hank's Balanced Salt Solution (HBSS), Heat-inactivated Fetal Bovine Serum (FBS), trypsin-ethylenediaminetetraacetic acid (EDTA), penicillin-streptomycin were purchased from Invitrogen (Auckland, New Zealand). Rat brain microvascular endothelial cells (RBMVECs), rat brain endothelial cell growth media was purchased from Cell Applications, Inc (San Diego, CA, USA). Rat astrocyte cell line was purchased by American Type Culture Collection (ATCC, Rockville, USA). Glycine-Proline-Glutamate (GPE), cyclic Glycine-Proline (cGP), Span 80, Tween 20, dimethyl sulfoxide (DMSO), hydroxylamine hydrochloride, tris(2-carboxyethyl)phosphine (TCEP), sodium azide, 3-(4, 5-dimethyl-thiazol-2-yl)-2, 5-diphenyl tetrazolium bromide (MTT), (Sodium tetraborate Succinimidyl-S-acetylthioacetate (SATA), cholesterol (CH) and dihexadecyl phosphate (DCP) were purchased from Sigma-Aldrich (Sigma, USA). Trifluoroacetic acid was purchased from Fluka (Fluka, Germany). Analytical reagent grade methanol and acetonitrile were purchased from Merck (Merck, Germany). DSPE-PEG (1,2-distearoyl-sn-glycero-3-phosphoethanolamine-N-amino(polyethylene

glycol)) was purchased from Avanti Polar Lipids (Avanti, USA), CD71 monoclonal antibody (RI7) was purchased from ThermoFisher scientific (Thermofisher, USA), Poly-L-arginine (PLR) was purchased from Alamanda Polymers (Alamanda, USA), Milli-Q water and deionized water was available from the Pharmaceutics Laboratory at the University of Auckland (Auckland, New Zealand). All other reagents and chemicals were of analytical grade.

5.3.2. Analysis of GPE and cGP

GPE and cGP were quantified using a previously developed and validated HPLC method described in Chapter 2. Briefly, both peptides were separated on the C18 HPLC column of Synergi™ Polar-RP C18 Column (250 x 4.6 mm; 4.0 µm particle size) fitted with a guard column. The mobile phase consisted of 3% acetonitrile and 97% Milli-Q water containing 0.025% trifluoroacetic acid to quantify GPE and cGP. A constant flow rate of 1 ml/min was used. The injection sample volume was 50 µl, and the column temperature was maintained at 25°C. The absorbance was determined at 220 nm. All mobile phases were filtered and degassed before use.

5.3.3. Preparation of GPE and cGP loaded bi-ligand niosomes

The fabrication method for GPE and cGP loaded bi-ligand niosomes was described in chapter 3. Briefly, the surfactant, DCP, cholesterol and PLR-PEG will be mixed and dissolved in a 4:1 mixture of chloroform in a round bottom flask. The resultant solution will be rotary evaporated (Laborota 4000, Buchi, Switzerland)) to form a thin, dry film. Then the drug solution dissolved in PBS will be added to hydrate the dry film to create the drug-loaded niosomes. Hydration was carried out for up to 2 hours under 58°C with constant stirring. The niosomes were left at room temperature for 30 minutes to anneal. The previously prepared RI7 conjugated is then incubated with niosomes in a ratio of 1:2.5 (peptide/lipid) overnight at 4°C. This will result in the niosomes conjugated with both the RI7 and PLR ligands.

5.3.4. Cell culture

Astrocytes were cultured in DMEM medium containing 10% FBS and penicillin-streptomycin (100 U/ml and 100 µg/ml, respectively) under the condition of 5% CO_2, 95% air atmosphere at 37°C. Cell culture mediums were changed every 2 to 3 days. When the

astrocytes reached the confluency, the cells were passaged using trypsin-EDTA digestion, and the cell culture medium was collected for the preparation of astrocyte-conditioned medium (ACM). To prepare ACM, the same volume of astrocytes medium was mixed with an equal volume of fresh RBMVECs growth medium. RBMVECs were cultured in collagen coated culture flasks (Biocoat^{TM}). The growth medium to culture RBMVECs which was purchased from Cell Applications Inc (San Diego, USA). The medium contained 10% FBS, variable agents including endothelial cell growth factor (ECGF) (1 ng/ml), insulin (5 µg/ml), transferrin (5 µg/ml), essential and nonessential amino acids, vitamins, trace elements, 100 U/ml penicillin and gentamicin. The RBMVECs were cultured and passaged until carrying out the cellular uptake and transport experiments.

5.3.4.1. BBB co-culture cell model

Before carrying out the transport co-culture work, the Transwell® insert were coated with rat tail collagen. The Collagen solution was prepared by dissolving 2 mg collagen in 1 ml of 0.1% acetic acid. Collagen solution was added to the top of each insert (100 µl per insert)followed by drying at 4°C, this step was repeated for the bottom insert. To begin the experiment, the astrocytes were seeded with the density of $1x10^5$ cells on the bottom side of the insert. The insert was turned over and was transferred into Transwell®, in which the astrocytes were firmly attached to the surface of the membranes. The apical chamber of the insert could hold 0.5 ml cell culture medium, and the basolateral chamber could hold 1.5 ml medium. Two or three days later (enough time for astrocytes to firmly attach), RBMVEC were seeded on the upper side of the insert at a density of $5x10^5$ cells/insert, the apical chamber was fed with ACM cell culture medium and fed the basolateral chamber with the astrocyte growth medium. The cellular uptake and transport experiment would start after RBMVECs reached confluency. Figure 5.1 is a schematic diagram of a completed Transwell® insert with RBMVECs seeded on the apical side and astrocytes seeded in the basolateral side.

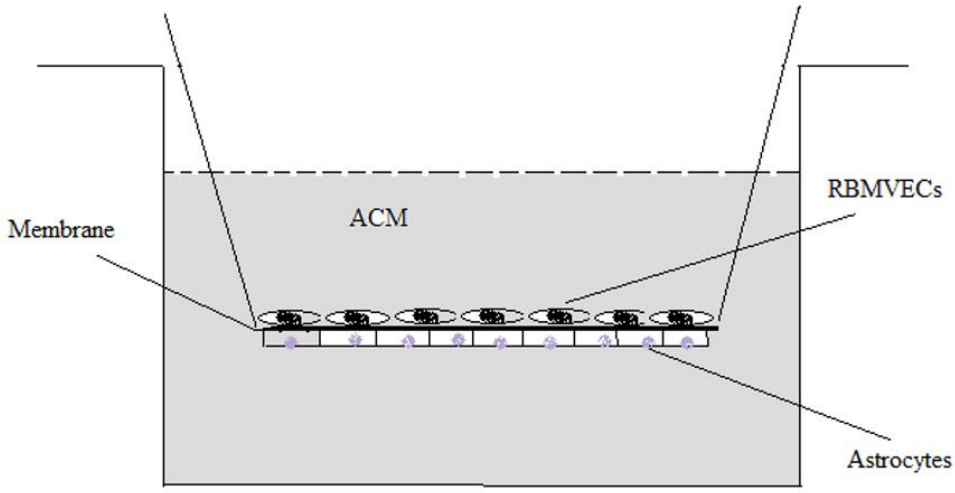

Figure 5.1. Diagram of a Transwell® insert showing RBMVECs seeded on apical side and Astrocytes seeded on basolateral side **(207)**.

5.3.4.2. TEER Measurement

Transepithelial/endothelial electrical resistance (TEER) measured with epithelial Volt/Ohm (TEER) Meter (World Precision Instruments, USA) is a useful method for assaying *in vitro* tissue barrier integrity (such as BBB integrity) in a non-invasive manner. TEER measurements can be performed by applying the electrodes on both sides of a cellular monolayer to measure the voltage and current and calculate the electrical resistance of the barrier in $\Omega.cm^2$. TEER was checked routinely throughout the experiments specifically before and after any trails to maintain consistency and repeatability.

5.3.5. Cytotoxicity Studies

Before carrying out the drug cellular uptake and transport studies, the concentrations of the drug candidate must be within the safe dosage range for the cells. Therefore, the cytotoxicity of the drug and drug-loaded formulations on the cells should be investigated. The cytotoxicity of free and loaded GPE and cGP niosomes toward the RBMVECs were examined using a 3-(4, 5-dimethyl-thiazol-2-yl)-2, 5-diphenyl tetrazolium bromide (MTT) assay for the assessment of cell viability. To begin, the 96-well plates (Corning, New York, USA) were coated with collagen solution and dried before each well was seeded 10^4 cells/cm^2. After cells were confluent, the medium was replaced with a serum-free medium containing various

concentrations of GPE, cGP, and their corresponding niosome formulations. In contrast, cells were treated with the serum-free medium as a control group. After the 8 hours incubation, 20μL of MTT (5 mg/mL in the serum-free medium) was added to each well, and then the cells were incubated for another 4 hours at 37°C. The supernatants were removed, and the precipitates were solubilised using a small amount of dimethyl sulfoxide (DMSO), then shaking for 15 minutes. The MTT assay assessed cell viability by measuring the enzymatic reduction of yellow tetrazolium MTT to a purple formazan at 570 nm using a SpectraMax Plus 384. The percentage of cell viability was then calculated and compared with positive and negative controls on the same plate. Concentrations within the safe range of cell viability for the specific drug or formulation were applied in all future cell experiments.

5.3.6. Cellular uptake studies for GPE or cGP loaded bi-ligand niosomes

To carry out the cellular uptake study, RBMVEC suspension at a density of 1×10^5 cells/cm^2 were seeded onto collagen coated Petri dishes (60 mm diameter, Corning, New York, USA) to allow cell attachment and proliferation. To promote cell growth, the RBMVECs growth medium was changed every three days. When the cells reached about 90% confluence, the culture medium was replaced with HBSS and incubated for 30 minutes before the uptake experiment. Then, the medium was replaced with a range of concentrations for GPE, cGP solution, or drug-loaded niosomal suspension and incubated up to 2 hours at 37°C to investigate the effect of temperature and drug concentrations on the cellular uptake.

To carry out the time-dependent uptake experiments, the fresh HBSS medium was replaced by solution of GPE, cGP or drug-loaded niosomal suspension, which contained variable drug concentrations. The drug-loaded Petri dishes were incubated for a large range of time points (5, 15, 30, 45, 60, 90 and 120 minutes) at 37°C. To determine the effect of temperature, uptake studies were also carried out in a 4°C environment for 120 minutes. To terminate the cellular uptake the HBSS medium that contained the drug was promptly removed, which means in the system the only drug left is the amount that has already been taken into the cells. After medium removal, the cells were immediately washed with PBS buffer five times and the cells were physically removed using a cell scraper (BD Biosciences, USA). The cell mixture was then transferred to an Eppendorf tube, containing lysis medium. The resulting suspension was centrifuged for 15 minutes to separate the supernatants and the heavy cell

pellets. The supernatant was quantified via HPLC (as described in Chapter 2) to determine the amount of drug which has not been uptaken by the cells. To establish the protein concentration involved in the cells, sodium hydroxide was used to dissolve the cell pellets. The solution was then subjected to a bicinchoninic acid (BCA) protein assay (Thermo Scientific, Waltham, USA) to determine the amount of protein in the cells. This is important as the amount of protein is directly related to the number of cells and even when the Petri dishes are accurately seeded with the same number of cells variations can and do occur. Assessing the amount of protein allows us to accurately express cell uptake as amount of drug (µg) uptake per mg cell protein, which is the more applicable method of presenting the data. This is all summarised in Figure 4.2.

5.3.7. Cellular uptake mechanism studies for GPE or cGP loaded bi-ligand niosomes

To investigate the cellular uptake mechanism of GPE or cGP bi-ligand niosomes, the RBMVECs were incubated into collagen coated Petri dishes and exposed to various conditions. To evaluate the effect of concentration on cellular uptake, cells were incubated with solution of GPE, cGP or drug-loaded niosomal suspension at 37°C for 120 minutes with GPE or cGP. To evaluate the effect of temperature on cellular uptake, cells were incubated with solution of GPE, cGP or drug-loaded niosomal suspension at 4°C and 37°C for 0, 5, 15, 30, 45, 60, 90 and 120 minutes. To determine the uptake mechanism variable inhibitors (sodium azide, chlorpromazine, protamine sulfate and filipin) were dissolved in the niosomal suspension before adding to the cells and incubating for 120 mins at 37°C. Both positive (GPE or cGP solution, with no inhibitor) and negative (solution with no drug) controls were also used for comparison, incubated with the same conditions.

5.3.8. Cellular transport studies for GPE or cGP loaded bi-ligand niosomes

Transport experiments were performed on *in vitro* co-culture BBB model (i.e., RBMVECs/astrocytes co-cultured cells) in 12-well Transwell® inserts (detailed in section 5.3.4.1). To carry out the transport studies, the RBMVECs/astrocytes were cultured for about 8 - 14 days at the same condition described in previous method section. Every 3 days, the apical chamber was fed with ACM cell culture medium and the basolateral chamber is fed with the astrocyte growth medium. The TEER was measured every 3 days using a Millicell®-ERS system to monitor the Cell membrane integrity. The monolayers with TEER values higher than

400 $\Omega.cm^2$ were used for the transport study. The medium in the apical and basolateral chambers were replaced with pre-warmed HBSS buffer, and the cells were allowed to equilibrate at 37°C for 30 min before the study. Apical chamber medium was then replaced with solution of GPE, cGP or drug-loaded niosomal suspension at a 0.1 mg/mL concentration and maintained at 37°C. At 0.5, 1, 1.5, 2 and 3 hours, an aliquot of the sample was removed from the basolateral chamber, and an equal volume of HBSS buffer was filled back to the basolateral chamber. Niosomes not loaded with any drug (unloaded niosomes) were used as a negative control to assess any significant HPLC result interference. There is a chance that the niosome components (without any drug) can interact with the cells/cell media and interfere with the HPLC results, so we had a negative control to check for this. The amount of transported GPE or cGP that was transported is determined using the HPLC (developed and validated in Chapter 2). The cumulative amount of GPE and cGP transported across the cell membrane was determined, and the transport rate flux and the permeability coefficient (P_{app}) were also calculated (196). The Flux was expressed in $\mu g/min/cm^2$ and calculated using equation 4.1. The dM/dt is the cumulative amount of drug in the basolateral side per unit time (µg/min), and A is the surface area of the insert membrane used (1.13 cm^2). The P_{app} was expressed in cm/s and C_i is the initial concentration and is calculated by equation 4.2.

5.4. Statistical analysis

All results from cellular uptake and transport are presented as mean ± SD with at least three replicates). A statistical analysis of one-way ANOVA followed by Turkey-test were used to evaluate any significant differences between the treatment and the control groups (SigmaStat 3.5, Systat Software, USA), with the significance level at $p < 0.05$.

5.5. Results and discussion

5.5.1. *In vitro* cytotoxicity studies towards RBMVECs

Cytotoxicity of free and loaded GPE or cGP bi-ligand niosome to RBMVECs was assessed using MTT assay. Figure 5.2 showed the percentage of cell viability of RBMVECs retained was more than 95% when incubated for 24 hours with GPE and cGP solutions up to 15 mM. Figure 5.3 showed the cell viability for the niosome counterparts' and significant cytotoxicity was observed in higher concentrations above 7.5 mM reaching as low as 38%. There was no significant difference ($p > 0.05$) compared to GPE solution and its niosome suspension after 24 hours incubation with RBMVECs at drug concentration of 5mM and lower. Similarly, there was no significant difference ($p > 0.05$) compared cGP solution and its niosome suspension after 24 hours incubation with RBMVECs at the drug concentration of 5 mM and lower. Compared to all the results, no significant cytotoxicity after 24 hours incubation at 5 mM (or lower) which indicates the biocompatibility of the excipients in the niosomes and the safety of the drug candidates within this range.

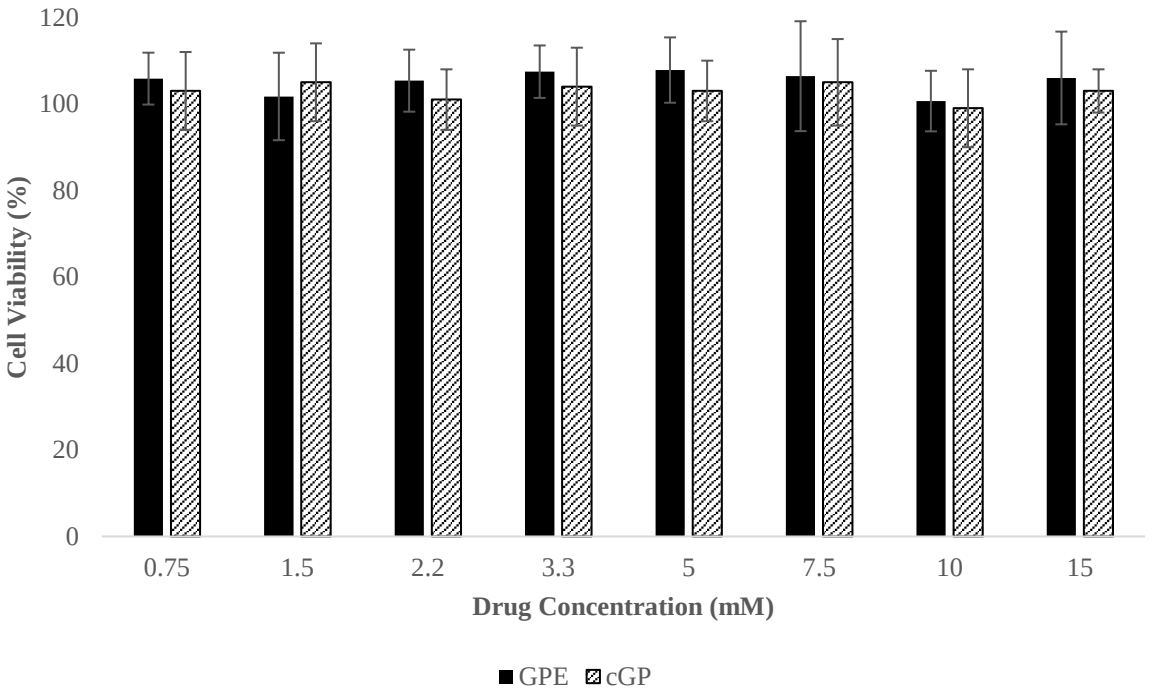

Figure 5.2. Cytotoxicity of GPE or cGP on RBMVECs for 8 hours. (Mean ± SD, n=5)

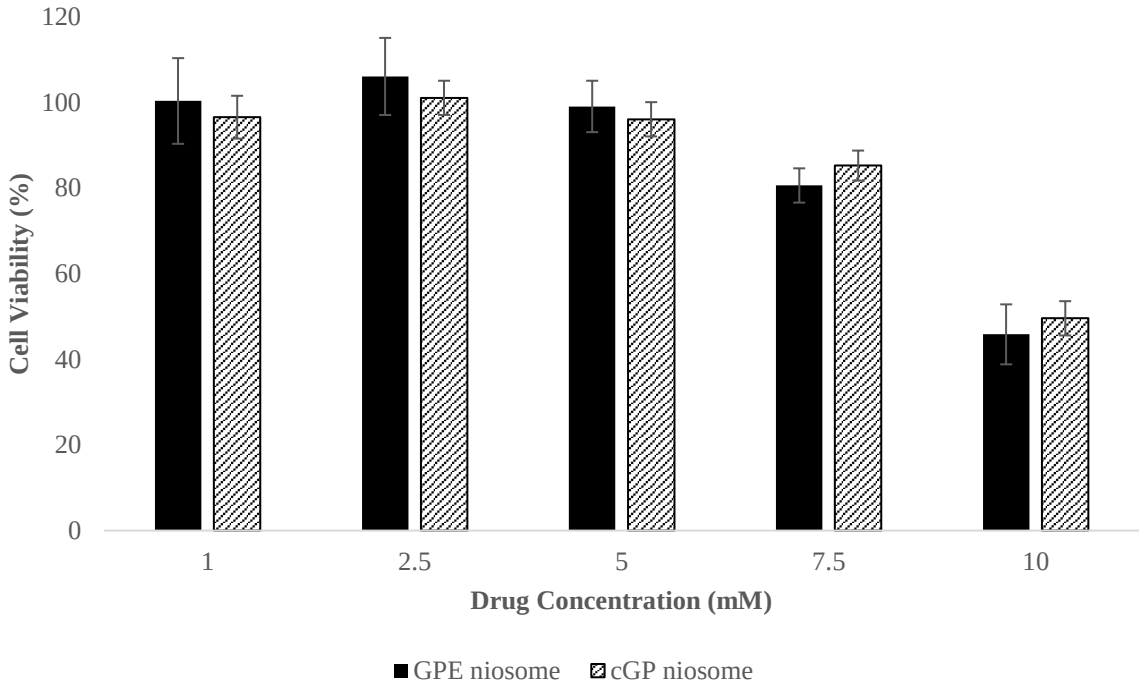

Figure 5.3. Cytotoxicity of GPE or cGP loaded bi-ligand niosomes on RBMVECs for 8 hours (Mean ± SD, n = 5).

5.5.2. *In vitro* cellular uptake studies towards RBMVECs

The cellular uptake of GPE and cGP by RBMVECs was investigated and quantified by HPLC and BCA assay. Figure 5.4A showed the uptake of GPE was concentration dependent with more drug uptake observed with higher amounts of GPE present (up to 1000 µg/ml). As there is no statistically significant difference between 500 µg/ml and 1000 µg/ml, uptake is likely saturated at 500 µg/ml. Figure 5.4B also showed the uptake of GPE by RBMVECs was time-dependent with more drug uptake observed with longer the uptake time (up to 120 minutes), with no deductions can be made if the transport is saturated. A very similar trend was found in Chapter 4 when carried out the uptake used Caco-2 cells. Figure 5.3C showed the uptake of GPE by RBMVECs was energy (temperature) dependent with less drug uptaken at colder temperatures (4°C vs 37°C).

Figure 5.5A showed the uptake of cGP was concentration-dependent up to 50 µg/ml. The amount uptaken seemed to be a linear increase until the 50 µg/ml which also indicated that it may be saturated as there was no statistical difference between 50 µg/ml and 100 µg/ml. Figure 5.5B also showed the uptake of cGP by RBMVECs was time-dependent as with longer uptake time, higher amount of drug was uptaken. The data suggests the uptake was saturated at 60 minutes; this is markedly different from the data received from Caco-2 cells in Chapter 4 where saturation could not be deduced up until the 120th minute. As expected in Figure 5.4C, temperature also has a significant impact on the uptake of cGP as in colder environments (4 °C vs 37 °C) the uptake was significant slower, which indicates the energy (temperature) dependent uptake involved in this uptake pathway.

Figure 5.6 A and B showed the cellular uptake comparison between either GPE or cGP and the corresponding niosomal suspension (with no additional ligands), niosomal suspension with one ligand attached and niosomal suspension with both ligands attached. The rank order of GPE cellular uptake by RBMVECs is bi-ligand ≈ poly-L-arginine (PLR) > RI7 > niosome (no ligand) ≈ free GPE. The rank order of cGP cellular uptake is bi-ligand > niosome (no ligand) > free cGP. Both formulations of GPE and cGP significantly increased the amount of drug uptaken into the RMBVECs when compared to control ($p < 0.01$). There was more than 2.5 times increase in uptake with the GPE bi-ligand niosome and more than 3 times increase with the cGP bi-ligand niosome.

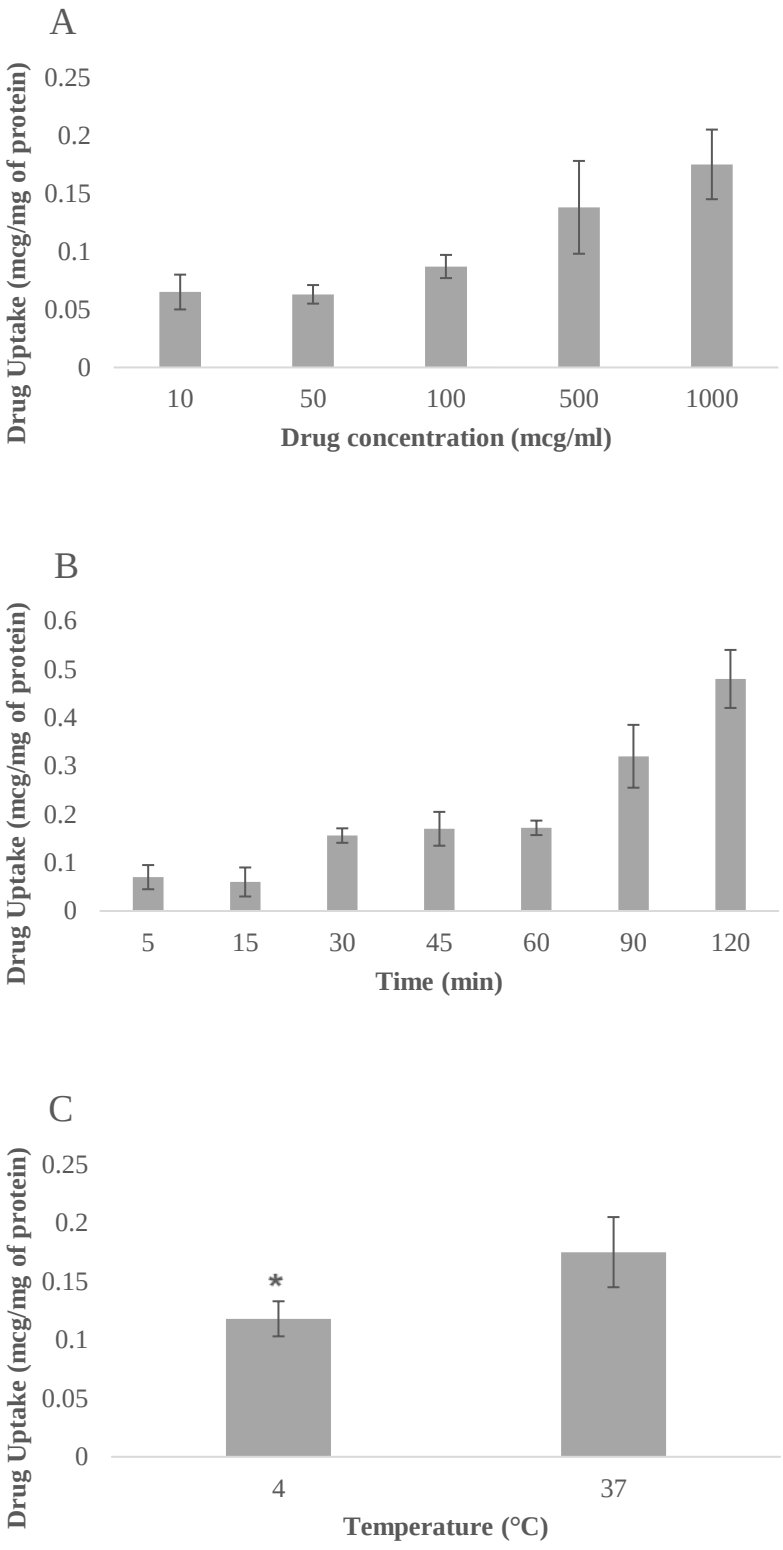

Figure 5.4. GPE uptake study at variable conditions on RBMVECs. A shows the concentration dependent effect on uptake, B shows the time dependent effect on uptake, C shows the temperature dependent effect on uptake (Mean ± SD, n = 3, *$p < 0.05$).

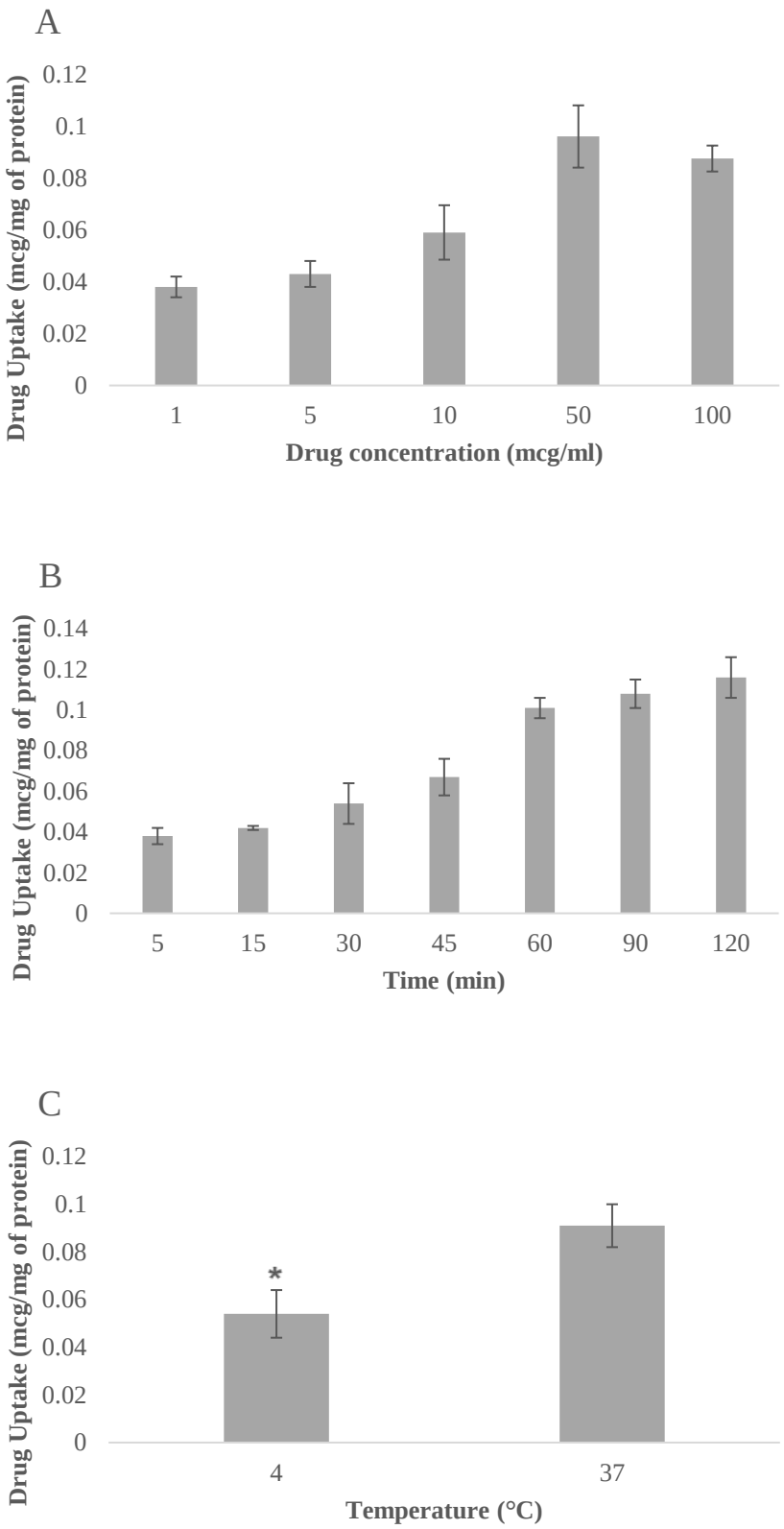

Figure 5.5. cGP uptake study at variable conditions on RBMVECs. A shows the concentration dependent effect on uptake, B shows the time dependent effect on uptake, C shows the temperature dependent effect on uptake (Mean ± SD, n = 3, *$p < 0.05$).

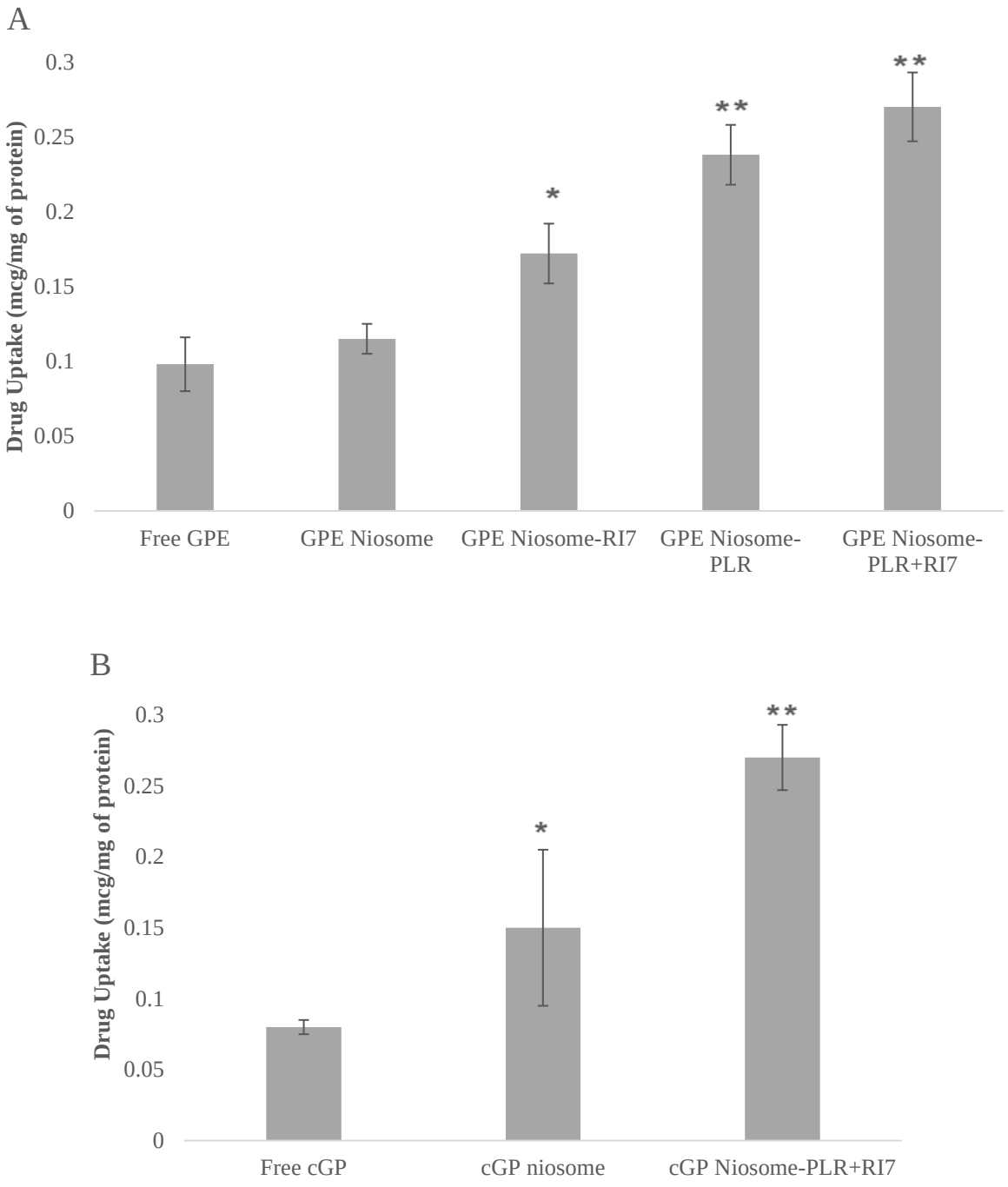

Figure 5.6 Cellular uptake of free and niosomal GPE or cGP niosomes on RBMVECs. **A** shows the effect of different ligands on GPE niosomes and Free GPE. **B** shows the effect of different ligands on cGP niosomes and Free cGP. (Mean ± SD, n = 3, *p < 0.05, **p < 0.01)

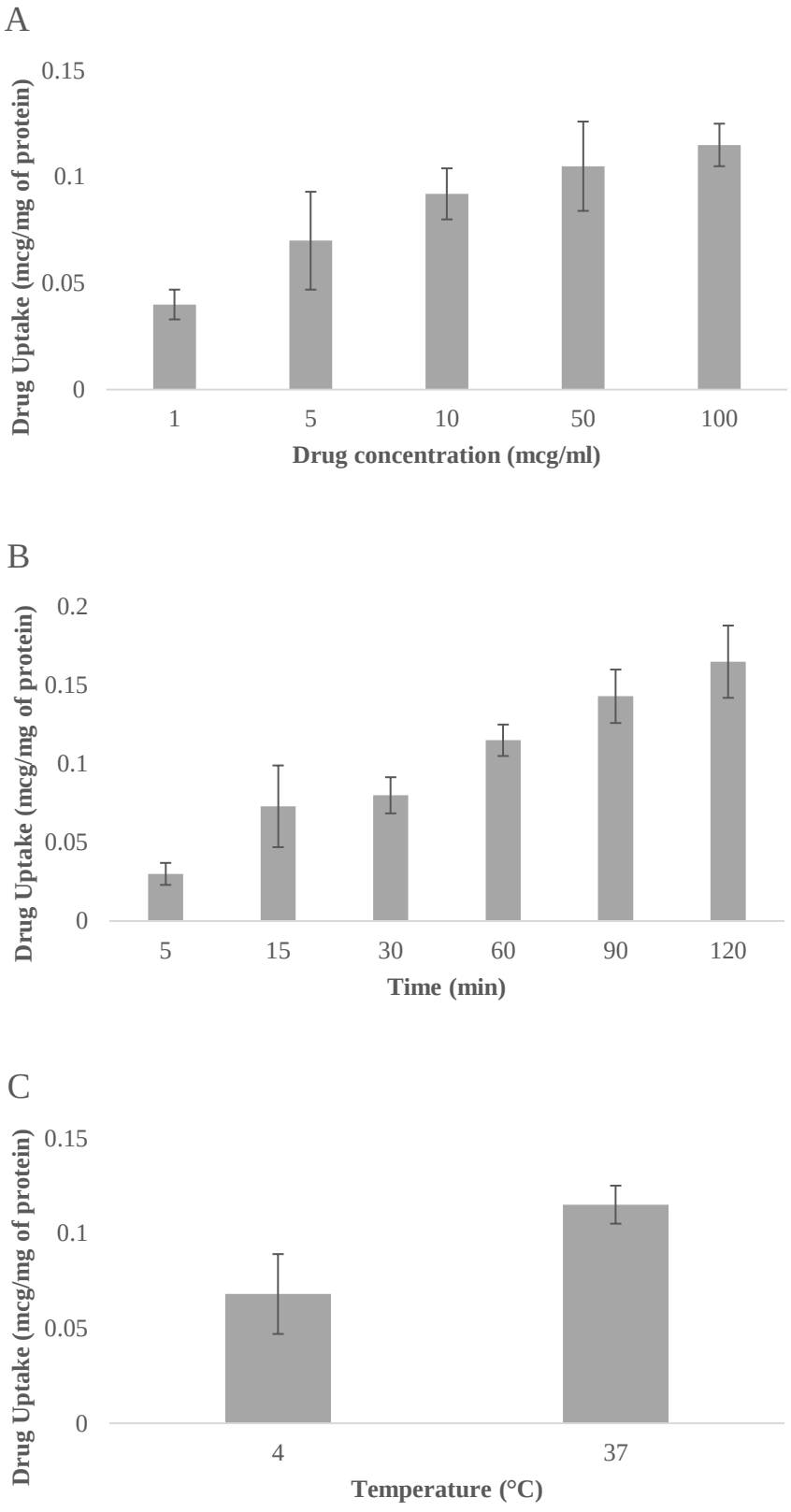

Figure 5.7 GPE niosome uptake study at variable conditions on RBMVECs. **A** shows the concentration dependent effect on uptake, **B** shows the time dependent effect on uptake, **C** shows the temperature dependent effect on uptake (Mean ± SD, n = 3).

For GPE uptake the addition ligands provided significantly improved uptake results compared with when GPE was simply formulated into a niosome with no ligands. For cGP uptake the results also showed that the niosome formulation by itself contributed to the increased uptake, but additional ligands also had significant effect. With the GPE niosome there were also tests with each individual ligand and both were more effective than the niosome by itself. Since the cell model is mimicking the BBB, it was expected to see an increased uptake with the RI7 ligand, but the non-specific PLR peptide still had better uptake amounts. This is markedly different than the Caco-2 cell experiments in chapter 4 where the RI7 ligand had no effect on uptake. This indicates to the specificity of the RI7 ligand but also the efficacy of the PLR ligand with its superior cell penetrating ability. The bi-ligand niosome has proven to significantly improve drug uptake into the RBMVEC cell model, of which has significant *in vivo* correlation to have improved penetration across the BBB when compared to free drug. According to Sivandzade and others, utilisation of both astrocytes and endothelial cells in a BBB model can properly predict future *in vivo* results (208-211). The cGP uptake experiments had the same trend as the GPE experiments and proved that this niosomal delivery system was effective in delivering both drugs. Figure 5.7 showed that the uptake mechanism of the niosomal formulation into the RBMVECs is time dependent, concentration dependent and temperature dependent. Higher concentrations (up to 100 µg/ml for GPE) and longer time (up to 120 minutes) resulted in larger uptake of drug. It was also observed that a higher temperature (37°C) had a larger amount of drug uptake when compared to colder temperatures (4°C), indicating energy dependent mechanism of uptake.

5.5.3. *In vitro* cellular uptake mechanism studies towards RBMVECs

Figure 5.8 shows the possible uptake mechanism for free and loaded the GPE niosome in the absence or presence of variable inhibitors. The cellular uptake experiment was carried out at 37ºC for up to 120 minutes of incubation. Various inhibitors used in this study were sodium azide (active transport inhibitor), protamine sulfate (adsorptive mediated endocytosis inhibitor), chlorpromazine (clathrin-mediated endocytosis inhibitor), and filipin (caveolae-mediated endocytosis inhibitor). Figure 5.6A and B showed the results of GPE and cGP with various inhibitors. After adding the inhibitors, the amount of drug uptaken by the RBMVE were decreased only in protamine group compared to the control group for both GPE and cGP ($p < 0.05$). This suggests adsorptive mediated endocytosis played a key role for GPE and cGP uptake in RBMVECs. Figure 5.6C showed the cellular uptake results of GPE loaded niosome in the presence of various inhibitors as described above. The results showed there was significant ($p < 0.05$) decreased of the amount of cellular uptake after adding sodium Azide, protamine sulfate and chlorpromazine (212,213). The uptake of the niosomes was at least partially involved in the three mechanism pathways: active transport, adsorptive mediated and clathrin mediated endocytosis. However, with the additions of Filipin the caveolae-mediated endocytosis inhibitor the uptake drug amount is not statistically different ($p > 0.05$), showing uptake did not occur through that pathway. The transport of drug loaded nanoparticles across BBB was reported to be via receptor-mediated endocytosis (212,213). Transferrin receptors present on the BBB can facilitate drug transport across BBB if the drug candidates or particles have the properties (or ligands) to bind to the receptors. Utilization of the RI7 ligand showed the great affinity to the transferrin reporter and improve the drug cellular uptake (33,104). From all the results shown above, the RBMVECs uptake of GPE or cGP bi-ligand niosomes was via receptor-mediated endocytosis is a concentration- and time-dependent process, which is consistent with those results present in the quantitative studies. Three different pathways have been identified active transport, adsorptive mediated transport and clathrin mediated transport as contributors to the uptake of the niosomal formulation.

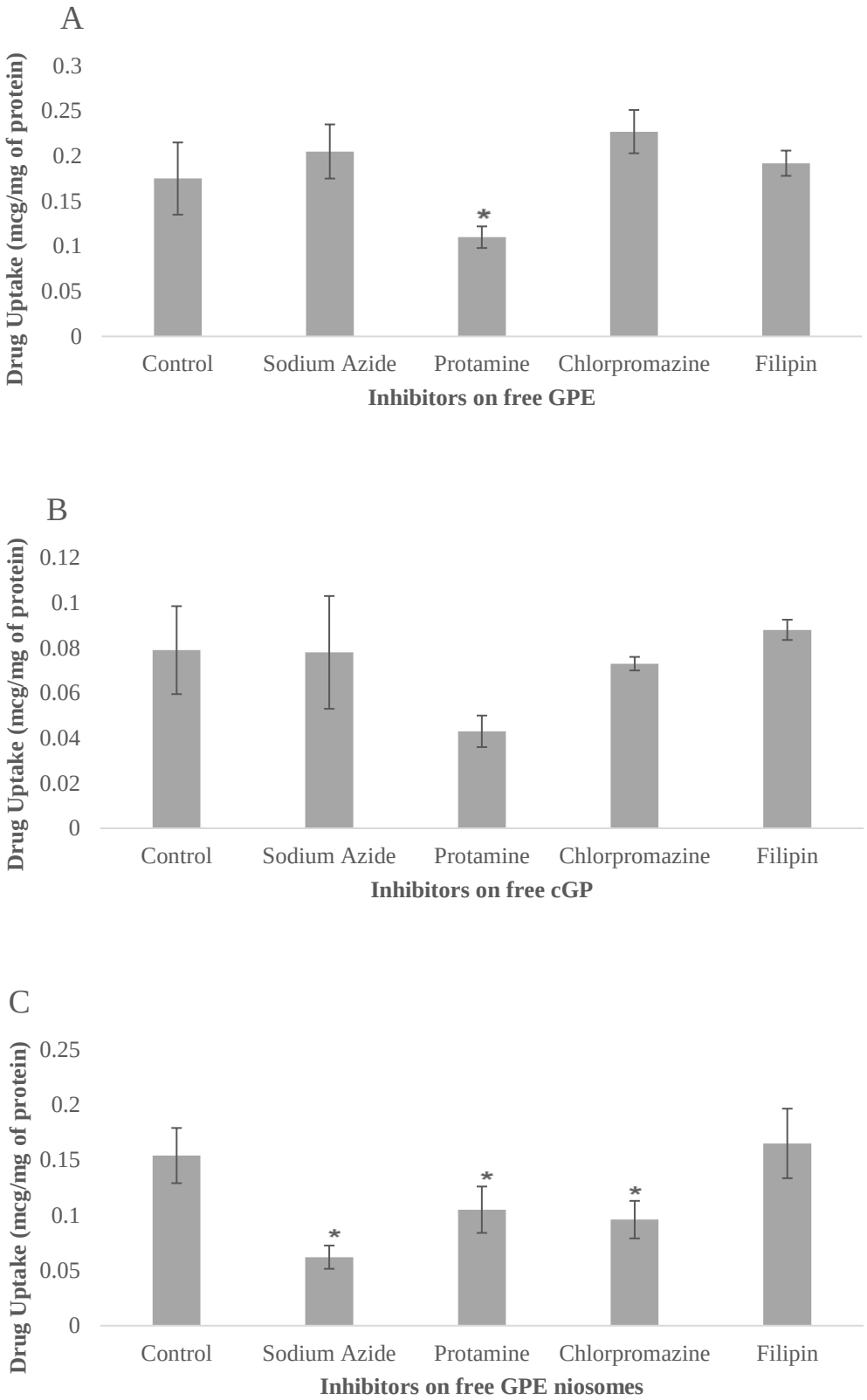

Figure 5.8 Mechanism uptake study with variable inhibitors on RBMVECs. A shows the inhibitors effect on GPE, B shows the inhibitors effect on cGP, C shows the inhibitors effect on GPE niosomes (Mean ± SD, n = 3, *p < 0.05).

5.5.4. *In vitro* cellular transport studies towards RBMVECs

Transport studies were carried out for both GPE and cGP niosomes (and their corresponding variables) to transport across a BBB model comprising of RBMVECs and astrocytes. Unfortunately, no drug was able to be quantified in the basolateral chamber of both the free GPE and cGP and the niosome versions as well. This is quite peculiar as it means that the drug was able to be uptaken into the cell but due to various reasons like degradation, intracellular lysosomal destruction and/or unable to exit the cells, as no drug was able to be found on the basolateral side. We suspect it is a mixture of multiple reasons including but not limited to the sensitivity of our quantification method.

5.6. Conclusion

The cytotoxicity results showed whether GPE and cGP drug solution or their drug-loaded bi-ligand niosome counterparts towards RBMVECs were a threat to cell viability. At all concentrations tested with both peptides GPE and cGP they showed no statistically significant cytotoxic effects at all. At the higher concentrations of niosome formulation there was a statistically significant decrease in cell viability, but concentrations below 5 mM showed no cytotoxic effects. The range tested did not give enough information to calculate the half-maximal inhibitory concentration (IC_{50}) of the niosome preparation but did give us a range to carry out future experiments effectively with cytotoxicity in mind.

An *in vitro* BBB model was fabricated by co-culturing RBMVECs and astrocytes. The cellular uptake of GPE or cGP loaded bi-ligand niosomes showed a significant increase when compared to the free drug ($p < 0.05$). GPE , cGP and GPE bi-ligand niosomes uptake was found to be concentration dependent, time dependent and energy dependent which seem to correlate with the mechanisms that we explored. Adsorptive-mediated endocytosis process dominated GPE and cGP uptake whereas active transport, adsorptive mediated transport and clathrin mediated transport were involved in uptake GPE loaded bi-ligand niosomes. No detectable amounts of the drug were seen present in the basolateral chamber of the attempted transport studies. The combined results suggests that both ligands present in the niosomes contributed to improve drug uptake, but no conclusion can yet be made about if they are able to transport across the cell.

Chapter 6
General discussion and future perspective

6.1. General discussion

Neurodegenerative diseases are becoming increasingly prevalent throughout New Zealand and worldwide. This is particularly an issue for countries with aging populations, as with New Zealand currently 10,000 people are living with Parkinson's disease (PD), 60,000 suffer long-term hospitalization or permanent disability due to stroke and 70,000 are living with dementia. Worldwide, dementia is expected to double every 20 years to an estimated 115.4 million in 2050. Alzheimer's Disease is the most common form of dementia which affects over 5.39 million people worldwide and is associated with cognitive decline, confusion, and forgetfulness, which severely effects not only those affected but also their families (1,214). Treating neurological conditions has been a great focus in modern medicine with a new treatment, management, and prevention developments. One main issue is there is currently no effective or efficient way to deliver medicine to the brain, even when we have many therapeutic agents that would be of great benefit. For a therapeutic agent to be used for these neurological conditions it must first be delivered to the brain, across the BBB. This is unfortunately not possible for most therapeutic agents which is why the research focus has shifted to enable them to cross the BBB, typically with the help of chemical modification and/or pharmaceutical formulations. This thesis focuses on developing a formulation that can orally deliver any drug to the brain, utilising a bi-ligand niosomal delivery system.

GPE and cGP are novel neuropeptides that have shown to possess neuroprotective effects in many neurological conditions (215). GPE is an endogenous tripeptide derived from the N-terminus of insulin-like growth factor 1 (IGF-1). The mechanism was reported to bind and activate to N-Methyl-D-aspartic acid (NMDA) receptors, which results in downregulation of inflammation, inhibition of apoptosis, promotion of astrocytosis and vascular remodelling (215). After GPE enters the blood circulation, it is rapidly metabolised into glutamic acid, and cyclic glycine-proline (cGP). Interestingly, cGP has been shown to bind to IGF-1 receptors, which increases IGF-1 bioavailability leading to improved neuroprotection (12). Many literatures reported GPE has offered neuroprotective effects, and it has shown the significant neuroprotection in rats and sheep with ischaemic injury (12,147,215,216). Nevertheless, the therapeutic effect of GPE is limited by its high hydrophilicity (very low partition coefficient) and susceptibility to enzymes in the gastrointestinal tract and peripheral blood system. As for cGP, it is more stable than GPE but has significant protein binding issues in the peripheral

blood system, preventing it from crossing the BBB. Oral administration is the most direct, non-invasive method to deliver drugs to the brain, which must cross the BBB.

The BBB is made up of endothelial cells which are connected by tight junctions, which prevents a large range of compounds, including drugs from entering the brain (217). These junctions were reported to be 100 times tighter than those found in other cells like the gastrointestinal epithelial cells, which makes penetration through the BBB very difficult and very selective (218). To maximise drug delivery across the BBB various chemical and formulation strategies can be attempted. These strategies include biochemical disruption of BBB, osmotic opening of BBB, direct injection, lipidation or cationization of drug molecules. Alternative route of administration or use of drug delivery systems such as polymeric nanoparticles, liposome, microemulsion, nanogel and niosome can also be used. Among all the drug delivery systems, niosomes has offered a great potential to delivery drug via oral administration due to its beneficial properties such as biodegradability, biocompatibility, non-immunogenicity, desirable release profiles and potential to include ligands in the structure. Therefore, the aim of this thesis is to develop, formulate and characterise a bi-ligand niosomal delivery system to orally deliver GPE and cGP across the BBB to maximise their concentration in brain. To achieve this aim, this thesis has explored several objectives.

In chapter 2, a novel HPLC analytical method was developed and validated according to ICH guidelines (148). HPLC is readily available, reliable, cost-effective technique to separate more than 90% of compounds and has been broadly used in pharmaceutical, nutraceutical, and biological sciences. The validation parameters such as linearity, specificity, repeatability, intermediate precision, sensitivity, recovery, and robustness were fully validated by using the developed HPLC methods for GPE and cGP. The HPLC method were used to quantify the GPE and cGP amounts in all experiments performed for this thesis. As with many published research, this was integral for the niosome release study, forced degradation study, optimising entrapment efficiency, quantify cellular uptake and transport in the cell studies (219-221). This chapter clearly exhibits that a sensitive and specific method was able to be developed and applied to the rest of the experiments with the possible exception being the unsuccessful transport experiments.

In chapter 3, neuropeptide GPE and cGP were formulated into niosomes, which was modified using two ligands: RI7 and PLR. The bi-ligand niosomal delivery systems can protect the GPE and cGP from degradation, improve their penetration and prevent large serum proteins from binding, as cGP was previously reported to have significant protein binding issues (12). To optimise the carrier systems, it is valuable to understand the carrier components, formation theory, and processing methods. Consequently, an efficient experimental factorial design was also implemented in chapter 3. As opposed to utilising the traditional step-by-step method, factorial design enables the testing of many factors simultaneously reducing the number of runs, utilised by many researchers including Witika et al. (168-170). Several formulation parameters were determined and implemented into the 2-level and 5 factor factorial design method to examine different factors like drug amount, pH of hydration medium, hydration time, surfactant to cholesterol ratio and the surfactant type to evaluate the optimum entrapment efficiency. These factors were chosen based on both literature search and preliminary experiments to narrow them down to the factors that have the highest likelihood of significantly influencing entrapment efficiency (222-224). The particle size, zeta-potential, FTIR, entrapment efficiency and *in vitro* release profiles were also fully investigated. The actual and predicted values of the entrapment efficiency of the drug delivery system was determined and compared. Sonication was found to be an important factor to reduce the particle size but can cause drug leakage as with similar findings by other researchers including Moghddam et al. (160,225). Three steps were involved in the fabrication of the bi-ligand niosome; synthesis of PLR-PEG; fabrication of dry film containing PLR-PEG and, -conjugation of the RI7 ligand. The particle size for GPE and cGP without ligand was 189.8 ± 6.4 nm and 183.4 ± 3.1 nm, respectively and with RI7 ligand, the particle size for GPE and cGP was increased to 263.1 ± 5.9 nm and 255.8 ± 4.3 nm, respectively. Interestingly, the addition of the ligands seems to increase the size of the niosomes which went against our aim as we wanted vesicles with the smallest size and the largest entrapment efficiency possible for optimum transport across GIT and BBB. The two ligands are integral to our uptake and transport studies as it improves penetration which outweighs the increase in particle size. Particle size still plays a crucial role in both GIT and BBB delivery with large vesicles (> 500 nm) were found not to be able to deliver the drug across the epithelial membranes (33,226). The ideal particle size to facilitate drug uptake and transport across both GIT and BBB should be less than 200 nm, although under 250 nm was also found to be acceptable (33-35). Zeta potential is another very important parameter, which provides essential information in determining the physical stability of

niosomes (164). It has been reported that niosomes with a zeta potential higher than +30 mV or lower than −30 mV is considered to have acceptable physical stability. This is due to their ability to cause electrostatic repulsion between the vesicles which prevent caking which is one of the main risks to long term stability (108,121,227). Electrostatic stabilization of the niosomes can strongly suppress their aggregation by inclusion of charge inducers such as DCP (228). In our study, DCP was used to stabilise the niosome as the surfactants used had no ionic charge. Comparing the results of entrapment efficiency between GPE and cGP, the entrapment efficiency of cGP was much higher than that of GPE (68% versus 28%). This is likely due to the difference of lipophilicity between the two peptides. cGP is more lipophilic in the structure compared to GPE and cGP would be more easily entrapped into the lipophilic bilayer of the niosome which could reduce drug leakage (118,155). The smaller the vesicle the less available volume is present at the centre of the vesicles (where a hydrophilic drug would be entrapped) in proportion to the bilayer, which means more opportunity of the lipophilic drug to be successfully entrapped in the bilayer. There is still very good potential for this method to entrap both hydrophilic and lipophilic drugs, however it seems like lipophilic drugs would be easier to entrap due to these reasons. The more hydrophilic drug, GPE would be partially entrapped inside of the niosomal vesicle and partially adhesive to the surface of niosomes which would be a disadvantageous compared to cGP. This adhesiveness to the surface of the niosome is also a possible explanation to the bi-phasic release seen in our *in vitro* release of GPE niosomes, seen by other researchers including Targhi et al. (229,230). *In vitro* release profiles showed that bi-ligand niosome exhibited an initial burst release followed by sustained/slow release up to 48 hrs. Surface adsorption of GPE, rather than entrapping the GPE in the vesicle, resulted in the initial burst release observed. The *in vitro* drug release mechanism was found to follow Korsmeyer-Peppas model, which indicates the drug release mimics that of diffusion through the matrix followed by matrix erosion. Although niosomes are not a type of matrix drug delivery system, this type of release profile was seen in by other researchers including Ghafelehbashi et al. (174,178-180).

In Chapter 4, *in vitro* studies of GPE and cGP loaded bi-ligand niosomes were assessed on Caco-2/E12 co-cultured cell model. Cytotoxicity studies showed the percentage of cell viability of Caco-2 cells retained was around 100% for both GPE and cGP for concentrations up to 15 mM. When the cells were exposed to the corresponding niosomal formulations cell viability decreased to about 60% at 10 mM concentration. The cytotoxicity results showed that

if the niosome concentration is kept at or below 5 mM, no significant toxicity would be experienced after 24-hour incubation. From the *in vitro* cell uptake study, it may be concluded that encapsulation into a niosomal delivery system and utilisation of ligands played a major role in uptake efficacy. The process of internalizing bi-ligand niosomes into Caco-2 cells was concentration, temperature, and time dependent uptake process for both GPE and cGP and their corresponding loaded niosomes. The rank order of the most effective GPE cellular uptake is bi-ligand niosome ≈ poly-L-arginine (PLR) > niosome > niosome (no ligand) ≈ RI7 niosome> free GPE (not encapsulated in niosome). The rank order of the most effective cGP cellular uptake is bi-ligand niosome > niosome (no ligand) > free GPE. This indicated that PLR ligand has played a key role to enhance cellular uptake, highlighting its superior cell penetrating properties. From the cellular mechanism study, with the additions of chlorpromazine and filipin, the uptake amount of GPE and cGP did not have a significant difference when compared to the control ($p > 0.05$). The free GPE and cGP uptake is not correlated to the caveolae and clathrin mediate endocytosis pathways (201,202,228). However, after adding protamine, an adsorptive-mediated endocytosis inhibitor, the uptake amount of GPE was significantly decreased compared to the control group ($p > 0.05$). A similar trend was seen with cGP and sodium azide, the active transport inhibitor. With GPE loaded bi-ligand niosome group, the addition of protamine, chlorpromazine, and sodium azide, the cellular uptake amount of GPE was significantly decreased. This demonstrated that the niosome formulation had different uptake mechanisms that is likely partly governed by active transport, adsorptive and clathrin mediated endocytosis (231,232). The addition of sodium azide the active transport inhibitor strangely increased uptake of free GPE into the cells, this can be attributed to the potential effect of sodium azide to compromising the cell and/or intracellular compartments (233). After multiple attempts at the transport experiments, there was no detectable amounts of GPE or cGP in the basolateral chamber of the Transwells®, indicating no transport across the Caco-2/E12 epithelial membrane. The absence of drug found across the cell model can be attributed to a variety of reasons, most likely additive of a few explanations. One potential explanation could be the unexpected and enormously large enzymatical degradation happening in the receptor chamber and/or basolateral chamber and/or inside the cells (194,195). There are more factors to consider, and this finding may either direct us to test other ligands or incorporate enzyme inhibitors into the formulation to ensure that degradation interference will be kept to a minimum (234,235). Although the addition of an enzyme inhibitor also brings with it other challenges like practical applicability and the potentially unknown side-effects it may have on

the cells. Another potential reason is the sensitivity of the quantitative method which could not detect the relatively lower levels of the drug in the basolateral chamber. Adopting and validating a liquid chromatography mass spectrometry (LCMS) method could alleviate this issue (236).

In chapter 5, an *in vitro* BBB model was re-established by co-culturing RBMVECs and Astrocytes. The BBB model was previously morphologically and functionally characterised by Dr Zhou (237-240). Cytotoxicity studies showed the percentage of cell viability of RBMVEC retained was around 100% for both GPE and cGP for concentrations up to 15 mM. When the cells were exposed to the corresponding niosomal formulations cell viability decreased to about 38% at 10 mM concentration. The cytotoxicity results showed that if the niosome concentration is kept at or below 5 mM, no significant toxicity would be experienced after 24-hour incubation. The process of internalising bi-ligand niosomes into RBMVECs was concentration, temperature, and time dependent uptake process for both GPE and cGP and their corresponding loaded niosomes. The rank order of GPE cellular uptake by RBMVECs is bi-ligand ≈ poly-L-arginine (PLR) > RI7 > niosome (no ligand) > free GPE. The rank order of cGP cellular uptake is bi-ligand > niosome (no ligand) > free cGP. This indicated that both PLR and RI7 ligands played a key role to enhance the cellular uptake into RBMVECs. Interestingly, there seems to be no statistical difference between both ligands and the PLR ligand niosomes, the main purpose of including the RI7 ligand was the BBB specificity. The RI7 ligand by itself showed a statistically significant increase compared to niosome with no ligand on RBMVECs. Chapter 4 and 5 results shows that the RI7 ligand is both effective and specific (to RBMVEC) as RI7 had little to negative influence on uptake on Caco-2 cells (42,43). These results were expected as the non-specific cell penetrating peptide PLR is still very effective in RBMVECs as it was in Caco-2 cells. The RI7 ligand has had a positive uptake effect on RBMVECs which is starkly different to the Caco-2 cells for which no significant difference was observed when compared to niosomes with no ligand. From the cellular mechanism study, with the additions of chlorpromazine and filipin, the clathrin and caveolae endocytosis inhibitors, the uptake amount of both GPE and cGP was not statistically significant from the control group ($p > 0.05$). However, after adding protamine, an adsorptive-mediated endocytosis inhibitor, the uptake amount of both GPE and cGP was significantly decreased compared to the control group ($p > 0.05$). Especially for the GPE loaded bi-ligand niosome group, with the addition of protamine, chlorpromazine, and sodium azide, the cellular uptake

amount of GPE was significantly decreased. This shows the niosomal uptake is at least partially governed by active transport, adsorptive and clathrin mediated endocytosis, and likely more pathways that we were not able to examine. This demonstrated that niosomal uptake is different from the free drug uptake of GPE and cGP and the potential uptake mechanisms to consider (231,232). After multiple attempts at the transport experiments, there was no detectable amounts of GPE or cGP in the basolateral chamber of the Transwells®, indicating no transport across the RBMVEC/Astrocytes BBB model. The absence of drug found across the cell model can be attributed to a variety of reasons, which are discussed in the previous paragraph. Due to the stricter TEER requirements of developing the BBB model the predicted amount of drug to be transported was to be lower than the GIT model (16,32,33). It is peculiar that both models resulted in no detectable amounts of drug, the enzymes present and interactions between the two models are different. Although the explanation could be the same, the BBB model likely has different reasons beyond just degradation of drug and the tight interactions between the RBMVEC and astrocytes could initially result in preventing the transport of niosomes due to their size and/or ligands present (33,34). A more sensitive quantitative method like LCMS could be adopted and validated which could have an increased chance of detecting the expected smaller amounts of drug in the BBB model.

6.2. Limitation and Future perspective

The production of this thesis study was taken place during COVID-19 period, in particular, level 3 and level 4 lockdown which greatly influenced the lab work progress both physically and mentally. There were a few issues and delays with the cell work irrespective of the lockdown which only further compounded the problems. Propagation of the cells were restarted multiple times due to a variety of reasons including but not limited to lockdowns, infections, and delayed orders.

A potential limitation of the thesis is the relatively low (28%) drug entrapment efficiency for GPE, due to multiple reasons of unable to improve this during optimization. To streamline the optimisation of the niosome encapsulation in the factorial design the initial factors chosen were limited due to preliminary studies. This meant many potential factors were not included which could have had a large effect on the entrapment efficiency of a hydrophilic drug like GPE, as cGP had acceptable entrapment efficiency of 68%. As explained in chapter

3 there were clear reasons for which some factors like drug amount and hydration time could not be expanded further due to practical reasons or simply not producing niosomes. There were other factors like the inclusion of only 2 surfactants, this could have easily been expanded to more surfactants but also with combination of surfactants. A more expanded selection of surfactants with different hydrophilic-lipophilic balance (HLB) values might have provided niosomes with more favourable entrapment efficiency for GPE (171-173). Other than the factorial design hydrophilic drugs are expected to have lower entrapment efficiency values than lipophilic drugs as the vesicles created are very small <250 nm which means with the low volume to surface area ratio, the drug physically has less space to be entrapped in (118,241,242). This is compared to the plentiful space between the bilayers where the more lipophilic drugs are entrapped. Morphology studies on the niosomes are also yet to be attempted which could provide more insight into the entrapment efficiency but also elucidate the unexpected *in vitro* release profile. Calculating entrapment efficiency comes with its own set of problems, many formulation papers focus on drug loading instead (243-245). Unfortunately, I did not dry weigh the final formulation for me to recalculate the drug loading from my optimization experiments. Future work will include drug loading which will be a more accurate and useful measure for drug dosing, in particular when it comes to *in vivo* evaluations (246).

There was also a large physical limitation of the drugs GPE and cGP in the study, the more preferable drug to use is cGP. In almost every conceivable way, cGP is the more ideal drug to carry out formulations with as it is found to be more stable and biologically effective than GPE with a much greater entrapment efficiency in our formulation. cGP is a very expensive compound and the budget that was available for this thesis did not allow the use of cGP in all stages. This meant cGP was only used in crucial comparisons with its GPE counterpart. Due to good planning, this provided results mostly with GPE, but we were still able to effectively show the efficacy of the niosome and each individual ligand and proof with cGP niosomes with similar trends in our uptake studies. Ideally, all tests should have been carried out with cGP to eliminate any potential gaps within the current thesis. The efficacy and mechanism of action of GPE and cGP in the brain has been extensively researched by other scientists, in particular Guan et al. (12,147,215). The result in the thesis is somewhat limited as it does not present any efficacy studies on GPE, cGP or their corresponding niosomal delivery systems. The mere encapsulation of GPE and cGP and/or the presence of the ligands used may significantly affect any efficacy tests. It could be a simple efficacy study as GPE and

cGP could be shown to promote cell proliferation or prevent damage. This can be shown by deliberately damaging the RBMVEC/Astrocyte cells, with high sheer stress or reactive oxygen species, as shown by Li et al. (247-249). The results also showed that uptake for both free drug and the niosomal delivery system is complex and occur through multiple pathways. I would like to explore more transport inhibitors and combination of inhibitors to define the major pathways more accurately as it was abundantly clear that every uptake mechanism explored was only partially responsible. If one of these combinations resulted in no uptake of drug, we could have more insightful information on the mechanisms involved.

With all the time delays and multiple failed attempts at the transport experiments the thesis could not delve deeper into more cell studies and/or animal studies which was originally proposed for this project. The cell uptake experiments results were successful, but the transport experiments resulted in no detectable amounts of drug. Early in the thesis there was little reason to conclude that the developed and validated HPLC method would not be sensitive enough for all experiments. When the transport experiments provide positive results, we can then pursue testing on animals to provide better insight into the *in vivo* applicability of this formulation (208-211). The issues with potential drug degradation, suboptimal niosome size (larger than 200 nm) and unsuccessful transport experiments makes the *in vivo* application of this project limited. In regard to oral delivery to the brain it is also expected that without preservation of the ligands (with a protectant like a polymer coating), then there could be extensive degradation in the extreme environments found in all areas of the GIT (11,17,21). Further modification of the niosomal delivery system might significantly alter its properties making it further unsuitable for BBB delivery. This means critically speaking the formulation in its current form will most likely be successful only if it is parenterally injected allowing it to be targeted to the BBB without overcoming the issues with the GIT. Our uptake results were very positive, highlighting the efficacy of the two ligands and how they influence uptake separately as well in both GIT and BBB models. The ligand selection is promising but more work is required if this delivery system is to be transformed for oral delivery to the brain.

6.3. Concluding remarks

From all the studies performed, this research fulfilled the objective of developing and optimising a bi-ligand niosomal delivery system for brain delivery of GPE and cGP. Specifically, these studies showed that:

i. A new HPLC analytical method was developed and validated. This method has been used for quantifying GPE and cGP in their formulation.

ii. The bi-ligand niosomes was successfully developed, optimised (using factorial design) and characterised in terms of particle size, drug entrapment efficiency, surface charge, *in vitro* drug release and drug-polymer compatibility (such as FTIR).

iii. The cellular uptake of GPE or cGP and the corresponding loaded bi-ligand niosomes was evaluated towards Caco-2 cells.

iv. *In vitro* BBB model was re-established and the cellular uptake of GPE or cGP and the corresponding loaded bi-ligand niosomes was evaluated towards RBMVECs.

This project has demonstrated that bi-ligand modified niosome can be utilised as a controlled release system for brain delivery of GPE and cGP. The bi-ligand niosome encapsulated with GPE and cGP can potentially be protected from enzymatical degradation in GI tract and peripheral blood system and improve uptake into GIT and BBB models. The novel niosomal system can also overcome protein binding and have improved peptide stability and permeability across the two different cell models.

References

(1) World Health Organization. Dementia. 2022; Available at: https://www.who.int/news-room/fact-sheets/detail/dementia.

(2) Egleton R, Davis T. Development of neuropeptide drugs that cross the blood-brain barrier. Neurotherapeutics 2005 Jan;2(1):44-53.

(3) Fosgerau K, Hoffmann T. Peptide therapeutics: current status and future directions. Drug Discovery Today 2015;20(1):122-128.

(4) Hamman JH, Enslin GM, Kotzé AF. Oral Delivery of Peptide Drugs. BioDrugs 2005;19(3):165-177.

(5) Siafaka PI, Okur ME, Erim PD, Çağlar EŞ, Özgenç E, Gündoğdu E, et al. Protein and Gene Delivery Systems for Neurodegenerative Disorders: Where Do We Stand Today? Pharmaceutics 2022;14(11):2425.

(6) Guan J, Mathai S, Harris P, Wen J, Zhang R, Brimble M, et al. Peripheral administration of a novel diketopiperazine, NNZ 2591, prevents brain injury and improves somatosensory-motor function following hypoxia–ischemia in adult rats. Neuropharmacology 2007;53(6):749-762.

(7) Baker AM, Batchelor DC, Thomas GB, Wen JY, Rafiee M, Lin H, et al. Central penetration and stability of N-terminal tripeptide of insulin-like growth factor-I, glycine-proline-glutamate in adult rat. Neuropeptides 2005;39(2):81-87.

(8) Antosova Z, Mackova M, Kral V, Macek T. Therapeutic application of peptides and proteins: parenteral forever? Trends Biotechnol 2009;27(11):628-635.

(9) Vlieghe P, Lisowski V, Martinez J, Khrestchatisky M. Synthetic therapeutic peptides: science and market. Drug Discov Today 2010;15(1-2):40-56.

(10) Joshi MD, Müller RH. Lipid nanoparticles for parenteral delivery of actives. European Journal of Pharmaceutics and Biopharmaceutics 2009;71(2):161-172.

(11) Morishita M, Peppas NA. Is the oral route possible for peptide and protein drug delivery? Drug Discovery Today 2006;11(19):905-910.

(12) Guan J, Gluckman P, Yang P, Krissansen G, Sun X, Zhou Y, et al. Cyclic glycine-proline regulates IGF-1 homeostasis by altering the binding of IGFBP-3 to IGF-1. Scientific reports 2014;4(1):1-9.

(13) Georgieva JV, Hoekstra D, Zuhorn IS. Smuggling drugs into the brain: an overview of ligands targeting transcytosis for drug delivery across the blood–brain barrier. Pharmaceutics 2014;6(4):557-583.

(14) Olivier J. Drug transport to brain with targeted nanoparticles. Neurotherapeutics 2005 Jan;2(1):108-119.

(15) Sharma G, Modgil A, Layek B, Arora K, Sun C, Law B, et al. Cell penetrating peptide tethered bi-ligand liposomes for delivery to brain in vivo: Biodistribution and transfection. Journal of Controlled Release 2013 Apr 10,;167(1):1-10.

(16) Choonara BF, Choonara YE, Kumar P, Bijukumar D, du Toit LC, Pillay V. A review of advanced oral drug delivery technologies facilitating the protection and absorption of protein and peptide molecules. Biotechnology Advances 2014 Nov 15,;32(7):1269-1282.

(17) Yun Y, Cho YW, Park K. Nanoparticles for oral delivery: Targeted nanoparticles with peptidic ligands for oral protein delivery. Advanced Drug Delivery Reviews 2013 Jun 15,;65(6):822-832.

(18) Madara JL, Pappenheimer JR. Structural basis for physiological regulation of paracellular pathways in intestinal epithelia. J Membr Biol 1987;100(1):149-164.

(19) Daugherty A, Mrsny R. Transcellular uptake mechanisms of the intestinal epithelial barrier Part one. Pharmaceutical science & technology today 1999 Apr;4(2):144.

(20) Russell-Jones GJ. The potential use of receptor-mediated endocytosis for oral drug delivery. Advanced Drug Delivery Reviews 2001;46(1):59-73.

(21) Bruno BJ, Miller GD, Lim CS. Basics and recent advances in peptide and protein drug delivery. Therapeutic delivery 2013 Nov;4(11):1443-1467.

(22) Thomson A, Dietschy JM. The role of the unstirred water layer in intestinal permeation. Pharmacology of intestinal permeation II: Springer; 1984. p. 165-269.

(23) Nellans HN. (B) Mechanisms of peptide and protein absorption: (1) Paracellular intestinal transport: modulation of absorption. Advanced Drug Delivery Reviews 1991;7(3):339-364.

(24) Bickel U, Yoshikawa T, Pardridge WM. Delivery of peptides and proteins through the blood–brain barrier. Adv Drug Deliv Rev 2001;46(1-3):247-279.

(25) Ulluwishewa D, Anderson RC, McNabb WC, Moughan PJ, Wells J, Roy NC. Regulation of Tight Junction Permeability by Intestinal Bacteria and Dietary Components. The Journal of Nutrition 2011;141(5):769-776.

(26) Hunter J, Hirst BH. Intestinal secretion of drugs. The role of P-glycoprotein and related drug efflux systems in limiting oral drug absorption. Adv Drug Deliv Rev 1997;25(2-3):129-157.

(27) Pauletti GM, Gangwar S, Siahaan TJ, Aubé J, Borchardt RT. Improvement of oral peptide bioavailability: Peptidomimetics and prodrug strategies. Adv Drug Deliv Rev 1997;27(2-3):235-256.

(28) Hooton D, Lentle R, Monro J, Wickham M, Simpson R. The secretion and action of brush border enzymes in the mammalian small intestine. Reviews of physiology, biochemistry and pharmacology: Springer; 2015. p. 59-118.

(29) Selma MV, Espín JC, Tomás-Barberán FA. Interaction between phenolics and gut microbiota: role in human health. Journal of agricultural and food chemistry 2009 Aug 12,;57(15):6485-6501.

(30) Rink R, Arkema-Meter A, Baudoin I, Post E, Kuipers A, Nelemans SA, et al. To protect peptide pharmaceuticals against peptidases. J Pharmacol Toxicol Methods 2010;61(2):210-218.

(31) Ballabh P, Braun A, Nedergaard M. The blood–brain barrier: an overview: Structure, regulation, and clinical implications. Neurobiology of Disease 2004;16(1):1-13.

(32) Abbott NJ, Patabendige AAK, Dolman DEM. Structure and function of the blood–brain barrier. Neurobiology of Disease 2009;37(1):13-25.

(33) Chen Y, Liu L. Modern methods for delivery of drugs across the blood–brain barrier. Advanced Drug Delivery Reviews 2012 May 15,;64(7):640-665.

(34) Pardridge WM. Drug targeting to the brain. Pharm Res 2007;24(9):1733-1744.

(35) Deeken JF, Löscher W. The Blood-Brain Barrier and Cancer: Transporters, Treatment, and Trojan Horses. Clinical Cancer Research 2007 Mar 15,;13(6):1663-1674.

(36) Jiang T, Zhang Z, Zhang Y, Lv H, Zhou J, Li C, et al. Dual-functional liposomes based on pH-responsive cell-penetrating peptide and hyaluronic acid for tumor-targeted anticancer drug delivery. Biomaterials 2012;33(36):9246-9258.

(37) Béduneau A, Saulnier P, Benoit J. Active targeting of brain tumors using nanocarriers. Biomaterials 2007;28(33):4947-4967.

(38) Mészáros M, Porkoláb G, Kiss L, Pilbat A, Kóta Z, Kupihár Z, et al. Niosomes decorated with dual ligands targeting brain endothelial transporters increase cargo penetration across the blood-brain barrier. European Journal of Pharmaceutical Sciences 2018 Oct 15,;123:228-240.

(39) Kibria G, Hatakeyama H, Ohga N, Hida K, Harashima H. Dual-ligand modification of PEGylated liposomes shows better cell selectivity and efficient gene delivery. Journal of Controlled Release 2011;153(2):141-148.

(40) Mishra V, Mahor S, Rawat A, Gupta PN, Dubey P, Khatri K, et al. Targeted brain delivery of AZT via transferrin anchored pegylated albumin nanoparticles. Journal of Drug Targeting 2006;14(1):45-53.

(41) Kleven MD, Jue S, Enns CA. Transferrin Receptors TfR1 and TfR2 Bind Transferrin through Differing Mechanisms. Biochemistry 2018 Mar 6,;57(9):1552-1559.

(42) Jones A, Shusta E. Blood–Brain Barrier Transport of Therapeutics via Receptor-Mediation. Pharm Res 2007 Sep;24(9):1759-1771.

(43) Lee HJ, Engelhardt B, Lesley J, Bickel U, Pardridge WM. Targeting Rat Anti-Mouse Transferrin Receptor Monoclonal Antibodies through Blood-Brain Barrier in Mouse. Journal of Pharmacology and Experimental Therapeutics 2000 Mar 1,;292(3):1048.

(44) Alata W, Paris-Robidas S, Emond V, Bourasset F, Calon F. Brain uptake of a fluorescent vector targeting the transferrin receptor: a novel application of in situ brain perfusion. Molecular pharmaceutics 2013;11(1):243-253.

(45) Paris-Robidas S, Brouard D, Emond V, Parent M, Calon F. Internalization of targeted quantum dots by brain capillary endothelial cells in vivo. Journal of Cerebral Blood Flow & Metabolism 2016;36(4):731-742.

(46) Fillebeen C, Descamps L, Dehouck M, Fenart L, Benaïssa M, Spik G, et al. Receptor-mediated transcytosis of lactoferrin through the blood-brain barrier. J Biol Chem 1999;274(11):7011-7017.

(47) Hu K, Li J, Shen Y, Lu W, Gao X, Zhang Q, et al. Lactoferrin-conjugated PEG–PLA nanoparticles with improved brain delivery: In vitro and in vivo evaluations. Journal of Controlled Release 2009;134(1):55-61.

(48) Elass-Rochard E, Roseanu A, Legrand D, Trif M, Salmon V, Motas C, et al. Lactoferrin-lipopolysaccharide interaction: involvement of the 28-34 loop region of human lactoferrin in the high-affinity binding to Escherichia coli 055B5 lipopolysaccharide. The Biochemical journal 1995 Dec 15,;312 (Pt 3)(Pt 3):839-845.

(49) Suzuki YA, Lopez V, Lönnerdal B. Mammalian lactoferrin receptors: structure and function. Cellular and molecular life sciences : CMLS 2005 Nov;62(22):2560.

(50) Ji B, Maeda J, Higuchi M, Inoue K, Akita H, Harashima H, et al. Pharmacokinetics and brain uptake of lactoferrin in rats. Life Sciences 2006;78(8):851-855.

(51) Huang R, Ke W, Han L, Liu Y, Shao K, Ye L, et al. Brain-targeting mechanisms of lactoferrin-modified DNA-loaded nanoparticles. Journal of Cerebral Blood Flow & Metabolism 2009;29(12):1914-1923.

(52) Ulbrich K, Knobloch T, Kreuter J. Targeting the insulin receptor: nanoparticles for drug delivery across the blood-brain barrier (BBB). Journal of Drug Targeting 2011 Feb;19(2):125-132.

(53) Ke Y, Qian ZM. Iron misregulation in the brain: a primary cause of neurodegenerative disorders. Lancet Neurology 2003;2(4):246-253.

(54) Wu D, Yang J, Pardridge WM. Drug targeting of a peptide radiopharmaceutical through the primate blood-brain barrier in vivo with a monoclonal antibody to the human insulin receptor. The Journal of clinical investigation 1997 Oct 1,;100(7):1804-1812.

(55) Zhang Y, Schlachetzki F, Pardridge WM. Global non-viral gene transfer to the primate brain following intravenous administration. Molecular Therapy 2003 Jan;7(1):11-18.

(56) Kuo Y, Ko H. Targeting delivery of saquinavir to the brain using 83-14 monoclonal antibody-grafted solid lipid nanoparticles. Biomaterials 2013;34(20):4818-4830.

(57) Gabathuler R. Approaches to transport therapeutic drugs across the blood–brain barrier to treat brain diseases. Neurobiol Dis 2010;37(1):48-57.

(58) Dehouck B, Fenart L, Dehouck M, Pierce A, Torpier G, Cecchelli R. A New Function for the LDL Receptor: Transcytosis of LDL across the Blood-Brain Barrier. The Journal of Cell Biology 1997 Aug 25,;138(4):877-889.

(59) Jeon H, Blacklow SC. Structure and physiologic function of the low-density lipoprotein receptor. Annual review of biochemistry 2005 Jan 1,;74:535-562.

(60) Demeule M, Currie J, Bertrand Y, Ché C, Nguyen T, Régina A, et al. Involvement of the low-density lipoprotein receptor-related protein in the transcytosis of the brain delivery vector Angiopep-2. Journal of Neurochemistry 2008 Aug;106(4):1534-1544.

(61) van Rooy I, Mastrobattista E, Storm G, Hennink WE, Schiffelers RM. Comparison of five different targeting ligands to enhance accumulation of liposomes into the brain. Journal of Controlled Release 2011;150(1):30-36.

(62) Böckenhoff A, Cramer S, Wölte P, Knieling S, Wohlenberg C, Gieselmann V, et al. Comparison of five peptide vectors for improved brain delivery of the lysosomal enzyme arylsulfatase A. The Journal of neuroscience : the official journal of the Society for Neuroscience 2014 Feb 26,;34(9):3122-3129.

(63) Kreuter J, Shamenkov D, Petrov V, Ramge P, Cychutek K, Koch-Brandt C, et al. Apolipoprotein-mediated Transport of Nanoparticle-bound Drugs Across the Blood-Brain Barrier. Journal of Drug Targeting 2002;10(4):317-325.

(64) Laskowitz DT, Thekdi SD, Thekdi AD, Han SKD, Myers JK, Pizzo SV, et al. Downregulation of Microglial Activation by Apolipoprotein E and ApoE-Mimetic Peptides. Experimental Neurology 2001 Jan;167(1):74-85.

(65) Gaillard PJ, Visser CC, de Boer AG. Targeted delivery across the blood–brain barrier. Expert opinion on drug delivery 2005;2(2):299-309.

(66) Gaillard PJ, Brink A, de Boer AG. Diphtheria toxin receptor-targeted brain drug delivery. International Congress Series 2005;1277:185-198.

(67) Gaillard PJ, de Boer AG. A novel opportunity for targeted drug delivery to the brain. Journal of Controlled Release 2006;116(2):e60-e62.

(68) Wang P, Xue Y, Shang X, Liu Y. Diphtheria toxin mutant CRM197-mediated transcytosis across blood–brain barrier in vitro. Cell Mol Neurobiol 2010;30(5):717-725.

(69) Gao H. Progress and perspectives on targeting nanoparticles for brain drug delivery. Acta Pharmaceutica Sinica B 2016 Jul;6(4):268-286.

(70) Wei X, Chen X, Ying M, Lu W. Brain tumor-targeted drug delivery strategies. Acta Pharmaceutica Sinica B 2014;4(3):193-201.

(71) Backos DS, Franklin CC, Reigan P. The role of glutathione in brain tumor drug resistance. Biochem Pharmacol 2012;83(8):1005-1012.

(72) Gawryluk JW, Wang J, Andreazza AC, Shao L, Young LT. Decreased levels of glutathione, the major brain antioxidant, in post-mortem prefrontal cortex from patients with psychiatric disorders. International Journal of Neuropsychopharmacology 2011;14(1):123-130.

(73) Rip J, Chen L, Hartman R, van den Heuvel A, Reijerkerk A, van Kregten J, et al. Glutathione PEGylated liposomes: pharmacokinetics and delivery of cargo across the blood-brain barrier in rats. Journal of Drug Targeting 2014 Jun;22(5):460-467.

(74) Rotman M, Welling MM, Bunschoten A, de Backer ME, Rip J, Nabuurs RJ, et al. Enhanced glutathione PEGylated liposomal brain delivery of an anti-amyloid single domain antibody fragment in a mouse model for Alzheimer's disease. J Controlled Release 2015;203:40-50.

(75) Lindqvist A, Rip J, van Kregten J, Gaillard P, Hammarlund-Udenaes M. In vivo Functional Evaluation of Increased Brain Delivery of the Opioid Peptide DAMGO by Glutathione-PEGylated Liposomes. Pharm Res 2016 Jan;33(1):177-185.

(76) Geldenhuys W, Mbimba T, Bui T, Harrison K, Sutariya V. Brain-targeted delivery of paclitaxel using glutathione-coated nanoparticles for brain cancers. J Drug Target 2011;19(9):837-845.

(77) Gaillard PJ, Visser CC, Appeldoorn CC, Rip J. Enhanced brain drug delivery: safely crossing the blood–brain barrier. Drug Discovery Today: Technologies 2012;9(2):e155-e160.

(78) Li-Li Zou, Jie-Lan Ma, Tao Wang, Tang-Bin Yang, Chang-Bai Liu. Cell-Penetrating Peptide-Mediated Therapeutic Molecule Delivery into the Central Nervous System. Current Neuropharmacology 2013 Mar;11(2):197-208.

(79) Li J, Zhou L, Ye D, Huang S, Shao K, Huang R, et al. Choline-Derivate-Modified Nanoparticles for Brain-Targeting Gene Delivery. Advanced Materials 2011 Oct 18,;23(39):4516-4520.

(80) Li J, Guo Y, Kuang Y, An S, Ma H, Jiang C. Choline transporter-targeting and co-delivery system for glioma therapy. Biomaterials 2013;34(36):9142-9148.

(81) Patching S. Glucose Transporters at the Blood-Brain Barrier: Function, Regulation and Gateways for Drug Delivery. Mol Neurobiol 2017 Mar;54(2):1046-1077.

(82) Qin Y, Fan W, Chen H, Yao N, Tang W, Tang J, et al. In vitro and in vivo investigation of glucose-mediated brain-targeting liposomes. J Drug Target 2010;18(7):536-549.

(83) Jiang X, Xin H, Ren Q, Gu J, Zhu L, Du F, et al. Nanoparticles of 2-deoxy- d -glucose functionalized poly(ethylene glycol)-co-poly(trimethylene carbonate) for dual-targeted drug delivery in glioma treatment. Biomaterials 2013;35(1):518-529.

(84) Radka Gromnicova, Heather A Davies, Peddagangannagari Sreekanthreddy, Ignacio A Romero, Torben Lund, Ivan M Roitt, et al. Glucose-Coated Gold Nanoparticles Transfer across Human Brain Endothelium and Enter Astrocytes In Vitro. PLoS One 2013 Dec 1,;8(12):e81043.

(85) Dufes C, Gaillard F, Uchegbu IF, Schätzlein AG, Olivier J, Muller J. Glucose-targeted niosomes deliver vasoactive intestinal peptide (VIP) to the brain. International Journal of Pharmaceutics 2004;285(1):77-85.

(86) Koren E, Vladimir P. Cell-penetrating peptides: breaking through to the other side. Trends in Molecular Medicine 2012;18(7):385-393.

(87) Vivès E, Schmidt J, Pèlegrin A. Cell-penetrating and cell-targeting peptides in drug delivery. BBA - Reviews on Cancer 2008;1786(2):126-138.

(88) Green M, Loewenstein PM. Autonomous functional domains of chemically synthesized human immunodeficiency virus tat trans-activator protein. Cell 1988;55(6):1179-1188.

(89) Järver P, Langel Ü. Cell-penetrating peptides—A brief introduction. BBA - Biomembranes 2006;1758(3):260-263.

(90) Cao G, Pei W, Ge H, Liang Q, Luo Y, Sharp FR, et al. In Vivo Delivery of a Bcl-xL Fusion Protein Containing the TAT Protein Transduction Domain Protects against Ischemic Brain Injury and Neuronal Apoptosis. Journal of Neuroscience 2002 Jul 1,;22(13):5423.

(91) Malhotra M, Tomaro-Duchesneau C, Prakash S. Synthesis of TAT peptide-tagged PEGylated chitosan nanoparticles for siRNA delivery targeting neurodegenerative diseases. Biomaterials 2012;34(4):1270-1280.

(92) Sancini G, Gregori M, Salvati E, Cambianica I, Re F, Ornaghi F, et al. Functionalization with TAT-Peptide Enhances Blood-Brain Barrier Crossing In vitro of Nanoliposomes Carrying a Curcumin-Derivative to Bind Amyloid-b Peptide. 2013.

(93) Kanazawa T, Akiyama F, Kakizaki S, Takashima Y, Seta Y. Delivery of siRNA to the brain using a combination of nose-to-brain delivery and cell-penetrating peptide-modified nano-micelles. Biomaterials 2013;34(36):9220-9226.

(94) Qin Y, Chen H, Yuan W, Kuai R, Zhang Q, Zhang Z, et al. Liposome formulated with TAT-modified cholesterol for enhancing the brain delivery. International Journal of Pharmaceutics 2011;419(1):85-95.

(95) Guidotti G, Brambilla L, Rossi D. Cell-Penetrating Peptides: From Basic Research to Clinics. Trends in Pharmacological Sciences 2017;38(4):406-424.

(96) Kamei N, Nielsen EJB, Khafagy E, Takeda-Morishita M. Noninvasive insulin delivery: the great potential of cell-penetrating peptides. Therapeutic delivery 2013 Mar;4(3):315-326.

(97) Sharma G, Modgil A, Zhong T, Sun C, Singh J. Influence of Short-Chain Cell-Penetrating Peptides on Transport of Doxorubicin Encapsulating Receptor-Targeted Liposomes Across Brain Endothelial Barrier. Pharm Res 2014 May;31(5):1194-1209.

(98) Tseng Y, Liu J, Hong R. Translocation of Liposomes into Cancer Cells by Cell-Penetrating Peptides Penetratin and Tat: A Kinetic and Efficacy Study. Molecular Pharmacology 2002 Oct 1,;62(4):864-872.

(99) Patel L, Zaro J, Shen W. Cell Penetrating Peptides: Intracellular Pathways and Pharmaceutical Perspectives. Pharm Res 2007 Nov;24(11):1977-1992.

(100) Wang S, Liu Y, Weng L, Ma X. Effect of the Molecular Weights of Poly-L-Arginine on Membrane Strength and Permeability of Poly-L-Arginine Group Microcapsules. Macromolecular Bioscience 2003;3(7):347-350.

(101) Westergren I, Johansson BB. Altering the blood-brain barrier in the rat by intracarotid infusion of polycations: a comparison between protamine, poly-L-lysine and poly-L-arginine. Acta physiologica Scandinavica 1993 Sep;149(1):99-104.

(102) Zhang C, Tang N, Liu X, Liang W, Xu W, Torchilin VP. siRNA-containing liposomes modified with polyarginine effectively silence the targeted gene. Journal of Controlled Release 2006;112(2):229-239.

(103) Opanasopit P, Tragulpakseerojn J, Apirakaramwong A, Ngawhirunpat T, Rojanarata T, Ruktanonchai U. The development of poly-L-arginine-coated liposomes for gene delivery. International journal of nanomedicine 2011;6:2245-2252.

(104) Lockman PR, Mumper RJ, Khan MA, Allen DD. Nanoparticle Technology for Drug Delivery Across the Blood-Brain Barrier. Drug Development and Industrial Pharmacy 2002;28(1):1-13.

(105) Kumari A, Yadav SK, Yadav SC. Biodegradable polymeric nanoparticles based drug delivery systems. Colloids and Surfaces B: Biointerfaces 2010;75(1):1-18.

(106) Patel T, Zhou J, Piepmeier JM, Saltzman WM. Polymeric nanoparticles for drug delivery to the central nervous system. Adv Drug Deliv Rev 2012;64(7):701-705.

(107) Costantino L, Boraschi D. Is there a clinical future for polymeric nanoparticles as brain-targeting drug delivery agents? Drug Discovery Today 2012 Apr;17(7-8):367-378.

(108) Kreuter J. Nanoparticulate systems for brain delivery of drugs. Advanced Drug Delivery Reviews 2001;47(1):65-81.

(109) Calvo P, Gouritin B, Chacun H, Desmaële D, D'Angelo J, Noel J, et al. Long-Circulating PEGylated Polycyanoacrylate Nanoparticles as New Drug Carrier for Brain Delivery. Pharm Res 2001 Aug;18(8):1157-1166.

(110) Cheng Q, Feng J, Chen J, Zhu X, Li F. Brain transport of neurotoxin-I with PLA nanoparticles through intranasal administration in rats: a microdialysis study. Biopharmaceutics & Drug Disposition 2008 Nov;29(8):431-439.

(111) Müller RH, Mäder K, Gohla S. Solid lipid nanoparticles (SLN) for controlled drug delivery – a review of the state of the art. European Journal of Pharmaceutics and Biopharmaceutics 2000;50(1):161-177.

(112) Almeida AJ, Souto E. Solid lipid nanoparticles as a drug delivery system for peptides and proteins. Advanced Drug Delivery Reviews 2007;59(6):478-490.

(113) Blasi P, Giovagnoli S, Schoubben A, Ricci M, Rossi C. Solid lipid nanoparticles for targeted brain drug delivery. Adv Drug Deliv Rev 2007;59(6):454-477.

(114) Wissing SA, Kayser O, Muller RH. Solid lipid nanoparticles for parenteral drug delivery. Advanced Drug Delivery Reviews 2004;56(9):1257-1272.

(115) Dhawan S, Kapil R, Singh B. Formulation development and systematic optimization of solid lipid nanoparticles of quercetin for improved brain delivery. Journal of Pharmacy and Pharmacology 2011 Mar;63(3):342-351.

(116) Mulik RS, Mönkkönen J, Juvonen RO, Mahadik KR, Paradkar AR. Transferrin mediated solid lipid nanoparticles containing curcumin: Enhanced in vitro anticancer activity by induction of apoptosis. International Journal of Pharmaceutics 2010;398(1):190-203.

(117) Ramalingam P, Ko YT. Enhanced oral delivery of curcumin from N-trimethyl chitosan surface-modified solid lipid nanoparticles: pharmacokinetic and brain distribution evaluations. Pharmaceutical research 2015 Feb;32(2):389-402.

(118) Mahale NB, Thakkar PD, Mali RG, Walunj DR, Chaudhari SR. Niosomes: Novel sustained release nonionic stable vesicular systems — An overview. Advances in Colloid and Interface Science 2012 Nov 15,;183-184:46-54.

(119) Samad A, Sultana Y, Aqil M. Liposomal Drug Delivery Systems: An Update Review. Current Drug Delivery 2007 Oct;4(4):297-305.

(120) Verma A, Tiwari A, Saraf S, Panda PK, Jain A, Jain SK. Emerging potential of niosomes in ocular delivery. Expert opinion on drug delivery 2021;18(1):55-71.

(121) Lohumi A. A NOVEL DRUG DELIVERY SYSTEM: NIOSOMES REVIEW. Journal of drug delivery and therapeutics 2012 Sep 15,;2(5).

(122) Tiwari G, Tiwari R, Sriwastawa B, Bhati L, Pandey S, Pandey P, et al. Drug delivery systems: An updated review. International journal of pharmaceutical investigation 2012 Jan;2(1):2-11.

(123) Hua S. Orally administered liposomal formulations for colon targeted drug delivery. Frontiers in Pharmacology 2014;5:138.

(124) Chen H, Tang W, Tang J, Tang L, Qin Y, Yin Y, et al. Lactoferrin-modified procationic liposomes as a novel drug carrier for brain delivery. European Journal of Pharmaceutical Sciences 2010;40(2):94-102.

(125) Bragagni M, Mennini N, Furlanetto S, Orlandini S, Ghelardini C, Mura P. Development and characterization of functionalized niosomes for brain targeting of dynorphin-B. European Journal of Pharmaceutics and Biopharmaceutics 2014 May;87(1):73-79.

(126) L Shinde R, B Jindal A, V Devarajan P. Microemulsions and nanoemulsions for targeted drug delivery to the brain. Current Nanoscience 2011;7(1):119-133.

(127) McClements DJ. Emulsion design to improve the delivery of functional lipophilic components. Annual review of food science and technology 2010;1:241-269.

(128) McClements DJ, Rao J. Food-grade nanoemulsions: formulation, fabrication, properties, performance, biological fate, and potential toxicity. Crit Rev Food Sci Nutr 2011;51(4):285-330.

(129) Anton N, Benoit J, Saulnier P. Design and production of nanoparticles formulated from nano-emulsion templates—a review. J Controlled Release 2008;128(3):185-199.

(130) McClements DJ. Nanoemulsions versus microemulsions: terminology, differences, and similarities. Soft matter 2012;8(6):1719-1729.

(131) Rao J, McClements DJ. Food-grade microemulsions and nanoemulsions: Role of oil phase composition on formation and stability. Food Hydrocoll 2012;29(2):326-334.

(132) Valduga CJ, Fernandes DC, Prete ACL, Azevedo CH, Rodrigues DG, Maranhão RC. Use of a cholesterol-rich microemulsion that binds to low-density lipoprotein receptors as vehicle for etoposide. J Pharm Pharmacol 2003;55(12):1615-1622.

(133) Kang BK, Chon SK, Kim SH, Jeong SY, Kim MS, Cho SH, et al. Controlled release of paclitaxel from microemulsion containing PLGA and evaluation of anti-tumor activity in vitro and in vivo. Int J Pharm 2004;286(1-2):147-156.

(134) Zhang Q, Jiang X, Jiang W, Lu W, Su L, Shi Z. Preparation of nimodipine-loaded microemulsion for intranasal delivery and evaluation on the targeting efficiency to the brain. Int J Pharm 2004;275(1-2):85-96.

(135) Shinde RL, Bharkad GP, Devarajan PV. Intranasal microemulsion for targeted nose to brain delivery in neurocysticercosis: role of docosahexaenoic acid. European Journal of Pharmaceutics and Biopharmaceutics 2015;96:363-379.

(136) Soni KS, Desale SS, Bronich TK. Nanogels: An overview of properties, biomedical applications and obstacles to clinical translation. Journal of Controlled Release 2016 Oct 28,;240:109-126.

(137) Azadi A, Hamidi M, Rouini M. Methotrexate-loaded chitosan nanogels as 'Trojan Horses' for drug delivery to brain: Preparation and in vitro/in vivo characterization. International Journal of Biological Macromolecules 2013 Nov;62:523-530.

(138) Blackburn WH, Dickerson E, Smith MH, McDonald JF, Lyon LA. Peptide-functionalized nanogels for targeted siRNA delivery. Bioconjugate chemistry 2009 May 20,;20(5):960-968.

(139) Soni S, Babbar Ak, Sharma Rk, Maitra A. Delivery of hydrophobised 5-fluorouracil derivative to brain tissue through intravenous route using surface modified nanogels. Journal of Drug Targeting 2006;14(2):87-95.

(140) Vinogradov SV, Batrakova EV, Kabanov AV. Nanogels for oligonucleotide delivery to the brain. Bioconjugate chemistry 2004 Jan;15(1):50-60.

(141) Neue UD, Van Tran K, Iraneta PC, Alden BA. Characterization of HPLC packings. Journal of Separation science 2003;26(3-4):174-186.

(142) Ahuja S, Dong MW. Handbook of pharmaceutical analysis by HPLC. 1st ed. ed. Amsterdam [u.a.]: Elsevier; 2005.

(143) Florence AT, Siepmann J. Modern Pharmaceutics Volume 1. Baton Rouge: CRC Press; 2010.

(144) Kazakevich YV, LoBrutto R. HPLC for Pharmaceutical Scientists. Hoboken: John Wiley & Sons, Incorporated; 2007.

(145) Lazarowych NJ, Pekos P. Use of fingerprinting and marker compounds for identification and standardization of botanical drugs: strategies for applying pharmaceutical HPLC analysis to herbal products. Drug information journal: DIJ/Drug Information Association 1998;32(2):497-512.

(146) Wen J, Davies N, Ledger R, Butt G, McLeod B, Tucker IG. Isocratic liquid chromatographic assay for monitoring the degradation of luteinizing hormone releasing hormone by extracts from the gastrointestinal tract of possums. Journal of Chromatography B 2002;779(2):221-227.

(147) Guan J, Harris P, Brimble M, Lei Y, Lu J, Yang Y, et al. The role for IGF-1-derived small neuropeptides as a therapeutic target for neurological disorders. Expert opinion on therapeutic targets 2015;19(6):785-793.

(148) Guideline IHT. Validation of analytical procedures: text and methodology. Q2 (R1) 2005;1(20):05.

(149) Cartwright AC. The British pharmacopoeia, 1864 to 2014: medicines, international standards and the state. : Routledge; 2016.

(150) Huynh-Ba K. Handbook of stability testing in pharmaceutical development: regulations, methodologies, and best practices. : Springer; 2009.

(151) Akbarzadeh A, Rezaei-Sadabady R, Davaran S, Joo SW, Zarghami N, Hanifehpour Y, et al. Liposome: classification, preparation, and applications. Nanoscale research letters 2013;8(1):1-9.

(152) Munin A, Edwards-Lévy F. Encapsulation of natural polyphenolic compounds; a review. Pharmaceutics 2011;3(4):793-829.

(153) Marianecci C, Di Marzio L, Rinaldi F, Celia C, Paolino D, Alhaique F, et al. Niosomes from 80s to present: the state of the art. Adv Colloid Interface Sci 2014;205:187-206.

(154) Rashidi L, Khosravi-Darani K. The applications of nanotechnology in food industry. Crit Rev Food Sci Nutr 2011;51(8):723-730.

(155) Moghassemi S, Hadjizadeh A. Nano-niosomes as nanoscale drug delivery systems: an illustrated review. J Controlled Release 2014;185:22-36.

(156) Abdelkader H, Ismail S, Kamal A, Alany RG. Design and evaluation of controlled-release niosomes and discomes for naltrexone hydrochloride ocular delivery. J Pharm Sci 2011;100(5):1833-1846.

(157) Muzzalupo R, Tavano L, La Mesa C. Alkyl glucopyranoside-based niosomes containing methotrexate for pharmaceutical applications: evaluation of physico-chemical and biological properties. Int J Pharm 2013;458(1):224-229.

(158) Basiri L, Rajabzadeh G, Bostan A. Physicochemical properties and release behavior of Span 60/Tween 60 niosomes as vehicle for α-Tocopherol delivery. LWT 2017;84:471-478.

(159) Tavano L, Rossi CO, Picci N, Muzzalupo R. Spontaneous temperature-sensitive Pluronic® based niosomes: Triggered drug release using mild hyperthermia. Int J Pharm 2016;511(2):703-708.

(160) Moghddam SRM, Ahad A, Aqil M, Imam SS, Sultana Y. Formulation and optimization of niosomes for topical diacerein delivery using 3-factor, 3-level Box-Behnken design for the management of psoriasis. Materials science and engineering: C 2016;69:789-797.

(161) Fu J, Tan DMY, Er HM, Chen YS, Nesaretnam K. Tumor-targeted niosome as novel carrier for intravenous administration of tocotrienol. Asian J Pharm Sci 2016;11:79-80.

(162) Kassem AA, Abd El-Alim SH, Asfour MH. Enhancement of 8-methoxypsoralen topical delivery via nanosized niosomal vesicles: Formulation development, in vitro and in vivo evaluation of skin deposition. Int J Pharm 2017;517(1-2):256-268.

(163) Mashal M, Attia N, Puras G, Martínez-Navarrete G, Fernández E, Pedraz JL. Retinal gene delivery enhancement by lycopene incorporation into cationic niosomes based on DOTMA and polysorbate 60. J Controlled Release 2017;254:55-64.

(164) Chen S, Hanning S, Falconer J, Locke M, Wen J. Recent advances in non-ionic surfactant vesicles (niosomes): Fabrication, characterization, pharmaceutical and cosmetic applications. European Journal of Pharmaceutics and Biopharmaceutics 2019;144:18-39.

(165) Li D, Martini N, Liu M, Falconer JR, Locke M, Wu Z, et al. Non-ionic surfactant vesicles as a carrier system for dermal delivery of ( )-Catechin and their antioxidant effects. J Drug Target 2021;29(3):310-322.

(166) Bragagni M, Mennini N, Furlanetto S, Orlandini S, Ghelardini C, Mura P. Development and characterization of functionalized niosomes for brain targeting of dynorphin-B. European Journal of Pharmaceutics and Biopharmaceutics 2014;87(1):73-79.

(167) Ruckmani K, Sankar V. Formulation and optimization of zidovudine niosomes. Aaps Pharmscitech 2010;11(3):1119-1127.

(168) Witika BA, Walker RB. Development, manufacture and characterization of niosomes for the delivery for nevirapine. Die Pharmazie-An International Journal of Pharmaceutical Sciences 2019;74(2):91-96.

(169) Mohammed AR, Weston N, Coombes A, Fitzgerald M, Perrie Y. Liposome formulation of poorly water soluble drugs: optimisation of drug loading and ESEM analysis of stability. Int J Pharm 2004;285(1-2):23-34.

(170) Motwani SK, Chopra S, Talegaonkar S, Kohli K, Ahmad FJ, Khar RK. Chitosan–sodium alginate nanoparticles as submicroscopic reservoirs for ocular delivery: Formulation, optimisation and in vitro characterisation. European Journal of Pharmaceutics and Biopharmaceutics 2008;68(3):513-525.

(171) Tavano L, de Cindio B, Picci N, Ioele G, Muzzalupo R. Drug compartmentalization as strategy to improve the physico-chemical properties of diclofenac sodium loaded niosomes for topical applications. Biomed Microdevices 2014;16(6):851-858.

(172) Bandyopadhyay P. Fatty alcohols or fatty acids as niosomal hybrid carrier: effect on vesicle size, encapsulation efficiency and in vitro dye release. Colloids and Surfaces B: Biointerfaces 2007;58(1):68-71.

(173) Gadhave A. Determination of hydrophilic-lipophilic balance value. Int.J.Sci.Res 2014;3(4):573-575.

(174) Korsmeyer RW, Gurny R, Doelker E, Buri P, Peppas NA. Mechanisms of solute release from porous hydrophilic polymers. Int J Pharm 1983;15(1):25-35.

(175) Jacobs C, Müller RH. Production and characterization of a budesonide nanosuspension for pulmonary administration. Pharm Res 2002;19(2):189-194.

(176) Basha M, Abd El-Alim SH, Shamma RN, Awad GE. Design and optimization of surfactant-based nanovesicles for ocular delivery of Clotrimazole. J Liposome Res 2013;23(3):203-210.

(177) Kumbhar D, Wavikar P, Vavia P. Niosomal gel of lornoxicam for topical delivery: in vitro assessment and pharmacodynamic activity. AAPS pharmscitech 2013;14(3):1072-1082.

(178) Wang M, Yuan Y, Gao Y, Ma H, Xu H, Zhang X, et al. Preparation and characterization of 5-fluorouracil pH-sensitive niosome and its tumor-targeted evaluation: in vitro and in vivo. Drug Dev Ind Pharm 2012;38(9):1134-1141.

(179) Costa P, Lobo JMS. Modeling and comparison of dissolution profiles. European journal of pharmaceutical sciences 2001;13(2):123-133.

(180) Ghafelehbashi R, Akbarzadeh I, Yaraki MT, Lajevardi A, Fatemizadeh M, Saremi LH. Preparation, physicochemical properties, in vitro evaluation and release behavior of cephalexin-loaded niosomes. Int J Pharm 2019;569:118580.

(181) Kumar YP, Kumar KV, Kishore VS. Preparation and evaluation of diclofenac niosomes by various techniques. Res J Pharm Tech 2013;6(10):1097-1101.

(182) El-Ridy MS, Abdelbary A, Essam T, Abd EL-Salam RM, Aly Kassem AA. Niosomes as a potential drug delivery system for increasing the efficacy and safety of nystatin. Drug Dev Ind Pharm 2011;37(12):1491-1508.

(183) Kassem AA, Abd El-Alim SH, Asfour MH. Enhancement of 8-methoxypsoralen topical delivery via nanosized niosomal vesicles: Formulation development, in vitro and in vivo evaluation of skin deposition. Int J Pharm 2017;517(1-2):256-268.

(184) Rana A, Dumka A, Singh R, Rashid M, Ahmad N, Panda MK. An Efficient Machine Learning Approach for Diagnosing Parkinson's Disease by Utilizing Voice Features. Electronics (Basel) 2022 Nov 17,;11(22):3782.

(185) Zhou XH, Po ALW. Peptide and protein drugs: I. Therapeutic applications, absorption and parenteral administration. Int J Pharm 1991;75(2-3):97-115.

(186) Yang CY, Dantzig AH, Pidgeon C. Intestinal peptide transport systems and oral drug availability. Pharm Res 1999;16(9):1331-1343.

(187) Nojima Y, Suzuki Y, Iguchi K, Shiga T, Iwata A, Fujimoto T, et al. Development of poly (ethylene glycol) conjugated lactoferrin for oral administration. Bioconjug Chem 2008;19(11):2253-2259.

(188) Renukuntla J, Vadlapudi AD, Patel A, Boddu SH, Mitra AK. Approaches for enhancing oral bioavailability of peptides and proteins. Int J Pharm 2013;447(1-2):75-93.

(189) Swider E, Koshkina O, Tel J, Cruz LJ, de Vries IJM, Srinivas M. Customizing poly (lactic-co-glycolic acid) particles for biomedical applications. Acta biomaterialia 2018;73:38-51.

(190) Mansoor S, Kondiah PP, Choonara YE, Pillay V. Polymer-based nanoparticle strategies for insulin delivery. Polymers 2019;11(9):1380.

(191) Béduneau A, Tempesta C, Fimbel S, Pellequer Y, Jannin V, Demarne F, et al. A tunable Caco-2/HT29-MTX co-culture model mimicking variable permeabilities of the human intestine obtained by an original seeding procedure. European Journal of Pharmaceutics and Biopharmaceutics 2014;87(2):290-298.

(192) Reale O, Huguet A, Fessard V. Co-culture model of Caco-2/HT29-MTX cells: A promising tool for investigation of phycotoxins toxicity on the intestinal barrier. Chemosphere 2021;273:128497.

(193) Hilgendorf C, Spahn-Langguth H, Regårdh CG, Lipka E, Amidon GL, Langguth P. Caco-2 versus caco-2/HT29-MTX co-cultured cell lines: permeabilities via diffusion, inside- and outside-directed carrier-mediated transport. J Pharm Sci 2000;89(1):63-75.

(194) Chen G, Svirskis D, Lu W, Ying M, Huang Y, Wen J. N-trimethyl chitosan nanoparticles and CSKSSDYQC peptide: N-trimethyl chitosan conjugates enhance the oral bioavailability of gemcitabine to treat breast cancer. J Controlled Release 2018;277:142-153.

(195) Jin Y, Song Y, Zhu X, Zhou D, Chen C, Zhang Z, et al. Goblet cell-targeting nanoparticles for oral insulin delivery and the influence of mucus on insulin transport. Biomaterials 2012;33(5):1573-1582.

(196) Shi Z, Wu Z, Gu C, Chen B, Zhang H, Yin W, et al. Calculation methods for the permeability coefficient of concrete face rockfill dam with cracks. Advances in Civil Engineering 2019;2019.

(197) Tanigawa T, Kanazawa S, Ichibori R, Fujiwara T, Magome T, Shingaki K, et al. ( )-Catechin protects dermal fibroblasts against oxidative stress-induced apoptosis. BMC complementary and alternative medicine 2014;14(1):1-7.

(198) Gerloff K, Albrecht C, Boots AW, Förster I, Schins RP. Cytotoxicity and oxidative DNA damage by nanoparticles in human intestinal Caco-2 cells. Nanotoxicology 2009;3(4):355-364.

(199) Bettencourt A, Gonçalves LM, Gramacho AC, Vieira A, Rolo D, Martins C, et al. Analysis of the characteristics and cytotoxicity of titanium dioxide nanomaterials following simulated In Vitro digestion. Nanomaterials 2020;10(8):1516.

(200) Gleeson JP, Ryan SM, Brayden DJ. Oral delivery strategies for nutraceuticals: Delivery vehicles and absorption enhancers. Trends Food Sci Technol 2016;53:90-101.

(201) Rejman J, Bragonzi A, Conese M. Role of clathrin-and caveolae-mediated endocytosis in gene transfer mediated by lipo-and polyplexes. Molecular therapy 2005;12(3):468-474.

(202) Mislick KA, Baldeschwieler JD. Evidence for the role of proteoglycans in cation-mediated gene transfer. Proceedings of the National Academy of Sciences 1996;93(22):12349-12354.

(203) Yu X, Lin S, Zhou Z, Chen X, Liang J, Duan W, et al. Tanshinone IIB, a primary active constituent from Salvia miltiorrhza, exhibits neuro-protective activity in experimentally stroked rats. Neurosci Lett 2007;417(3):261-265.

(204) Zhou YZ, Alany RG, Chuang V, Wen J. Optimization of PLGA nanoparticles formulation containing L-DOPA by applying the central composite design. Drug Dev Ind Pharm 2013;39(2):321-330.

(205) Soni V, Kohli DV, Jain SK. Transferrin coupled liposomes for enhanced brain delivery of doxorubicin. Vascular Disease Prevention 2007;4(1):31-38.

(206) Jin Y, Wen J, Garg S, Liu D, Zhou Y, Teng L, et al. Development of a novel niosomal system for oral delivery of Ginkgo biloba extract. International journal of nanomedicine 2013;8:421.

(207) Bagchi S, Chhibber T, Lahooti B, Verma A, Borse V, Jayant RD. In-vitro blood-brain barrier models for drug screening and permeation studies: an overview. Drug design, development and therapy 2019;13:3591.

(208) Cai P, Zheng Y, Sun Y, Zhang C, Zhang Q, Liu Q. New blood–brain barrier models using primary Parkinson's Disease rat brain endothelial cells and astrocytes for the development of central nervous system drug delivery systems. ACS Chemical Neuroscience 2021;12(20):3829-3837.

(209) Sivandzade F, Cucullo L. In-vitro blood–brain barrier modeling: A review of modern and fast-advancing technologies. Journal of Cerebral Blood Flow & Metabolism 2018;38(10):1667-1681.

(210) Pardridge WM. The isolated brain microvessel: a versatile experimental model of the blood-brain barrier. Frontiers in physiology 2020;11:398.

(211) Demeuse P, Kerkhofs A, Struys-Ponsar C, Knoops B, Remacle C, de Aguilar, Ph van den Bosch. Compartmentalized coculture of rat brain endothelial cells and astrocytes: a syngenic model to study the blood–brain barrier. J Neurosci Methods 2002;121(1):21-31.

(212) Jones AR, Shusta EV. Blood–brain barrier transport of therapeutics via receptor-mediation. Pharm Res 2007;24(9):1759-1771.

(213) Lockman PR, Koziara JM, Mumper RJ, Allen DD. Nanoparticle surface charges alter blood–brain barrier integrity and permeability. J Drug Target 2004;12(9-10):635-641.

(214) World Health Organisation. Mental health: neurological disorders. 2016; Available at: https://www.who.int/news-room/questions-and-answers/item/mental-health-neurological-disorders#:~:text=Neurological%20disorders%20are%20diseases%20of,%2C%20neuromuscular%20junction%2C%20and%20muscles.

(215) Guan J, Gluckman PD. IGF-1 derived small neuropeptides and analogues: a novel strategy for the development of pharmaceuticals for neurological conditions. Br J Pharmacol 2009;157(6):881-891.

(216) Cacciatore I, Cornacchia C, Baldassarre L, Fornasari E, Mollica A, Stefanucci A, et al. GPE and GPE analogues as promising neuroprotective agents. Mini reviews in medicinal chemistry 2012;12(1):13-23.

(217) Daneman R, Prat A. The Blood–Brain Barrier. Cold Spring Harbor perspectives in biology 2015 Jan 5,;7(1):a020412.

(218) Lockman PR, Mumper RJ, Khan MA, Allen DD. Nanoparticle technology for drug delivery across the blood-brain barrier. Drug Dev Ind Pharm 2002;28(1):1-13.

(219) Song Q, Li D, Zhou Y, Yang J, Yang W, Zhou G, et al. Enhanced uptake and transport of ( )-catechin and (−)-epigallocatechin gallate in niosomal formulation by human intestinal Caco-2 cells. International Journal of Nanomedicine 2014;9:2157.

(220) Zhang Y, Zhang K, Wu Z, Guo T, Ye B, Lu M, et al. Evaluation of transdermal salidroside delivery using niosomes via in vitro cellular uptake. Int J Pharm 2015;478(1):138-146.

(221) Hong M, Zhu S, Jiang Y, Tang G, Pei Y. Efficient tumor targeting of hydroxycamptothecin loaded PEGylated niosomes modified with transferrin. J Controlled Release 2009;133(2):96-102.

(222) Obeid MA, Khadra I, Albaloushi A, Mullin M, Alyamani H, Ferro VA. Microfluidic manufacturing of different niosomes nanoparticles for curcumin encapsulation: Physical characteristics, encapsulation efficacy, and drug release. Beilstein journal of nanotechnology 2019;10(1):1826-1832.

(223) Hao Y, Zhao F, Li N, Yang Y. Studies on a high encapsulation of colchicine by a niosome system. Int J Pharm 2002;244(1-2):73-80.

(224) Arunachalam A, Jeganath S, Yamini K, Tharangini K. Niosomes: a novel drug delivery system. International journal of novel trends in pharmaceutical sciences 2012;2(1):25-31.

(225) Kumbhar D, Wavikar P, Vavia P. Niosomal gel of lornoxicam for topical delivery: in vitro assessment and pharmacodynamic activity. AAPS pharmscitech 2013;14(3):1072-1082.

(226) de Almeida MS, Susnik E, Drasler B, Taladriz-Blanco P, Petri-Fink A, Rothen-Rutishauser B. Understanding nanoparticle endocytosis to improve targeting strategies in nanomedicine. Chem Soc Rev 2021;50(9):5397-5434.

(227) Okore VC, Attama AA, Ofokansi KC, Esimone CO, Onuigbo EB. Formulation and evaluation of niosomes. Indian Journal of Pharmaceutical Sciences 2011;73(3):323.

(228) Sonia TA, Sharma CP. Oral delivery of insulin. : Elsevier; 2014.

(229) Varshosaz J, Taymouri S, Pardakhty A, Asadi-Shekaari M, Babaee A. Niosomes of ascorbic acid and α-tocopherol in the cerebral ischemia-reperfusion model in male rats. Biomed research international 2014;2014.

(230) Targhi AA, Moammeri A, Jamshidifar E, Abbaspour K, Sadeghi S, Lamakani L, et al. Synergistic effect of curcumin-Cu and curcumin-Ag nanoparticle loaded niosome: Enhanced antibacterial and anti-biofilm activities. Bioorg Chem 2021;115:105116.

(231) Song Q, Li D, Zhou Y, Yang J, Yang W, Zhou G, et al. Enhanced uptake and transport of ( )-catechin and (−)-epigallocatechin gallate in niosomal formulation by human intestinal Caco-2 cells. International Journal of Nanomedicine 2014;9:2157.

(232) Mészáros M, Porkoláb G, Kiss L, Pilbat A, Kóta Z, Kupihár Z, et al. Niosomes decorated with dual ligands targeting brain endothelial transporters increase cargo penetration across the blood-brain barrier. European journal of pharmaceutical sciences 2018;123:228-240.

(233) Skovsgaard T. Transport and binding of daunorubicin, adriamycin, and rubidazone in Ehrlich ascites tumour cells. Biochem Pharmacol 1977;26(3):215-222.

(234) Ungell A, Andreasson A, Lundin K, Utter L. Effects of enzymatic inhibition and increased paracellular shunting on transport of vasopressin analogues in the rat. J Pharm Sci 1992;81(7):640-645.

(235) Iversen T, Skotland T, Sandvig K. Endocytosis and intracellular transport of nanoparticles: Present knowledge and need for future studies. Nano today 2011;6(2):176-185.

(236) Grebe SK, Singh RJ. LC-MS/MS in the clinical laboratory–where to from here? The Clinical biochemist reviews 2011;32(1):5.

(237) Gaillard PJ, Voorwinden LH, Nielsen JL, Ivanov A, Atsumi R, Engman H, et al. Establishment and functional characterization of an in vitro model of the blood–brain barrier, comprising a co-culture of brain capillary endothelial cells and astrocytes. European journal of pharmaceutical sciences 2001;12(3):215-222.

(238) Demeuse P, Kerkhofs A, Struys-Ponsar C, Knoops B, Remacle C, de Aguilar, Ph van den Bosch. Compartmentalized coculture of rat brain endothelial cells and astrocytes: a syngenic model to study the blood–brain barrier. J Neurosci Methods 2002;121(1):21-31.

(239) Jeliazkova-Mecheva VV, Bobilya DJ. A porcine astrocyte/endothelial cell co-culture model of the blood–brain barrier. Brain research protocols 2003;12(2):91-98.

(240) Yong Zhou. Development and Optimisation of Nanoparticulate System for Brain Delivery of L-DOPA. University of Auckland; 2012.

(241) Khan R, Irchhaiya R. Niosomes: a potential tool for novel drug delivery. Journal of pharmaceutical investigation 2016;46(3):195-204.

(242) Okore VC, Attama AA, Ofokansi KC, Esimone CO, Onuigbo EB. Formulation and evaluation of niosomes. Indian Journal of Pharmaceutical Sciences 2011;73(3):323.

(243) Xu Y, Hanna MA. Electrospray encapsulation of water-soluble protein with polylactide: Effects of formulations on morphology, encapsulation efficiency and release profile of particles. Int J Pharm 2006;320(1-2):30-36.

(244) Salatin S, Barar J, Barzegar-Jalali M, Adibkia K, Kiafar F, Jelvehgari M. An alternative approach for improved entrapment efficiency of hydrophilic drug substance in PLGA nanoparticles by interfacial polymer deposition following solvent displacement. Jundishapur Journal of Natural Pharmaceutical Products 2018;13(4).

(245) Al-Qadi S, Grenha A, Carrión-Recio D, Seijo B, Remuñán-López C. Microencapsulated chitosan nanoparticles for pulmonary protein delivery: in vivo evaluation of insulin-loaded formulations. J Controlled Release 2012;157(3):383-390.

(246) Misra A, Jinturkar K, Patel D, Lalani J, Chougule M. Recent advances in liposomal dry powder formulations: preparation and evaluation. Expert opinion on drug delivery 2009;6(1):71-89.

(247) Li M, Zhao M, Kumar Durairajan SS, Xie L, Zhang H, Kum W, et al. Protective effect of tetramethylpyrazine and salvianolic acid B on apoptosis of rat cerebral microvascular endothelial cell under high shear stress. Clin Hemorheol Microcirc 2008;38(3):177-187.

(248) Zuluaga M, Gueguen V, Letourneur D, Pavon-Djavid G. Astaxanthin-antioxidant impact on excessive Reactive Oxygen Species generation induced by ischemia and reperfusion injury. Chem Biol Interact 2018;279:145-158.

(249) Auten RL, Davis JM. Oxygen toxicity and reactive oxygen species: the devil is in the details. Pediatr Res 2009;66(2):121-127.